PR12-22-005

A Search for a Nonzero Strange Form Factor of the Proton at 2.5 $(GeV/c)^2$

R.Beminiwattha, S.P.Wells, N.Simicevic, C. Palatchi, K.Paschke, S.Ali, X.Bai, G.Cates, R.Lindgren, N.Liyanage, V.Nelyubin, X.Zheng, **B.Wojtsekhowski**, S.Barcus, A.Camsonne, R.Carlini, S.Covrig Dusa, P.Degtiarenko, D.Gaskell, O.Hansen, D.Higinbotham, D.Flay, D.Jones, M.Jones, C.Keppel, D.Meekins, R.Michaels, B.Raydo, G.Smith, H.Szumila-Vance, A.S.Tadepalli, T.Horn, E.Cisbani, E.King, J.Napolitano, P.M.King, P.A.Souder, D.Hamilton, O.Jevons, R.Montgomery, P.Markowitz, E.Brash, P.Monaghan, T.Hobbs, G.Miller, J.Lichtenstadt, T.Kolar, E.Piasetzky, G.Ron, D.Armstrong, T.Averett, S.Mayilyan, H.Mkrtchyan, A.Mkrtchyan, A.Shahinyan, V.Tadevosyan, H.Voskanyan, W.Tireman, P.Datta, E.Fuchey, A.J.R.Puckett, S.Seeds, C.Munoz-Camacho

LaTech, Indiana, UVa, JLab, CUA, INFN - Roma, Temple, Ohio, Syracuse, Glascow, FIU, CNU, Fermilab, UWashington, Tel Aviv U, Hebrew U, W&M, AANL Yerevan, Northern Michigan, UConn, Orsay

Charge symmetry and the nucleon form factors

Charge Symmetry

$$G_E^p = \frac{2}{3} G_E^{u,p} - \frac{1}{3} G_E^{d,p}$$

$$G_E^n = \frac{2}{3} G_E^{u,n} - \frac{1}{3} G_E^{d,n}$$

Charge symmetry is assumed for the form factors, $G_E^{u,p} = G_E^{d,n}$, *etc.*
and used to find the flavor separated form-factors,
measuring $G_{E,M}^{p,n}$ to find $G_{E,M}^{u,d}$

$$G_E^p = \frac{2}{3} G_E^{u,p} - \frac{1}{3} G_E^{d,p} - \frac{1}{3} G_E^s$$

$$G_E^n = \frac{2}{3} G_E^{u,n} - \frac{1}{3} G_E^{d,n} - \frac{1}{3} G_E^s$$

But this can broken! One way is to have a non-zero strange form-factor, which breaks the "2 equations and 2 unknowns" system

The weak form factor provides a third linear combination:

$$G_E^{p,Z} = \left(1 - \frac{8}{3}\sin^2\theta_W\right) G_E^{u,p} + \left(-1 + \frac{4}{3}\sin^2\theta_W\right) G_E^{d,p} + \left(-1 + \frac{4}{3}\sin^2\theta_W\right) G_E^s$$

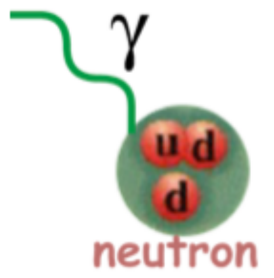

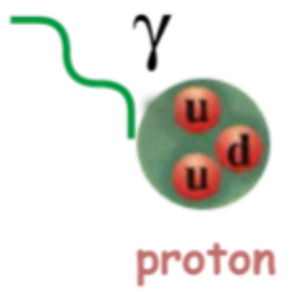

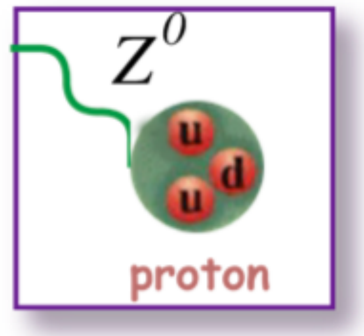

A strange quark form factor would be indistinguishable from a broken charge symmetry in u,d flavors

$$\delta G_E^u \equiv G_E^{u,p} - G_E^{d,n}$$

$$\delta G_E^d \equiv G_E^{d,p} - G_E^{u,n}$$

So, more generally: this experiment tests the assumption of charge symmetry which is crucial to the flavor decomposition of the form factors

Strangeness form factors

Polarized electron beam elastic e-p scattering

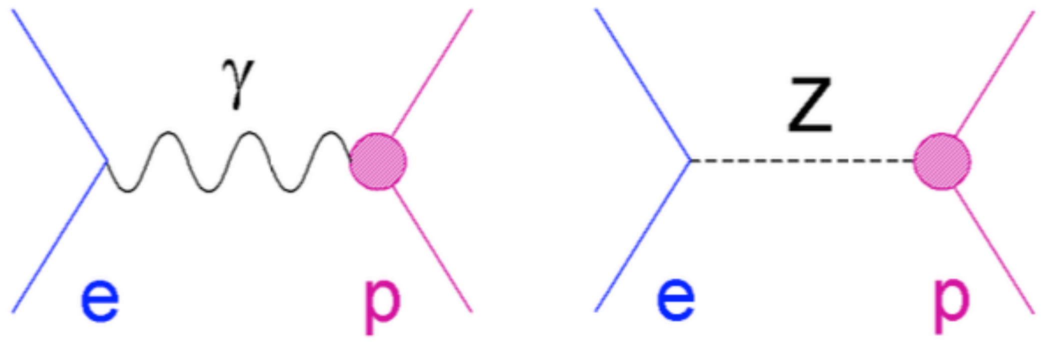

$$A_{PV} = -\frac{G_F Q^2}{4\pi\alpha\sqrt{2}} \cdot [(1 - 4\sin^2\theta_W) - \frac{\epsilon G_E^p G_E^n + \tau G_M^p G_M^n}{\epsilon (G_E^p)^2 + \tau (G_M^p)^2} - \frac{\epsilon G_E^p G_E^s + \tau G_M^p G_M^s}{\epsilon (G_E^p)^2 + \tau (G_M^p)^2}$$

$$+ \epsilon'(1 - 4\sin^2\theta_W) \frac{G_M^p G_A^{Zp}}{\epsilon (G_E^p)^2 + \tau (G_M^p)^2}]$$

A_{PV} = 150 ppm at θ = 15.5°, Q^2 = 2.5 GeV^2 (for sFF = 0)

A_{PV} = (-226 ppm) *[0.075 + 0.542 – 6.43*($G_M^s + 0.32\, G_E^s$) + 0.038]

Q_w EMFF axial

strange form-factors

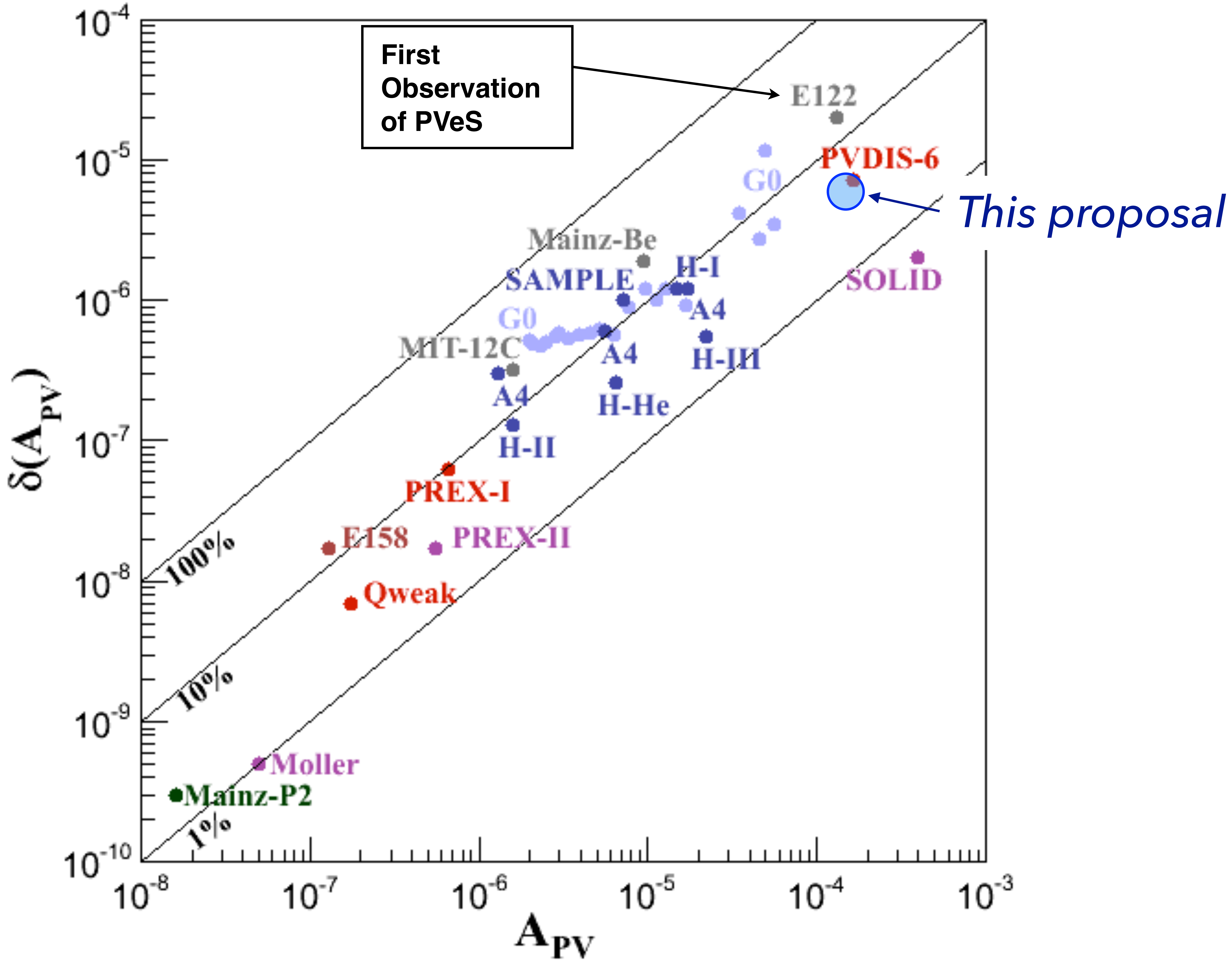
First Observation of PVeS
E122
PVDIS-6
This proposal
G0
Mainz-Be
SAMPLE
H-I
SOLID
A4
G0
MIT-12C
A4
H-III
H-He
A4
H-II
PREX-I
E158
PREX-II
Qweak
100%
10%
1%
Moller
Mainz-P2
$\delta(A_{PV})$
A_{PV}
10^{-4}
10^{-5}
10^{-6}
10^{-7}
10^{-8}
10^{-9}
10^{-10}
10^{-8}
10^{-7}
10^{-6}
10^{-5}
10^{-4}
10^{-3}

PVES "counting" experiments

Mainz A4

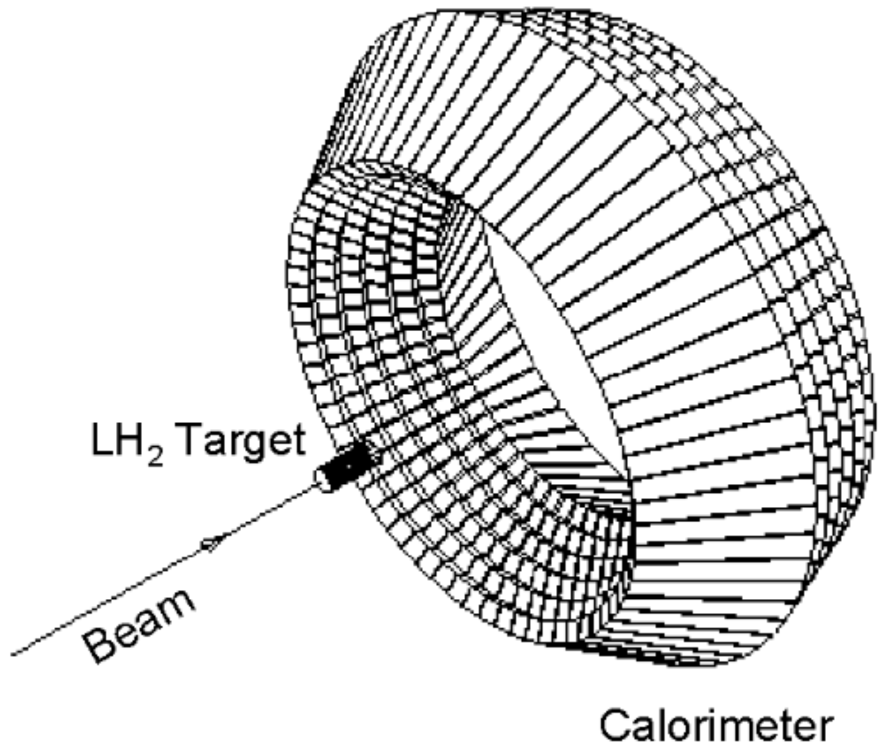

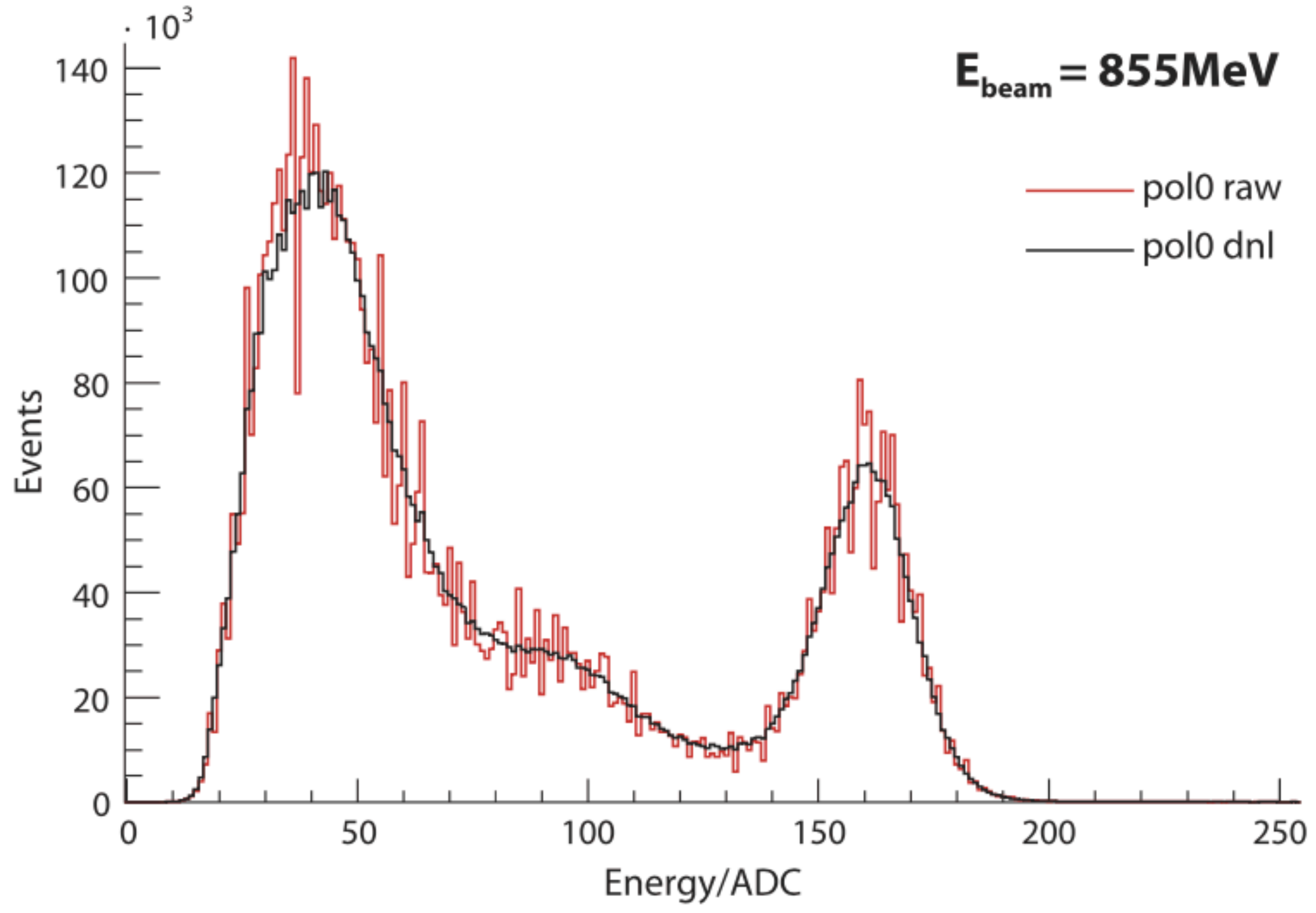

Total energy of electron

G0

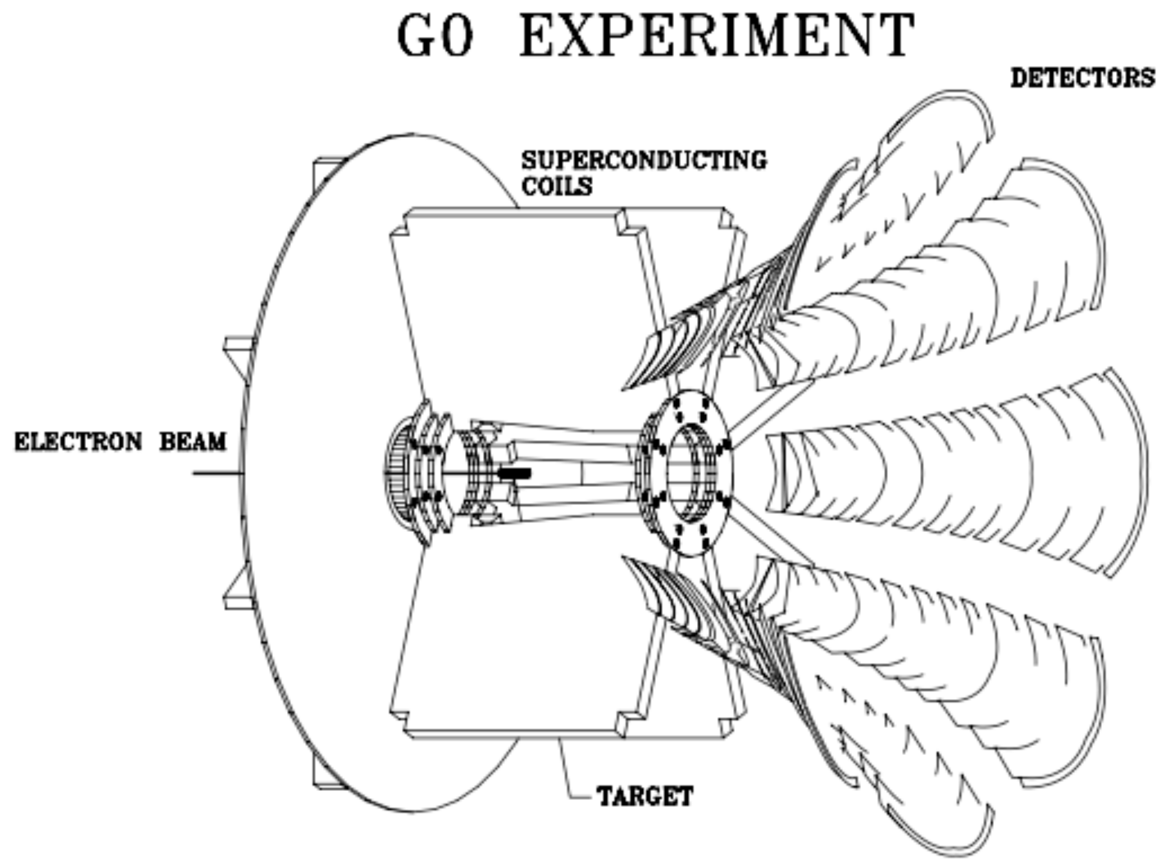

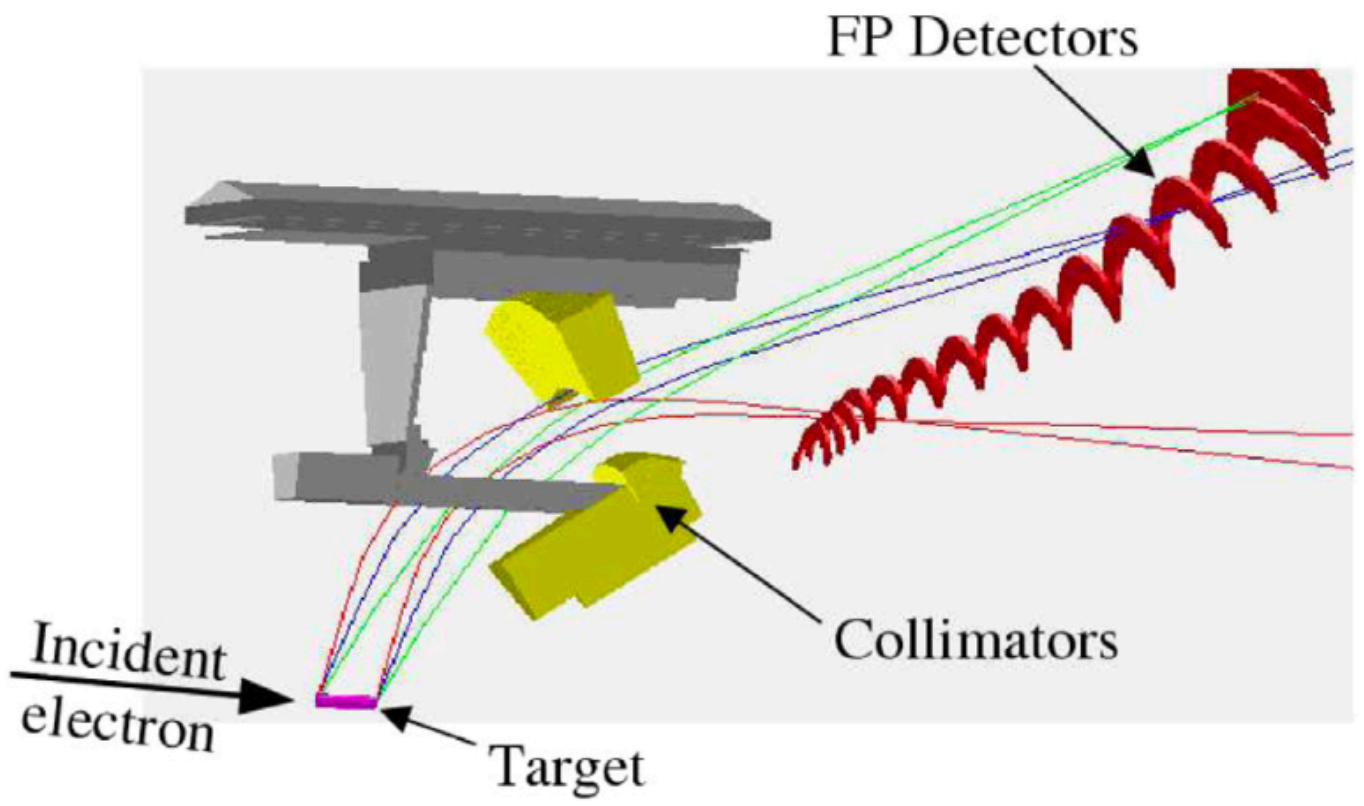

Time of flight of recoil proton

PVDIS-6

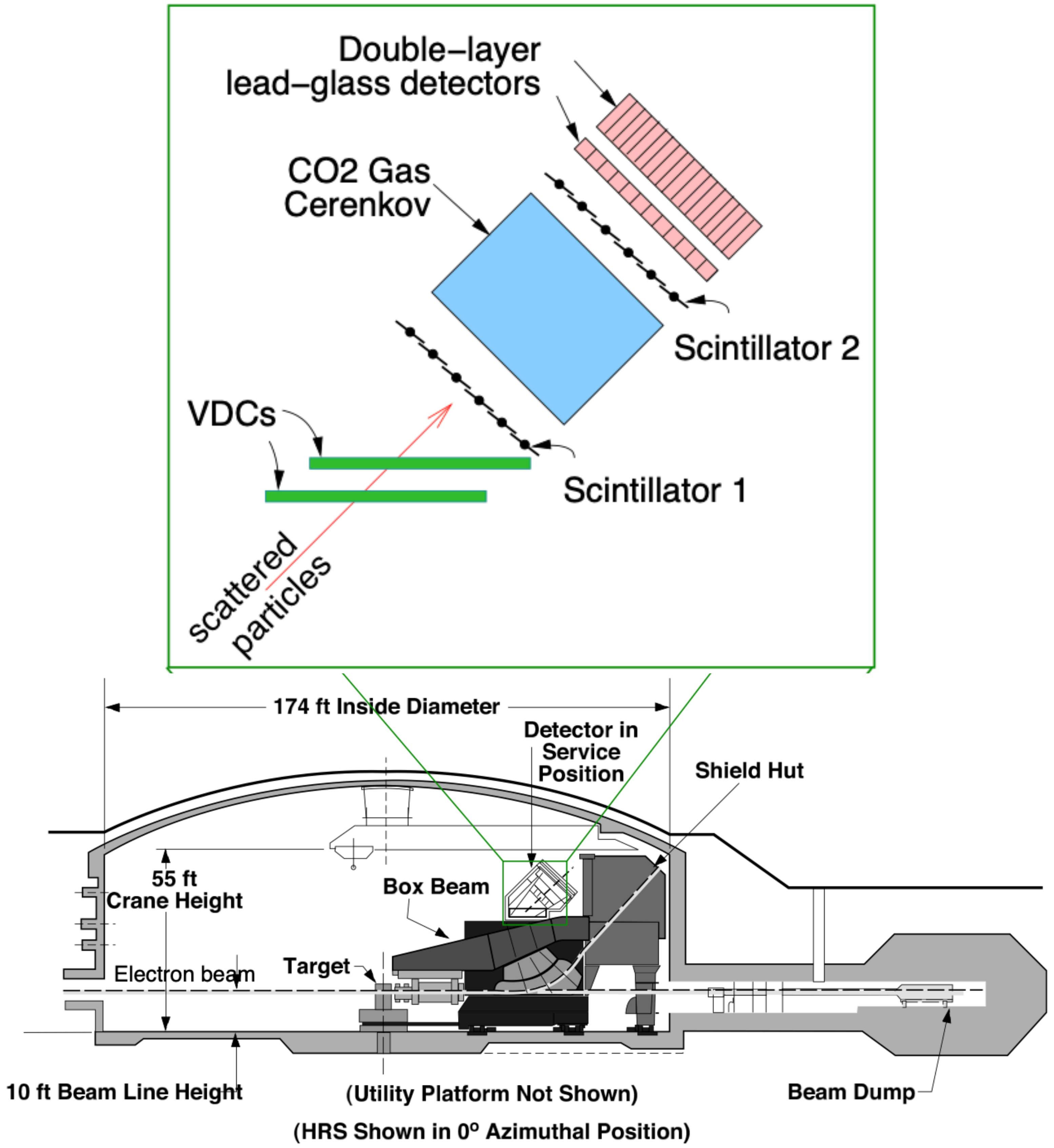

Calorimetry + Cerenkov PID

Proton strange form factors via parity violating elastic electron scattering

Strange form factors consistent with zero at low Q^2, but do not rule out non-zero values at higher Q^2, especially for magnetic form factor which is more accessible at higher Q^2

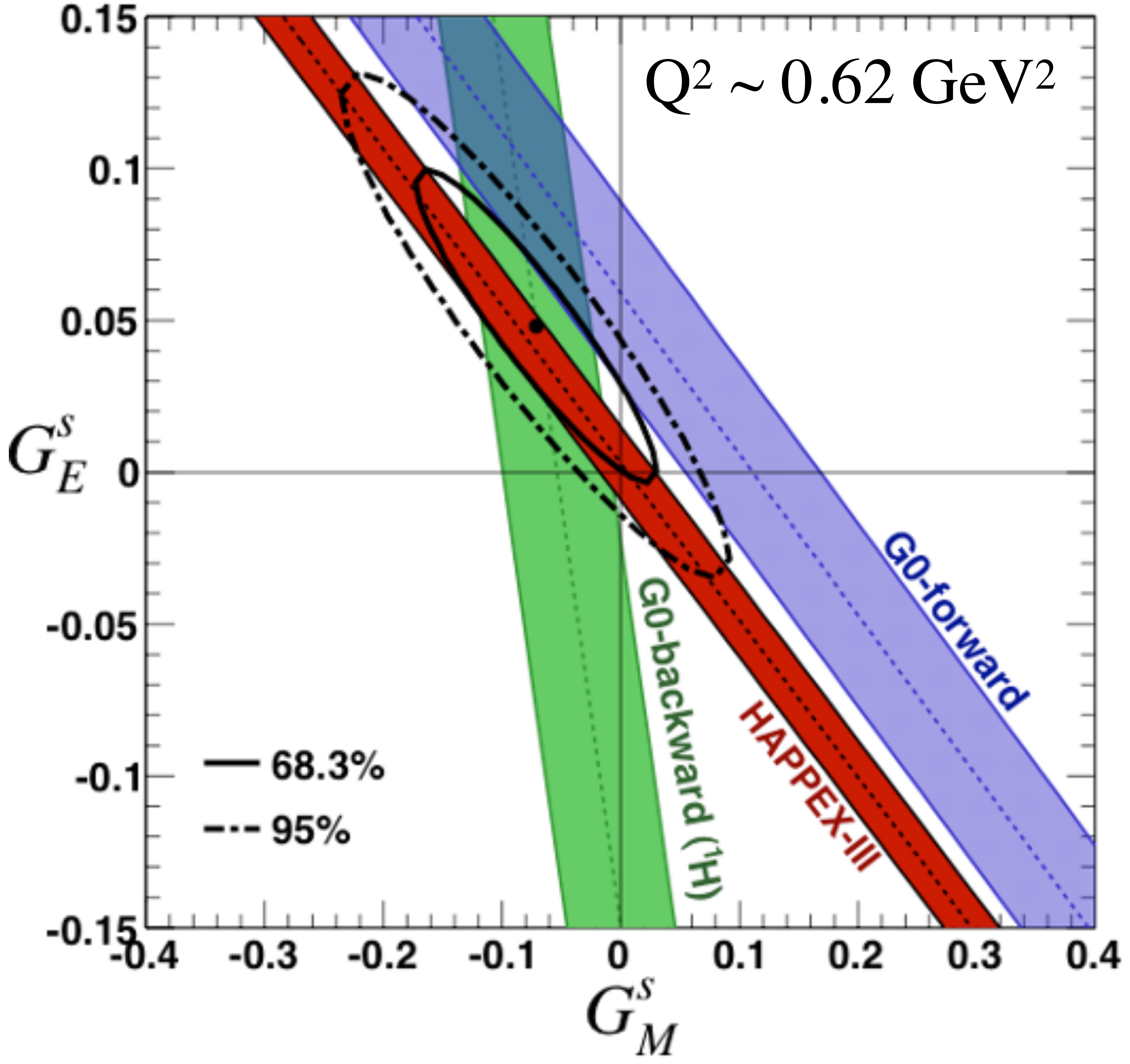

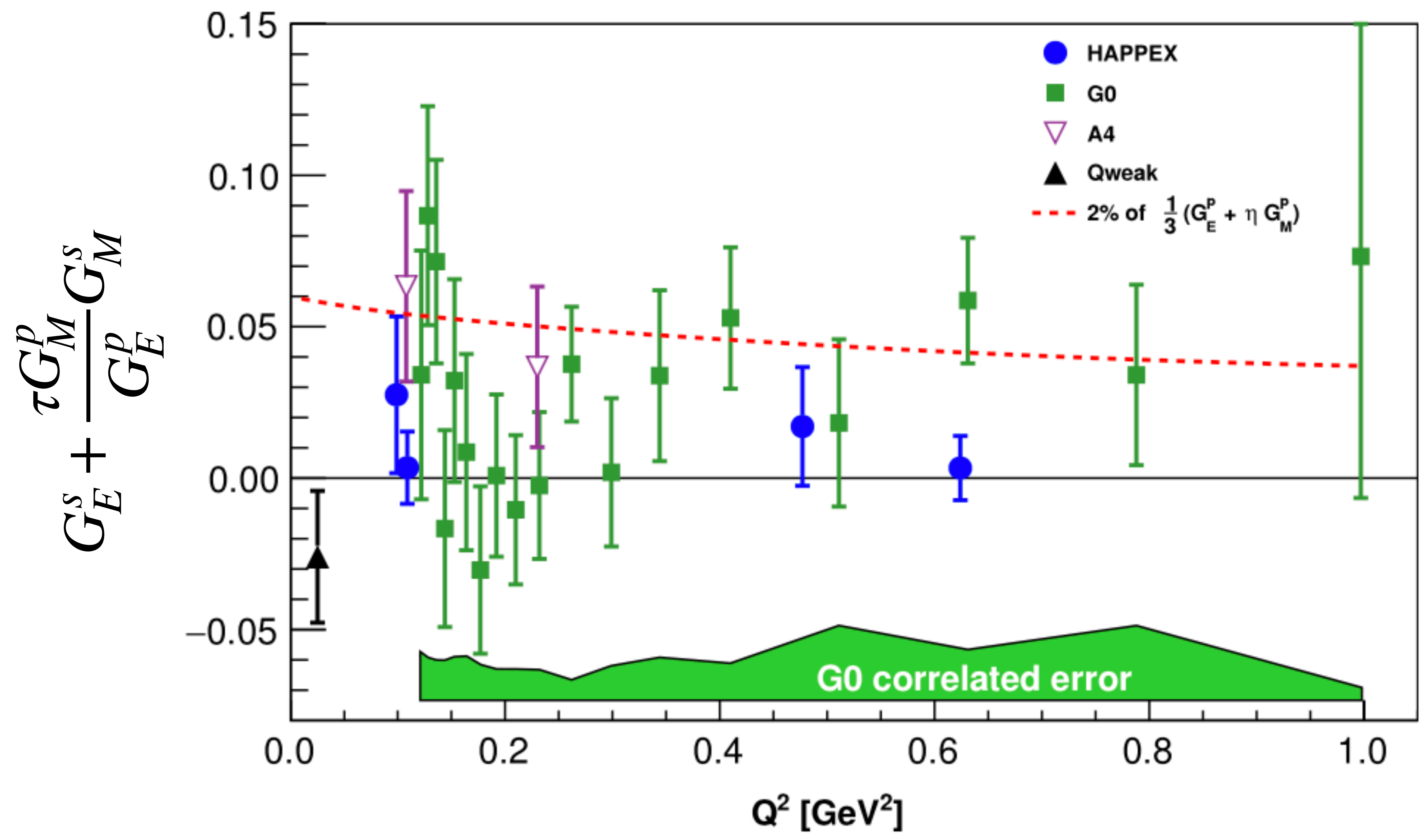

Strange form-factor predictions

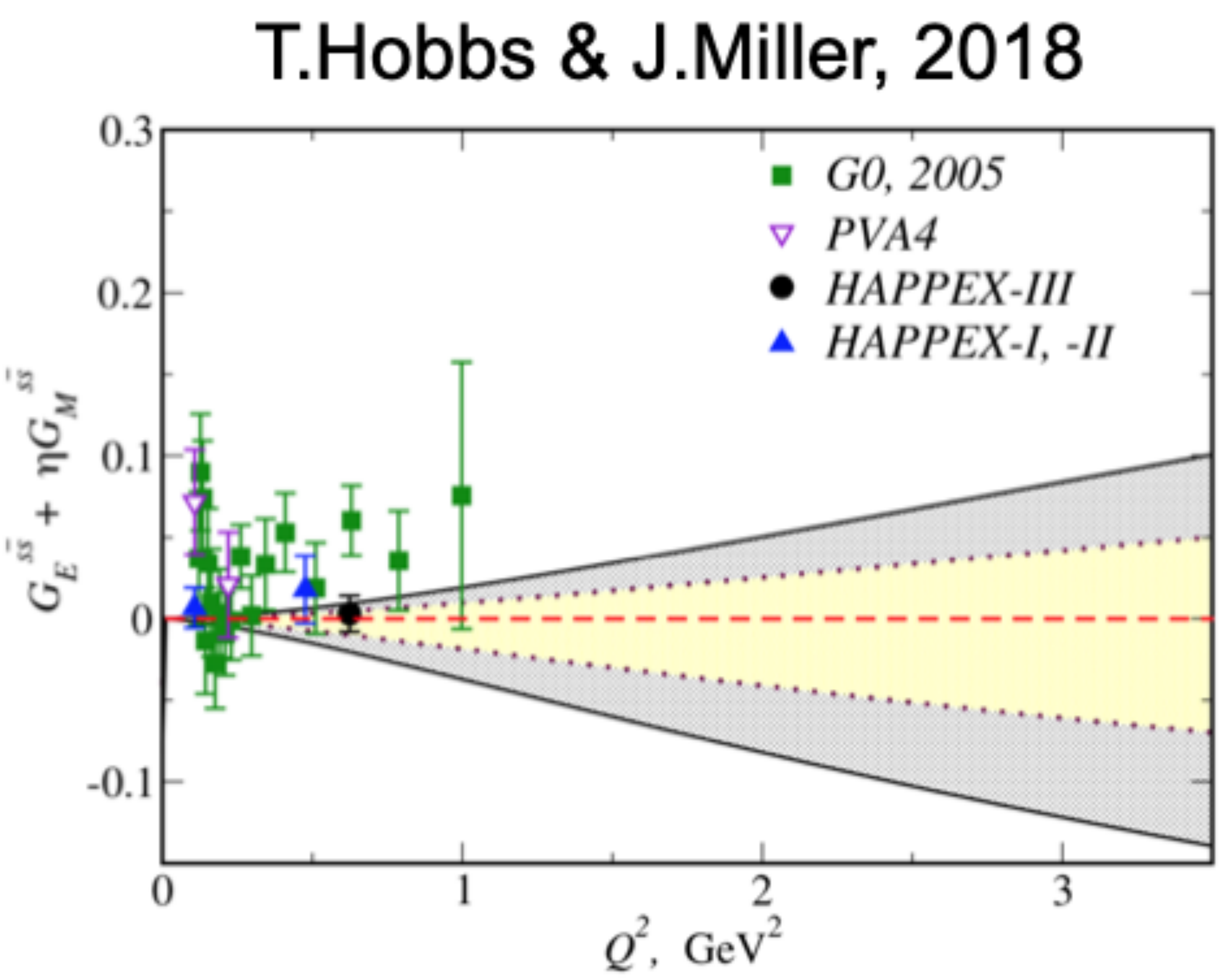

Follows work from *Phys.Rev.C* 91 (2015) 3, 035205
(LFWF to tie DIS and elastic measurements in a simple model)

Conclusion: sFF small (but non-zero) at low Q^2, but quite reasonable to think they may grow relatively large at large Q^2

G_D = 0.0477 at 2.5 GeV^2
uncertainty here ranges from (0.036,-0.051)

G_s/G_D ~ 1 is not excluded

Tim Hobbs and Jerry Miller have both joined the collaboration

Strange form-factors on the lattice

J.Green etal, 2015

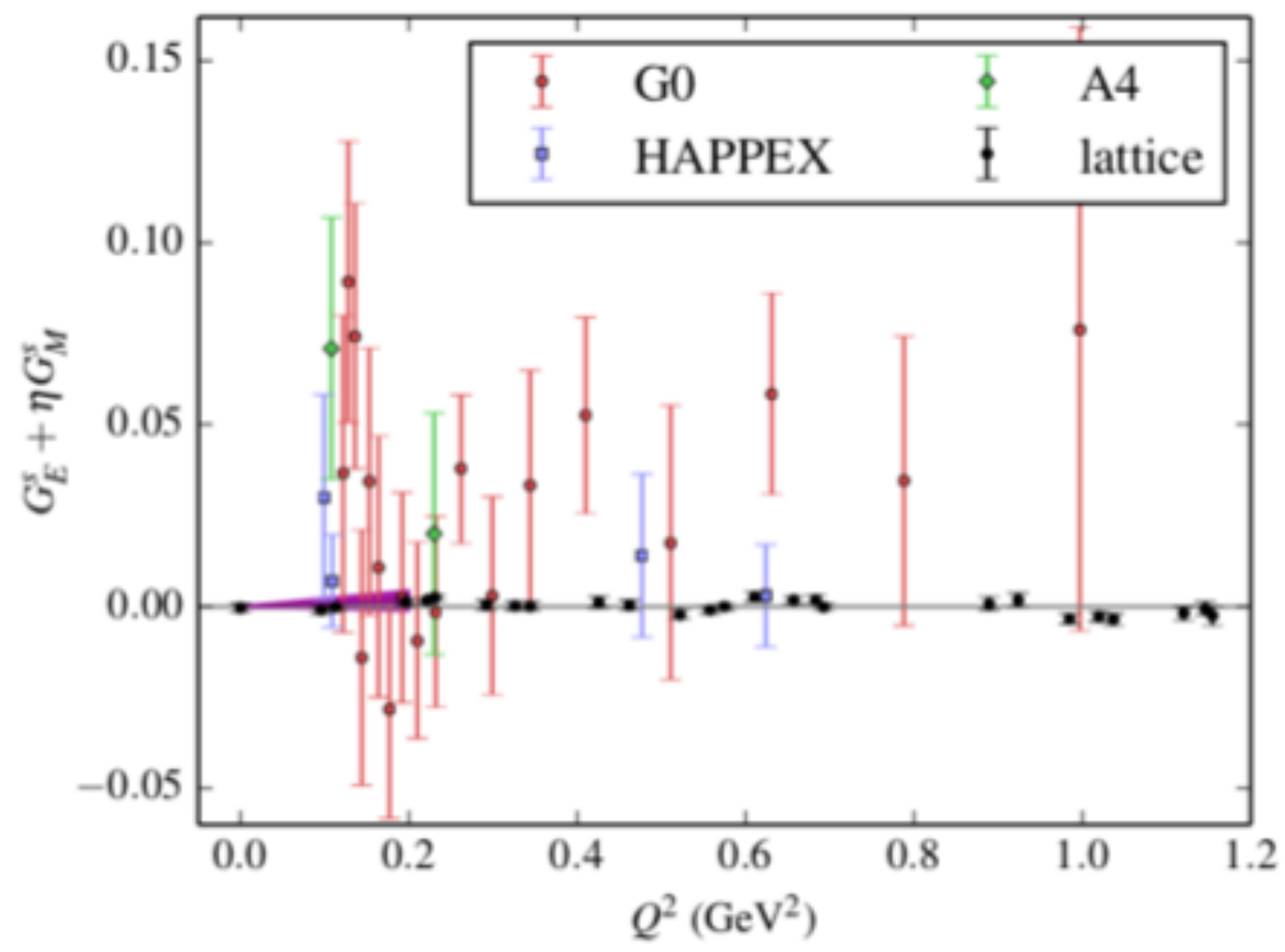

Some lattice calculations predict non-zero central values that would be visible with the proposed precision

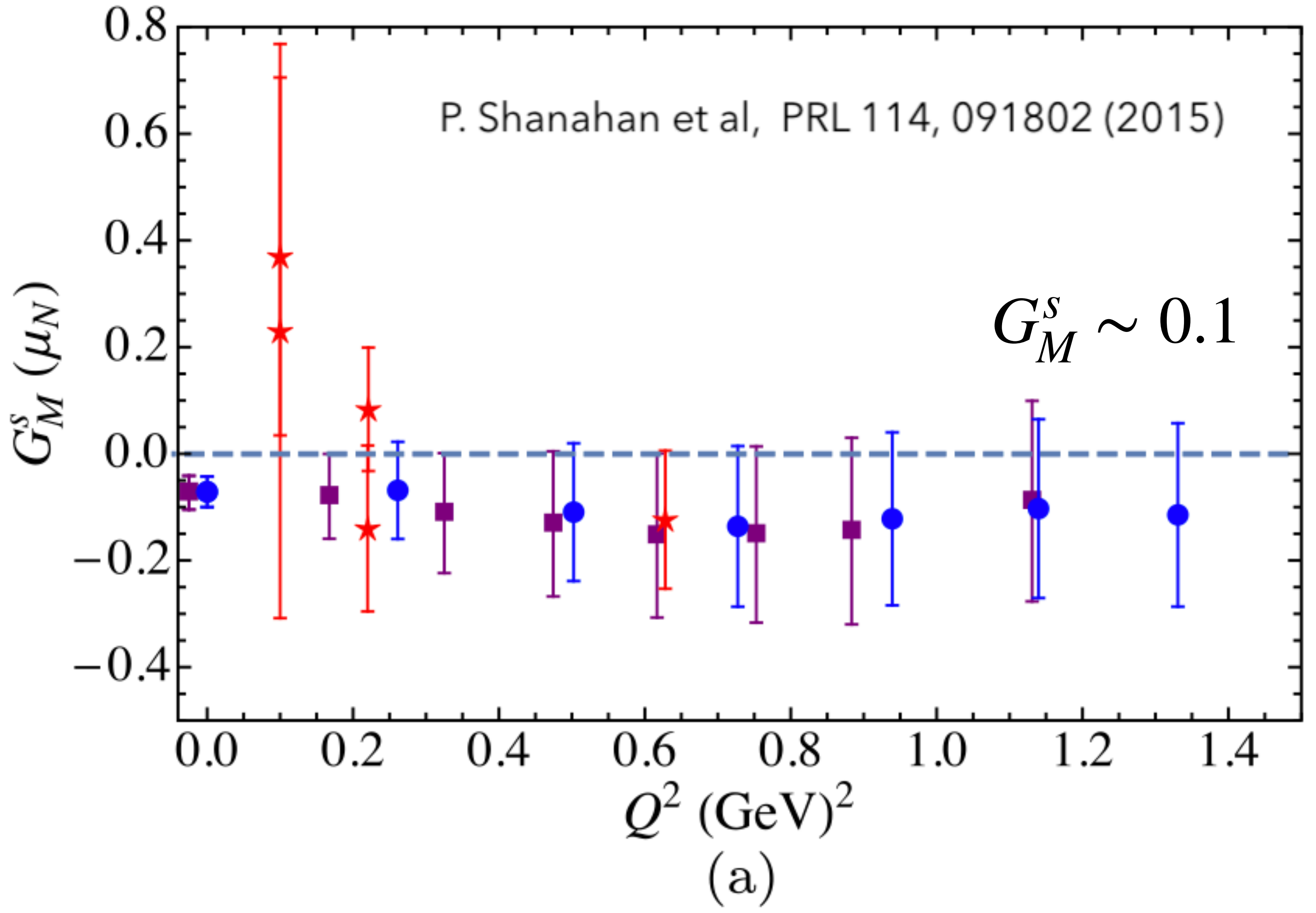

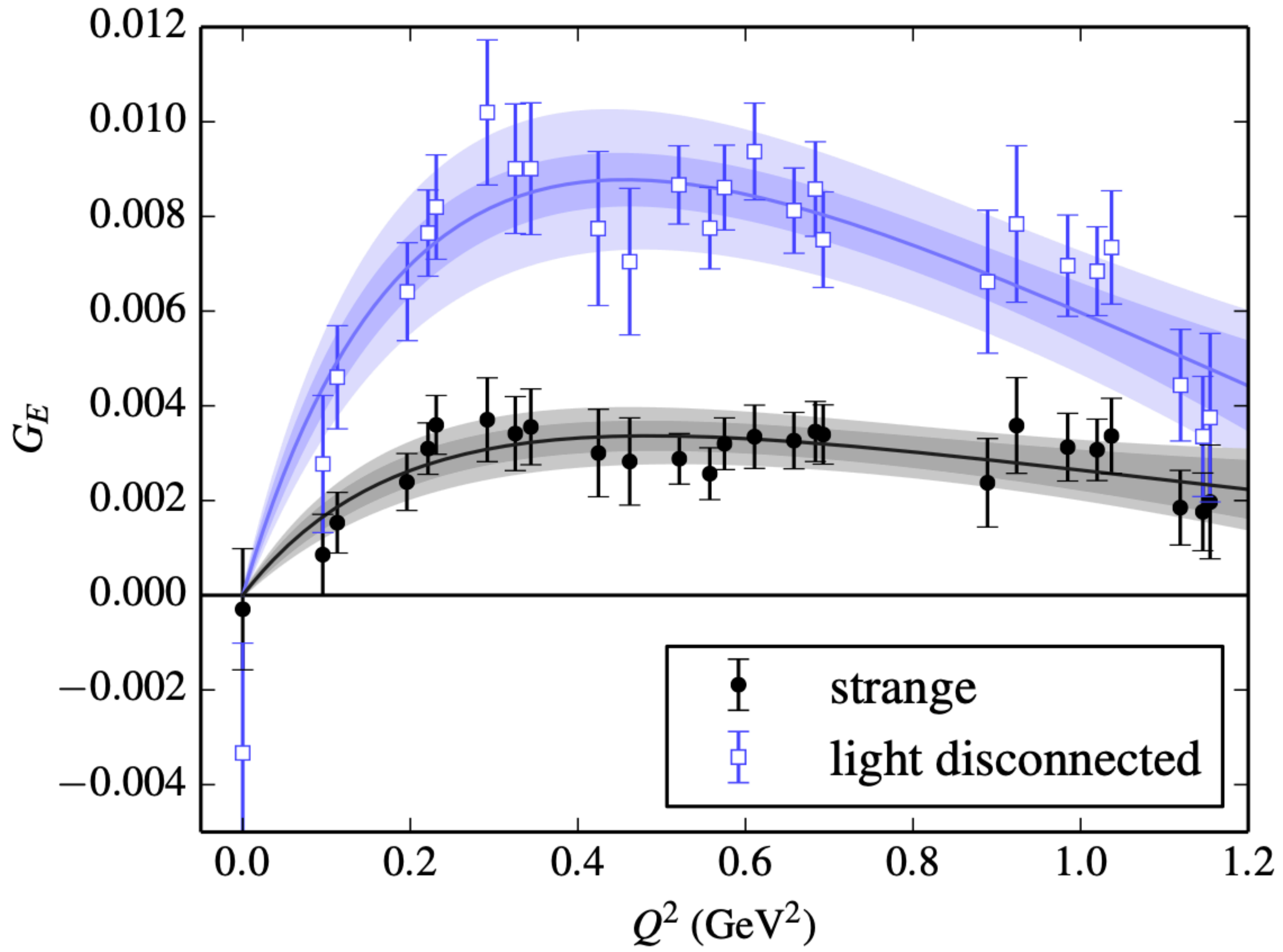

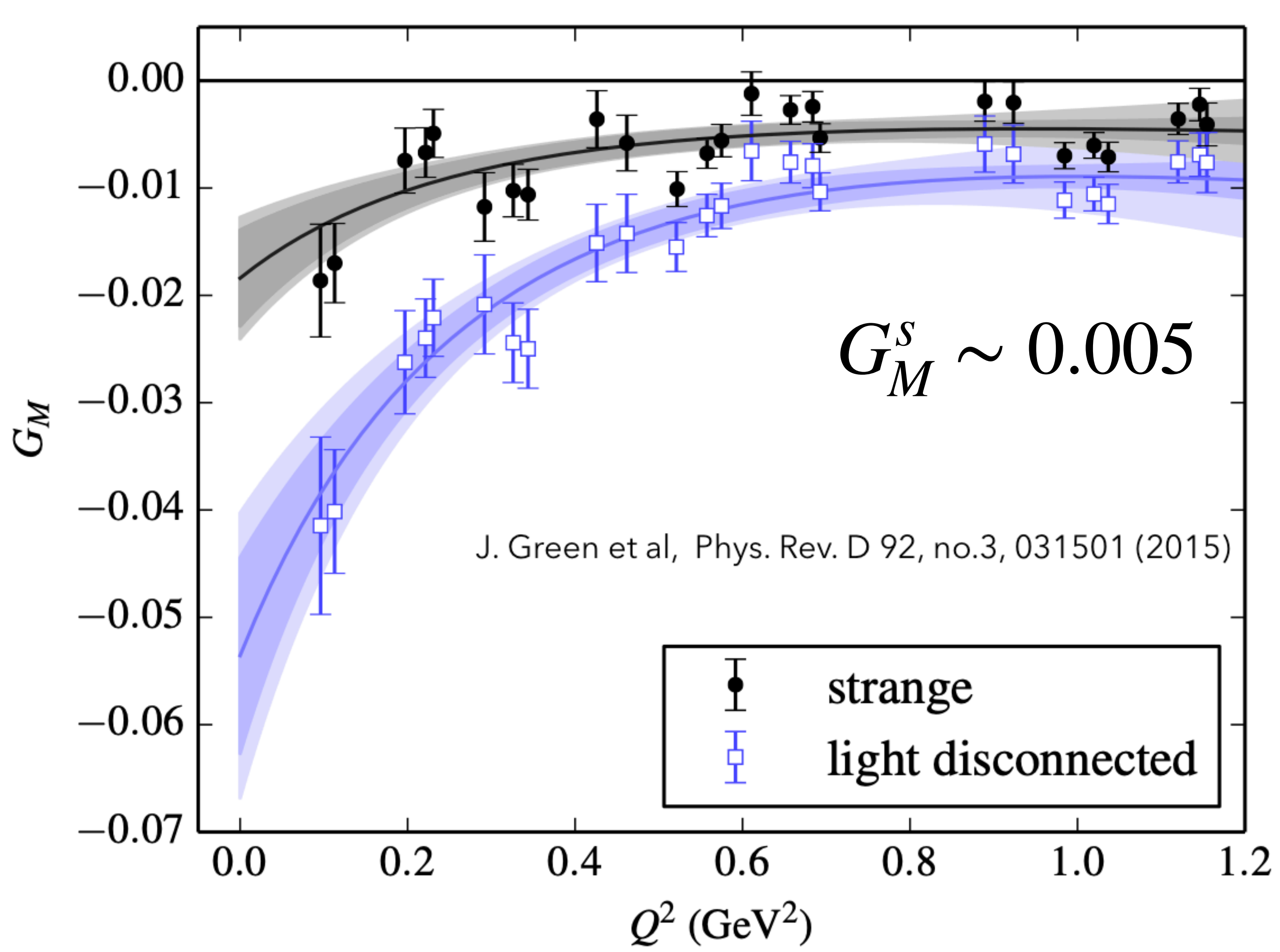

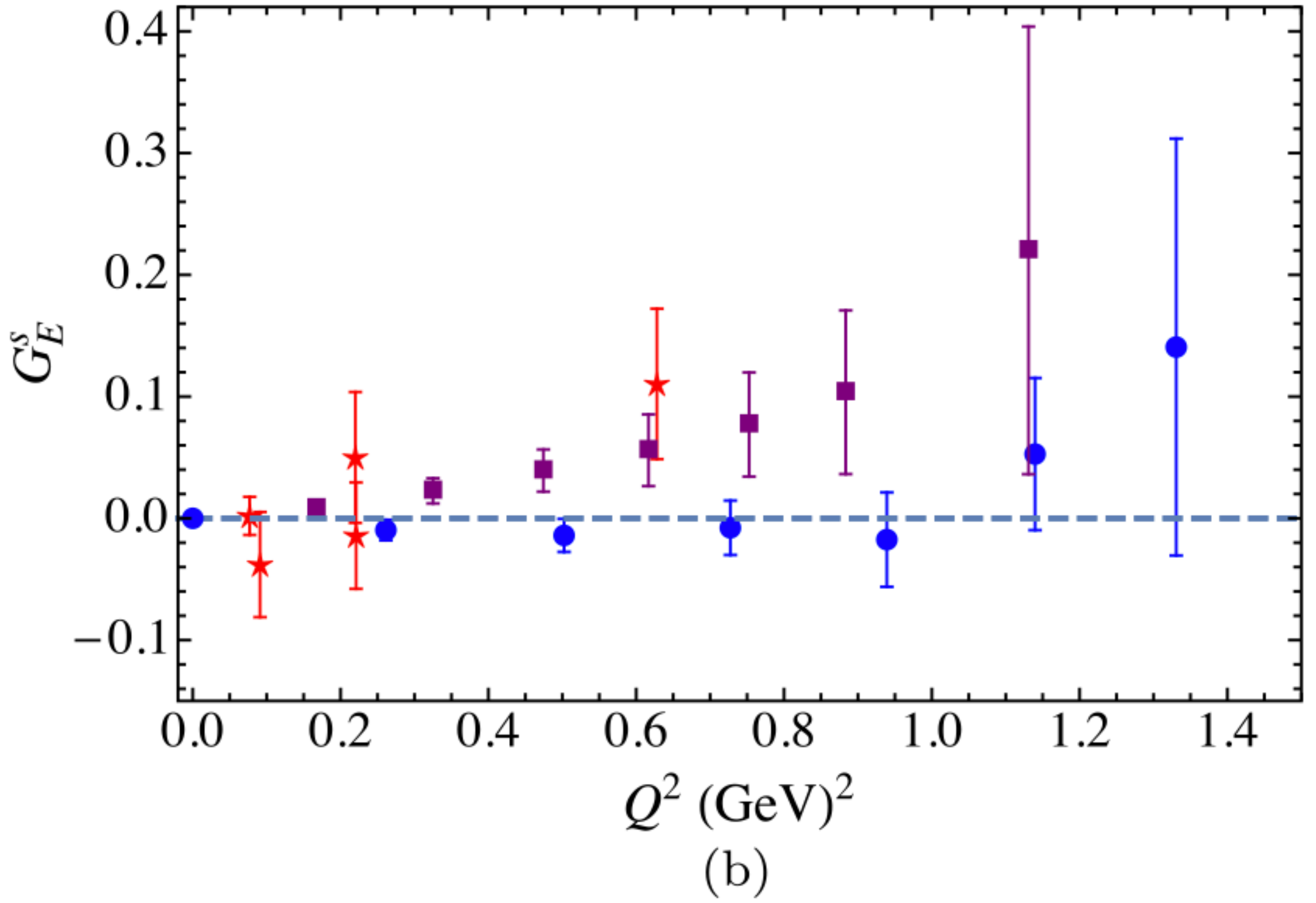

Q^2 dependence of F_2/F_1

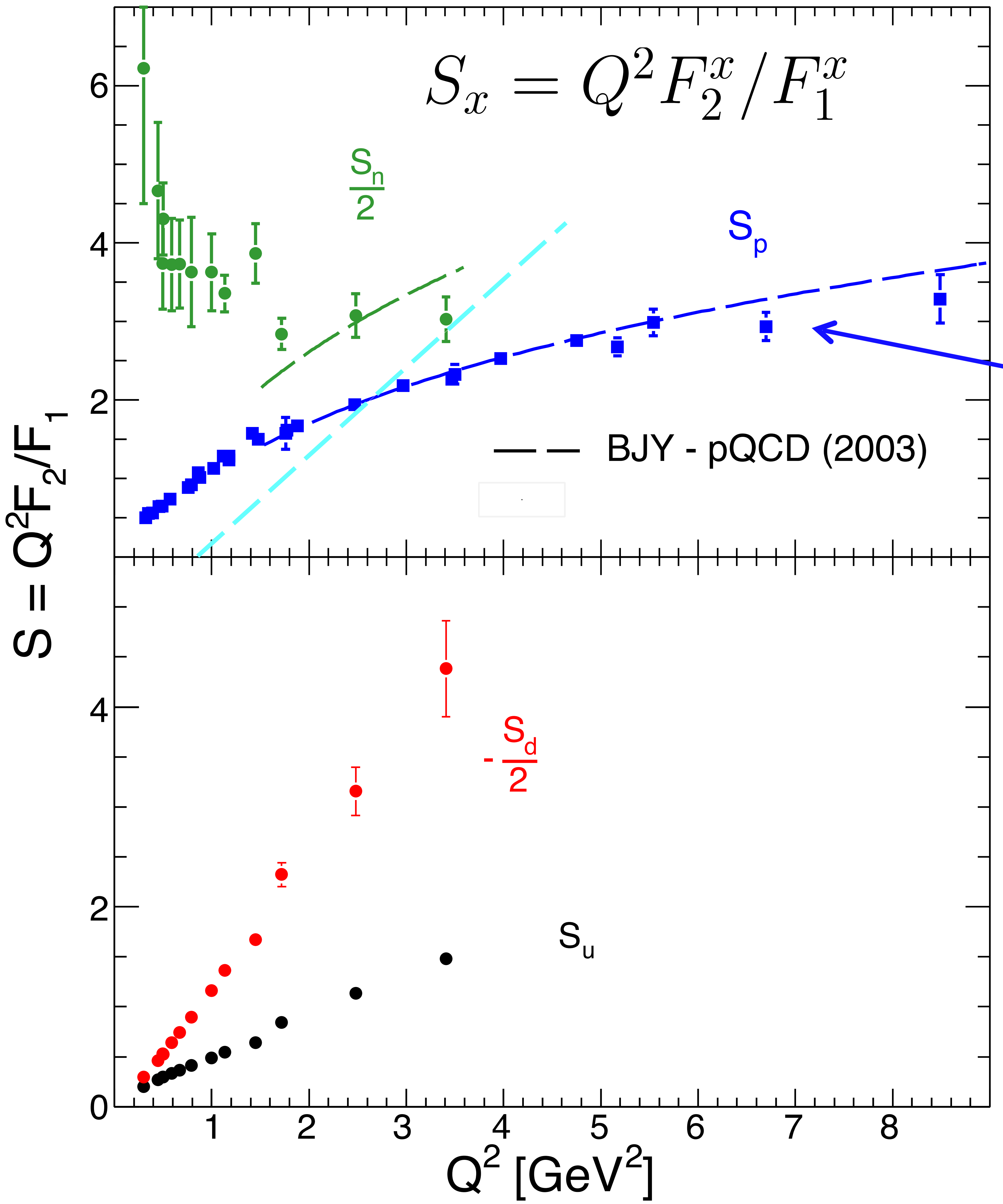

pQCD prediction for large Q^2:

$$S \to Q^2 F_2/F_1$$

pQCD updated prediction:

$$S \to \left[Q^2/\ln^2(Q^2/\Lambda^2)\right] F_2/F_1$$

Flavor separated contributions: the log scaling for the proton form factor ratio at few GeV^2 is likely “accidental”.

The lines for individual flavor are straight!

Cates, de Jager, Riordan, Wojtsekowski, Phys.Rev.Lett. 106 (2011) 252003

Q^2 dependence of Q^4F_1

$$F_{1p} = e_u\, F_1^u \; + \, e_d\, F_1^d \; + \, e_s\, F_1^s$$

$$F_{1n} = e_u\, F_1^d \; + \, e_d\, F_1^u \; + \, e_s\, F_1^s$$

$$F_1^u = 2F_{1p} + F_{1n} - F_1^s \qquad F_1^d = 2F_{1n} + F_{1p} - F_1^s$$

Assuming $\delta G^s_{E,M} \sim G_D \sim 0.048 \longrightarrow \delta(Q^4 F_1^u) \sim \pm\, 0.17$

$$F_1 = \frac{G_E + \tau G_M}{1+\tau} = \frac{G_E + 0.7 G_M}{1.7} \sim \frac{G_D}{1.7}$$

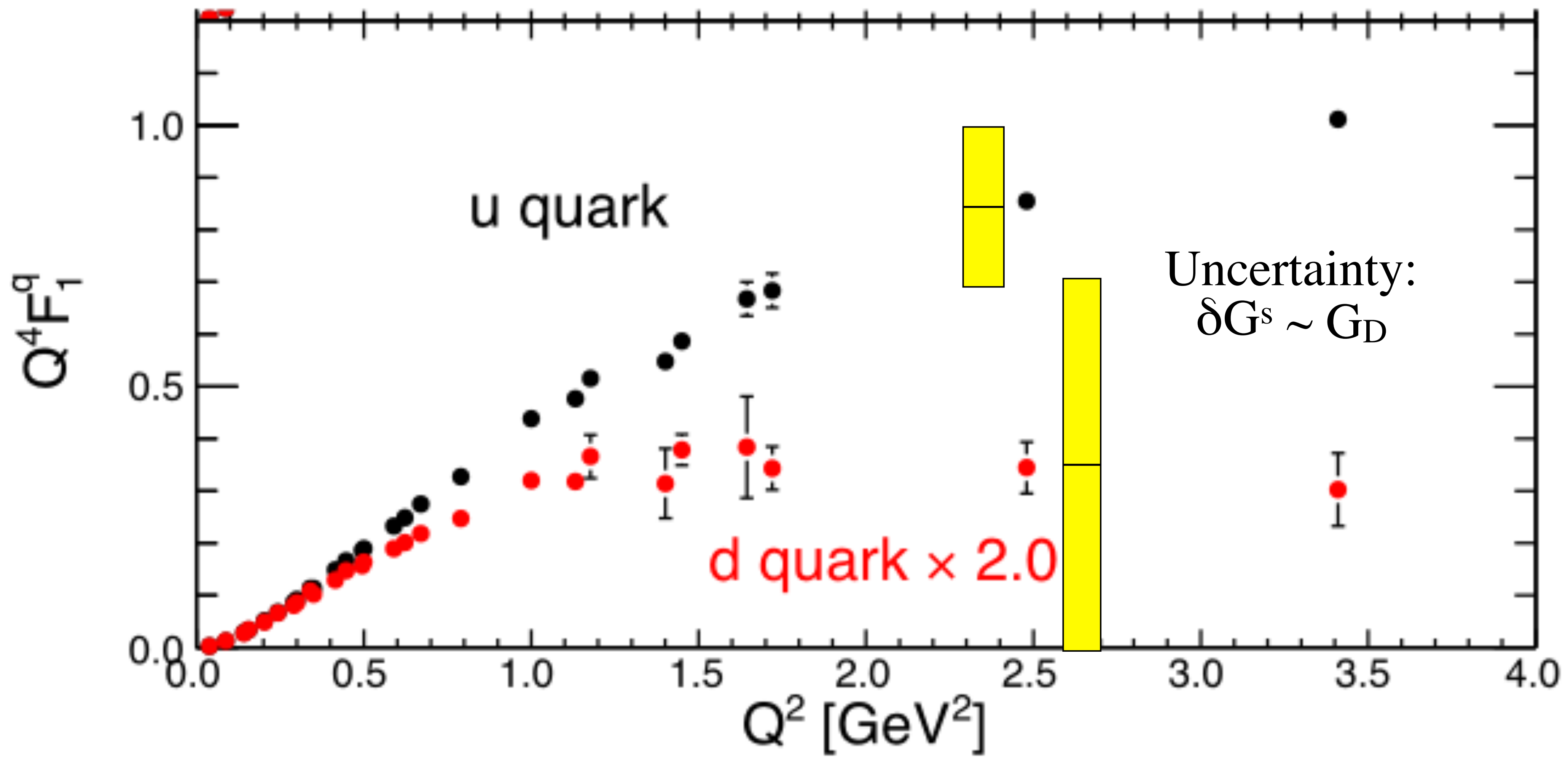

- Form factors are a crucial constraint on GPDs, and the flavor content must be understood
- Whatever future data informs GPDs and the nucleon femtography project, form-factors will remain an important constraint
- The quark flavor content of the form-factor must be known for this purpose!

Experimental concept

- Elastic kinematics between electron and proton
- Full azimuthal coverage, ~42 msr
- High resolution calorimeter for electron arm
- Angular correlation e-p

- 6.6 GeV beam
- Scattered electron at 15.5 degrees
- Scattered proton at 42.4 degrees
- 10 cm LH_2 target, 60 μA, $\mathcal{L}$ =1.6 x 10^{38} cm^{-2}/s

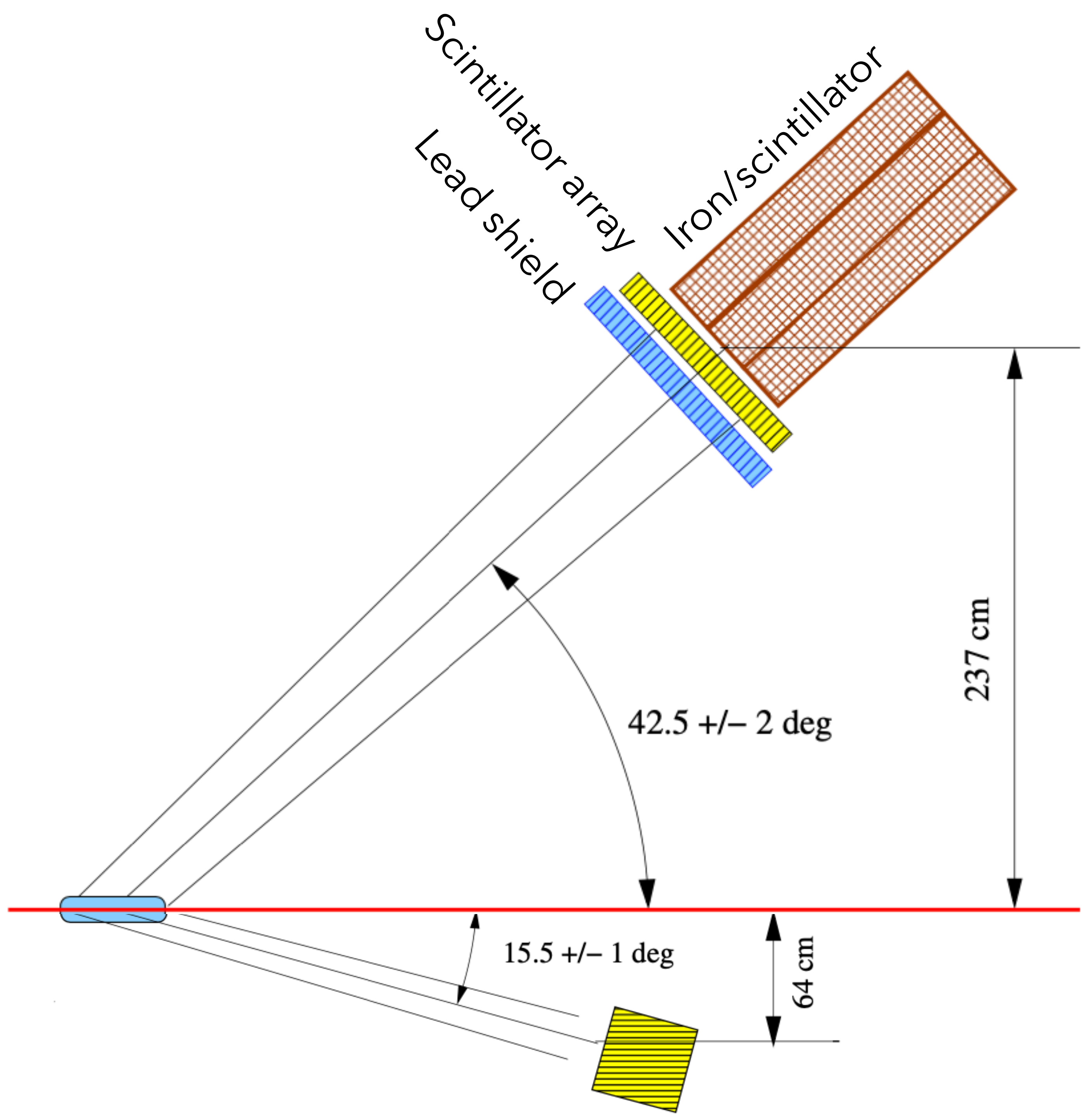

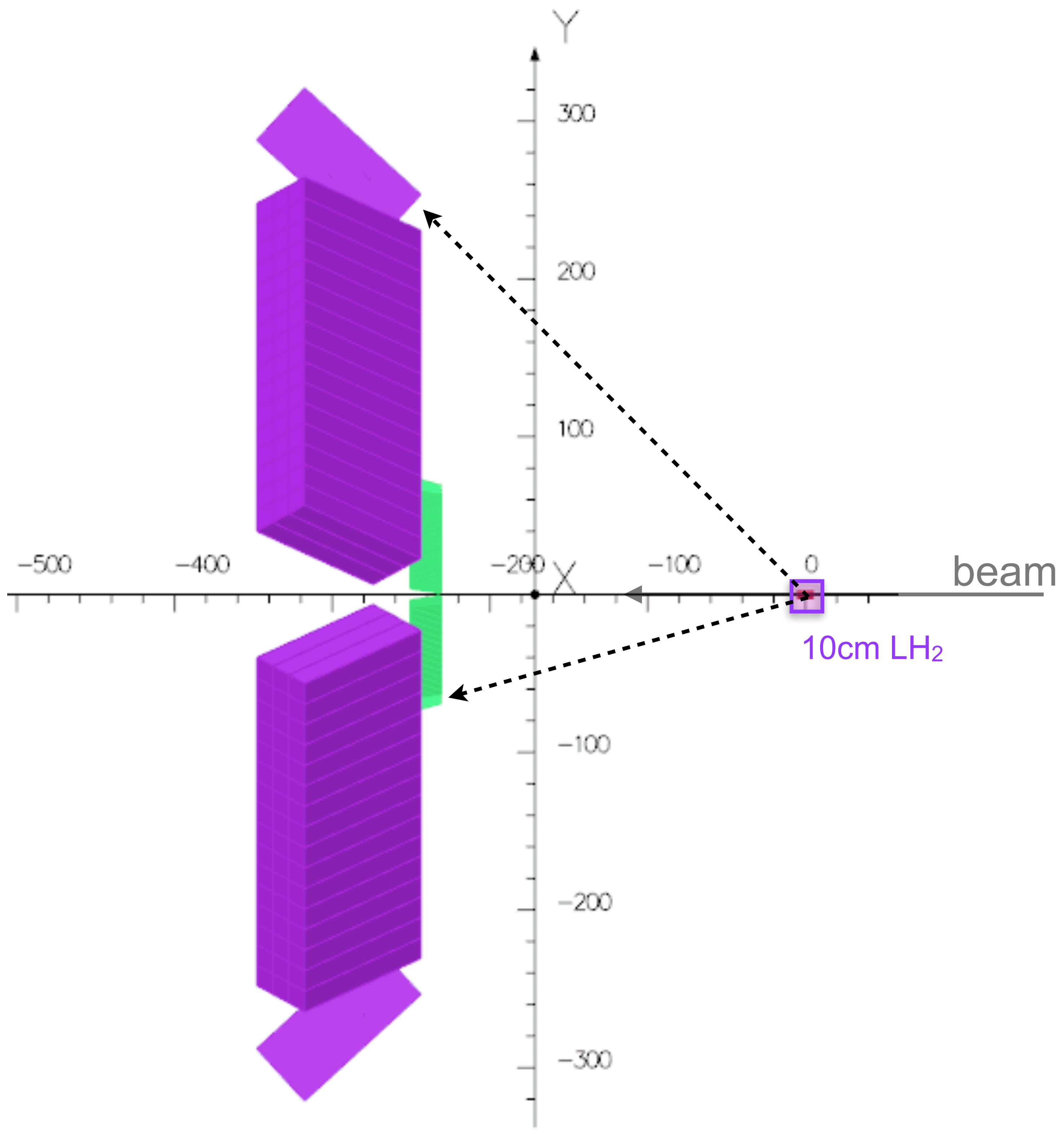

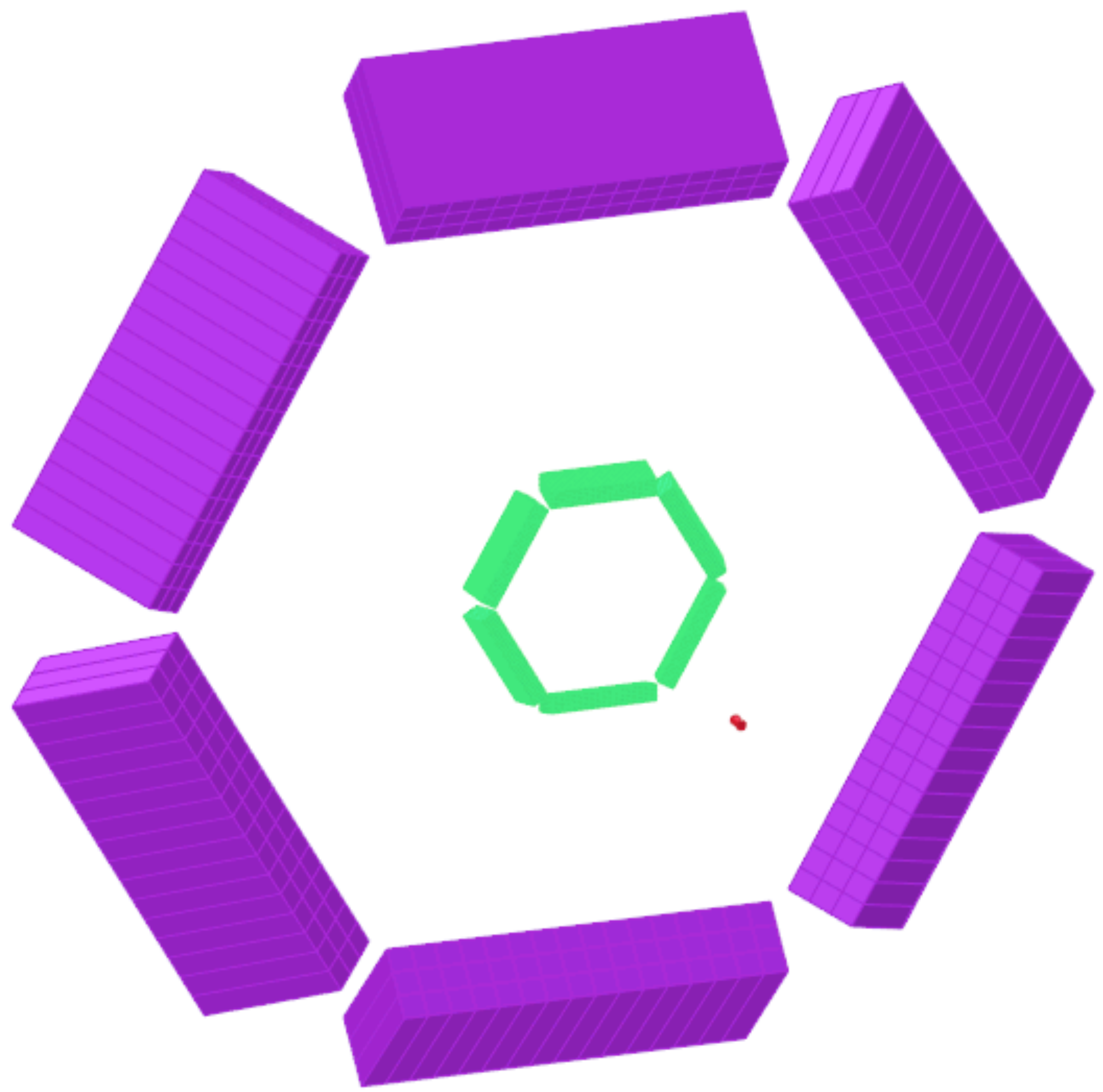

Detector System

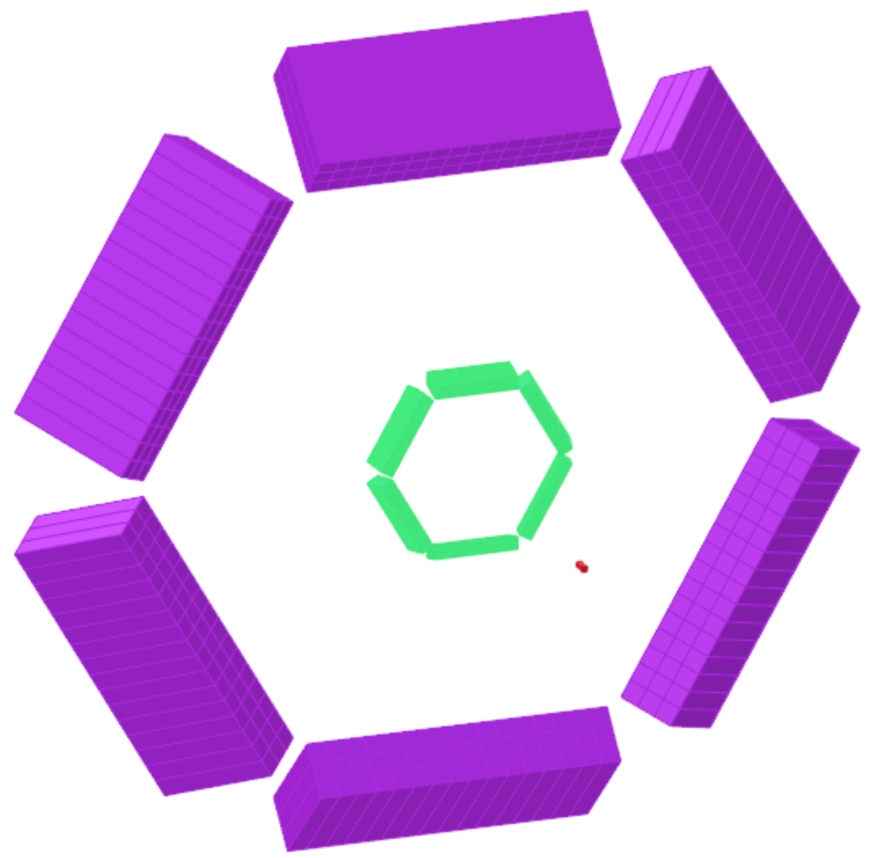

HCAL - hadron calorimeter

- Reassembled from detector elements from the SBS HCAL
- 288 blocks, each 15.5 x 15.5 x 100 cm^3
- iron/scintillator sandwich with wavelength shifting fiber readout

ECAL - electron calorimeter

- Reassembled from detector elements from the NPS calorimeter
- 1000 blocks, each 2 x 2 x 20 cm^3
- $PbWO_4$ scintillator

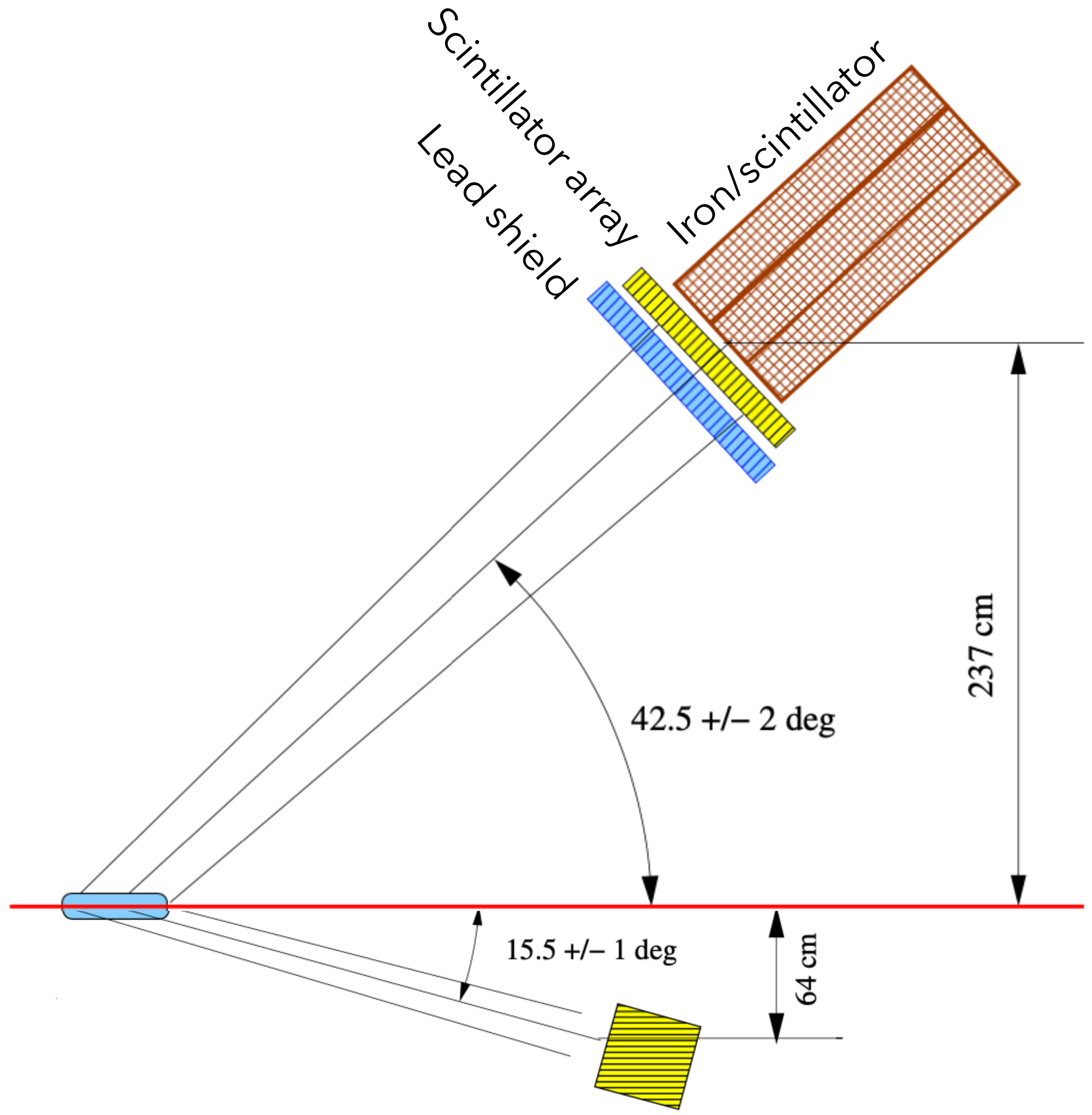

Scintillator array

- Used for improved position resolution in front of HCAL
- Not used to form trigger
- 7200 blocks, each 3 x 3 x 10 cm^3
- Lead shield in front (thickness to be optimized) to reduce photon load

Calorimeters reusing components

NPS electromagnetic calorimeter

- 1080 $PBWO_4$ scintillators, PMTs + bases
- will run in future NPS experiment

SBS hadronic calorimeter

- 288 iron/scintillator detectors, PMTs + bases
- Already in use with SBS

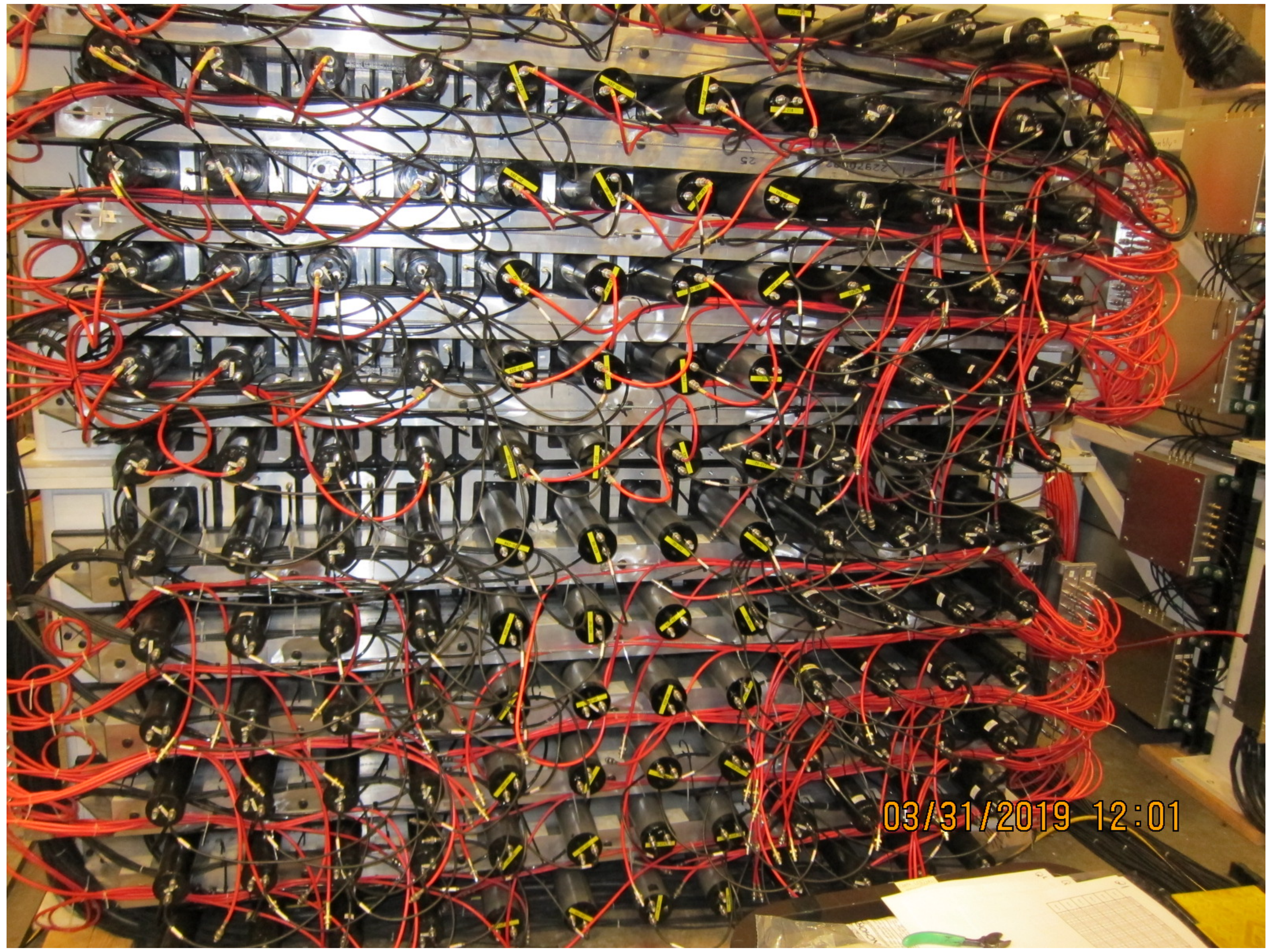

Scintillator Array

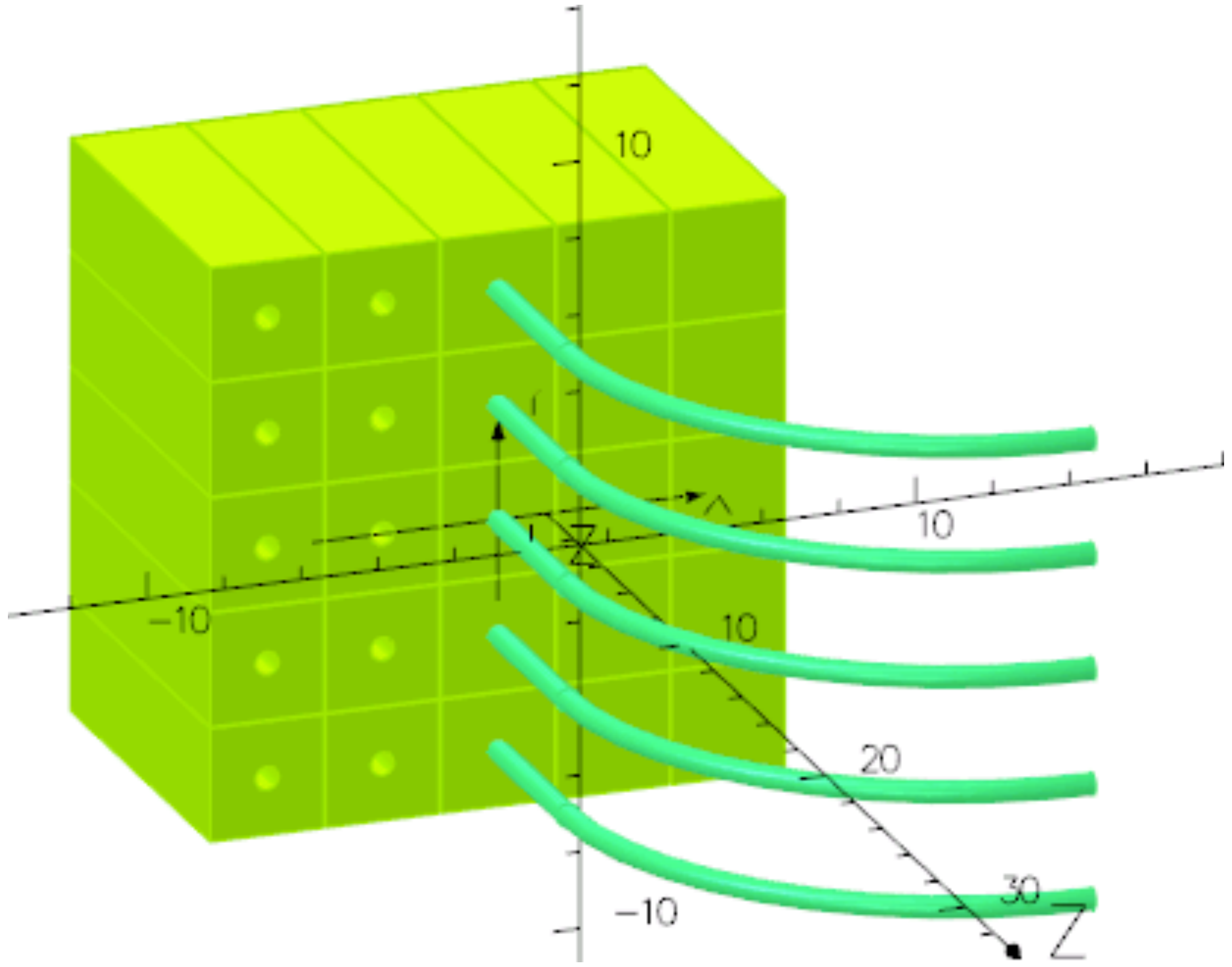

- New detector, must be built for this experiment
- Extruded plastic scintillator block
- Readout with wavelength-shifting fiber
- Each fiber read by pixel on multi-anode PMT
- Originally proposed for 2x2 cross-section, but 3x3 provides sufficient resolution
- 7200 blocks, each 3 x 3 x 10 cm^3

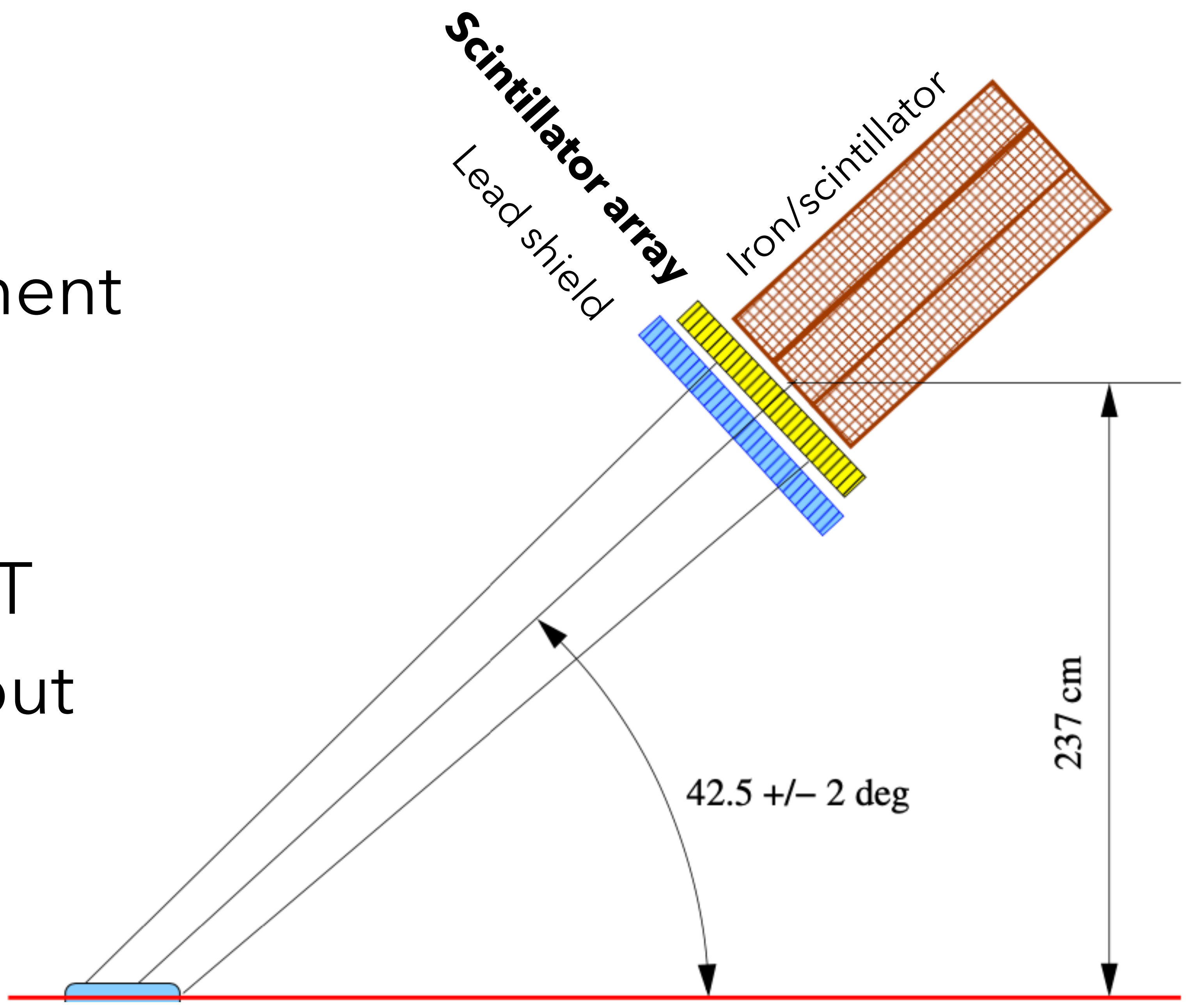

Design matches scintillator array built for GEP

- 2400 elements, 0.5 x 4 x 50 cm^3
- Already built, will run next year

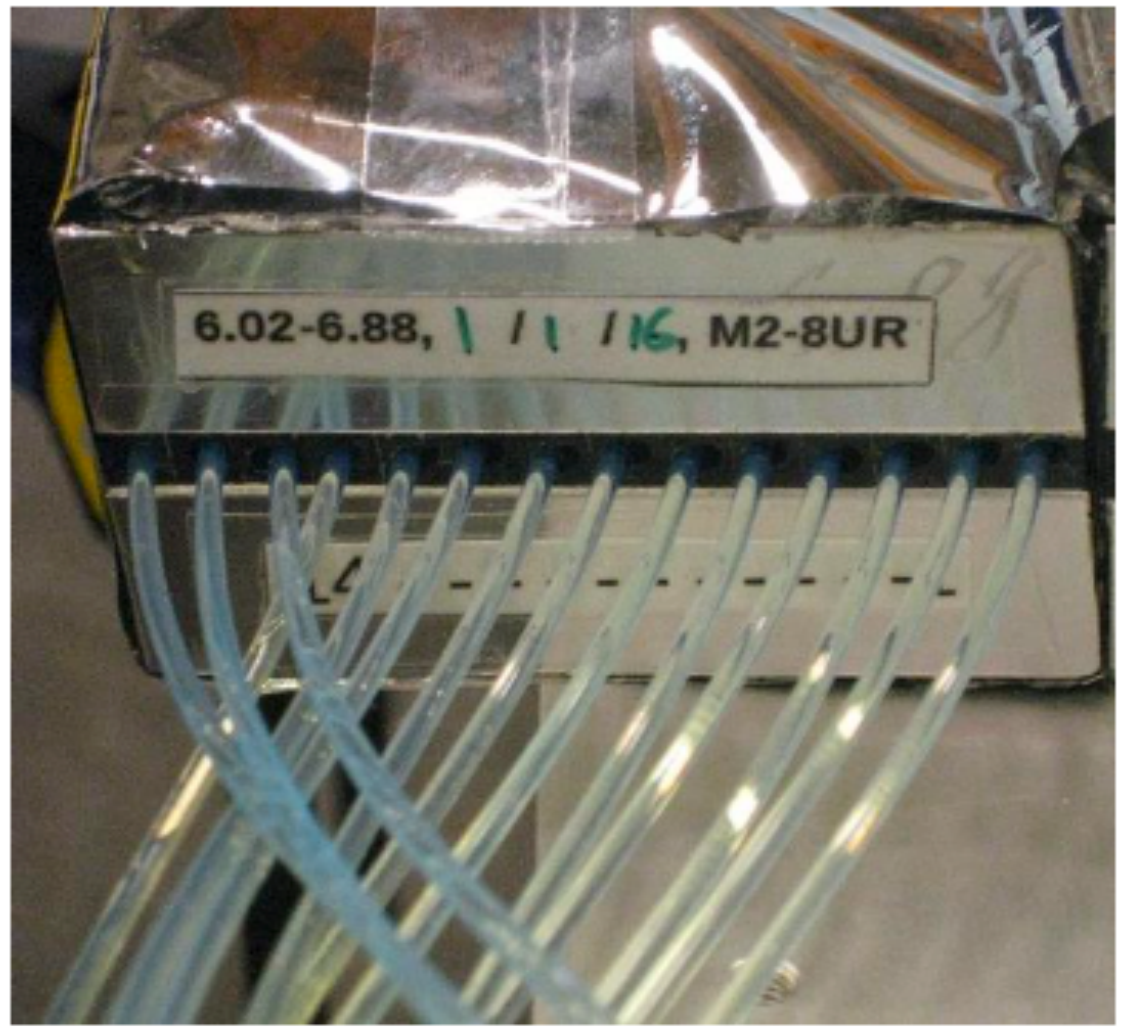

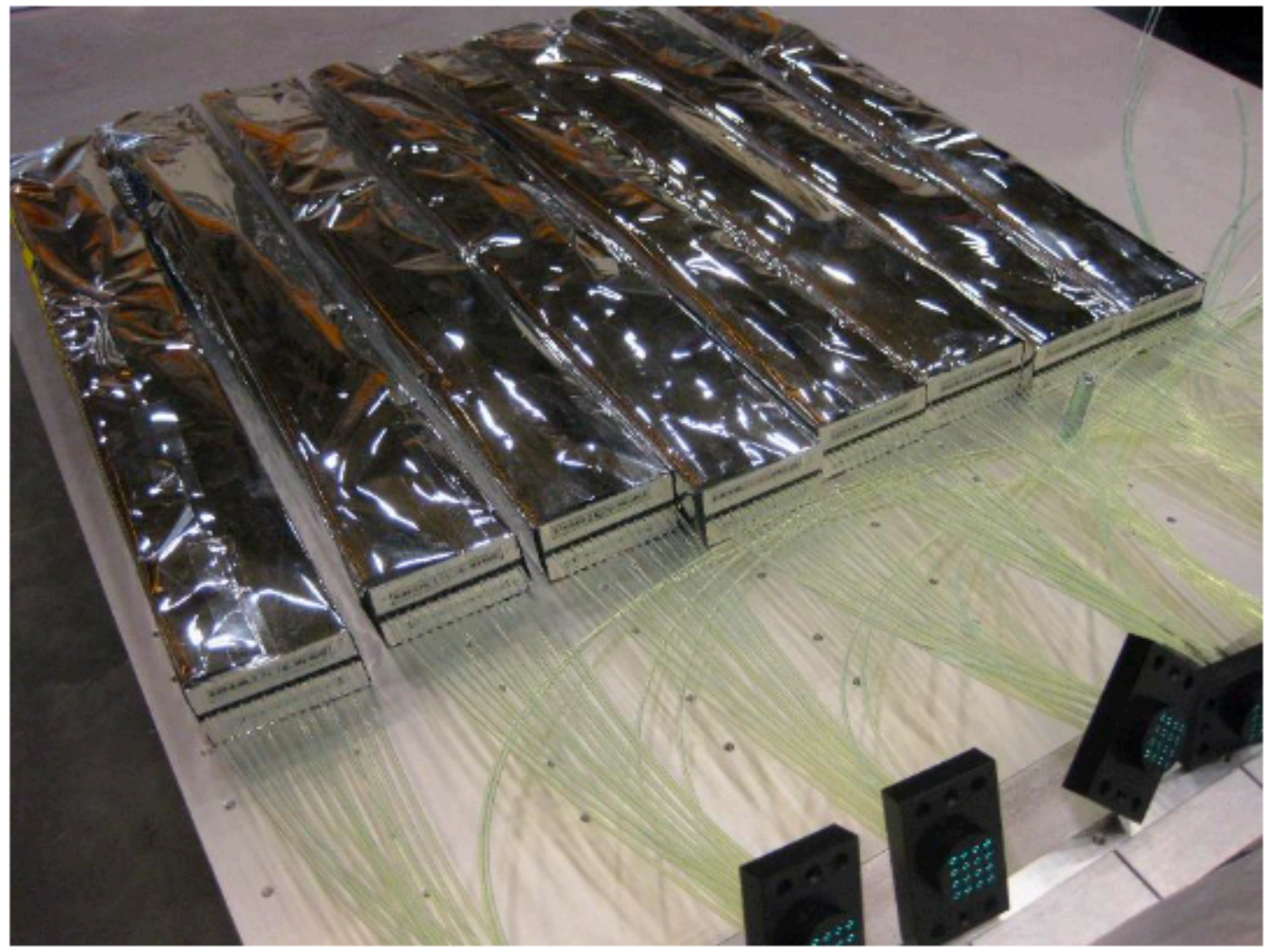

Scattering chamber

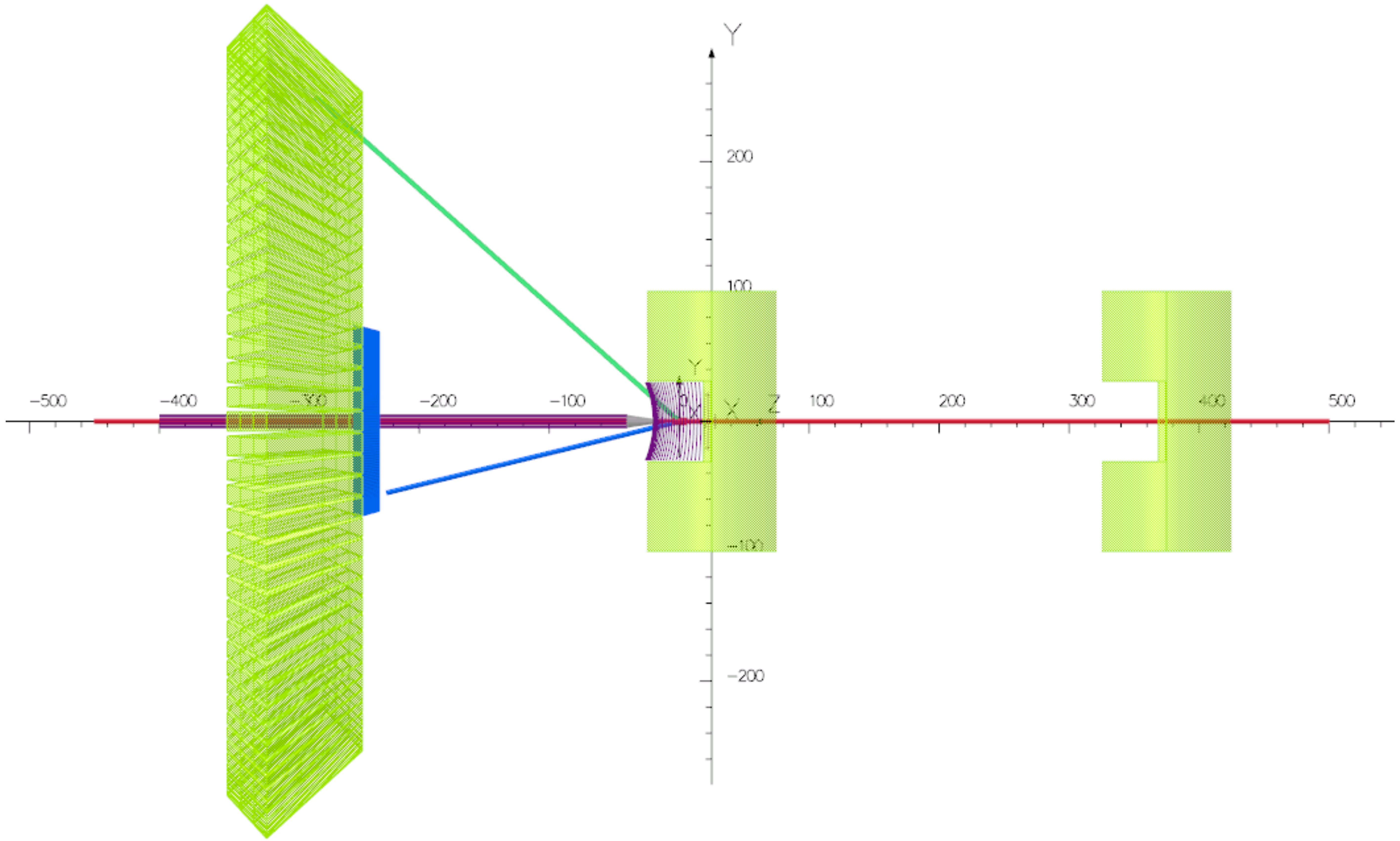

3.5 m target shift downstream from pivot due to space limitation on the SHMS side
A standard cylindrical scattering chamber with <1cm window to pass 15° electrons and 45° protons is sufficient

ECAL and HCAL rates

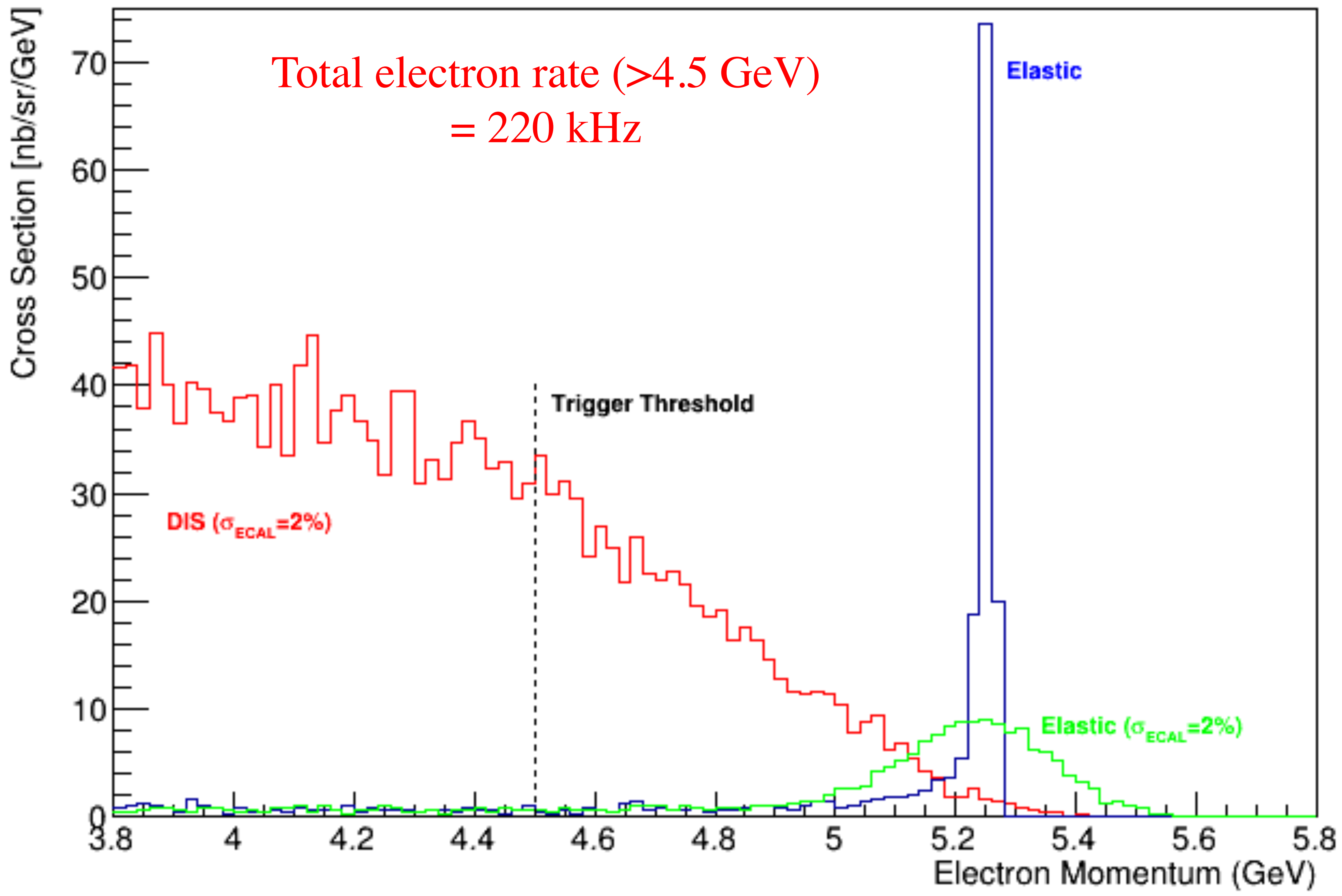

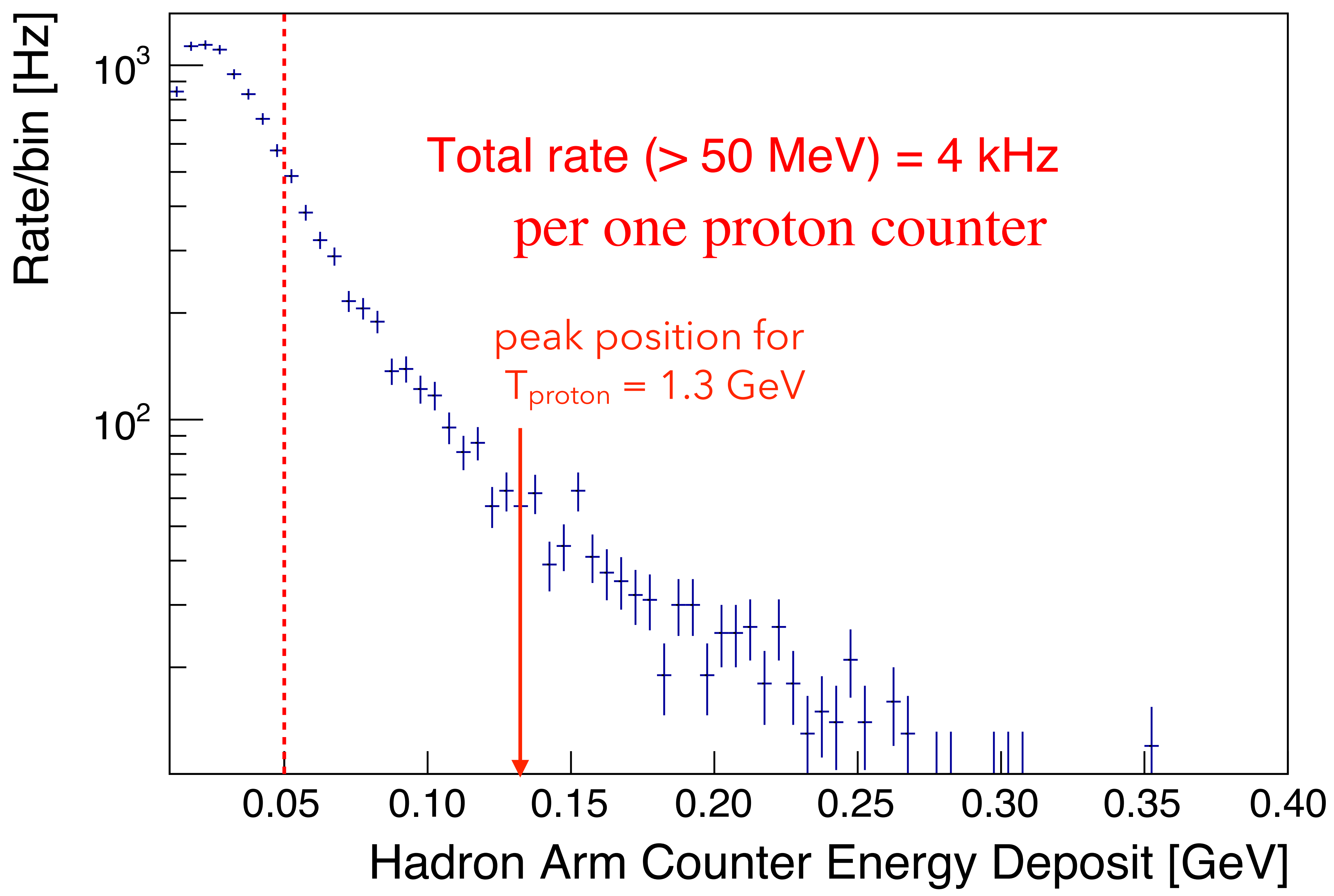

Inelastic:

E_e> 4.5 GeV rate is 220 kHz

E_e> 4.8 GeV rate is 85 kHz

E_e> 5.0 GeV rate is 18 kHz

E_e> 5.2 GeV rate is 2.8 kHz

Triggering and Analysis

Grouping into "subsystems" for energy threshold and coincidence triggering

- each polar column of detectors, overlapping with neighbors
- sum amplitude with conservative coincidence timing window
- compare to conservative energy threshold
- trigger when complementary (ECAL and HCAL) subsystems are both above threshold

Electron subsystems

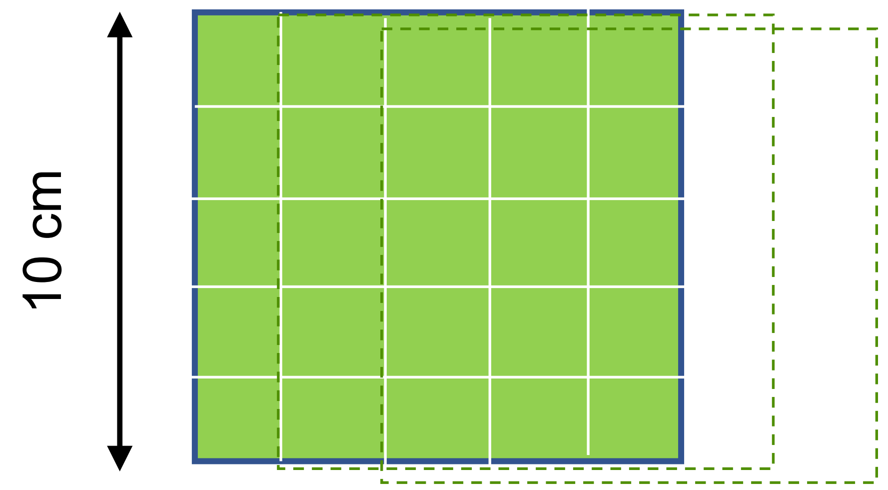

- 1000 $PbWO_4$ crystals
- 2x2x20 cm^3
- 5x5 grouping for subsystem
- 200 overlapping subsystems

Proton subsystems

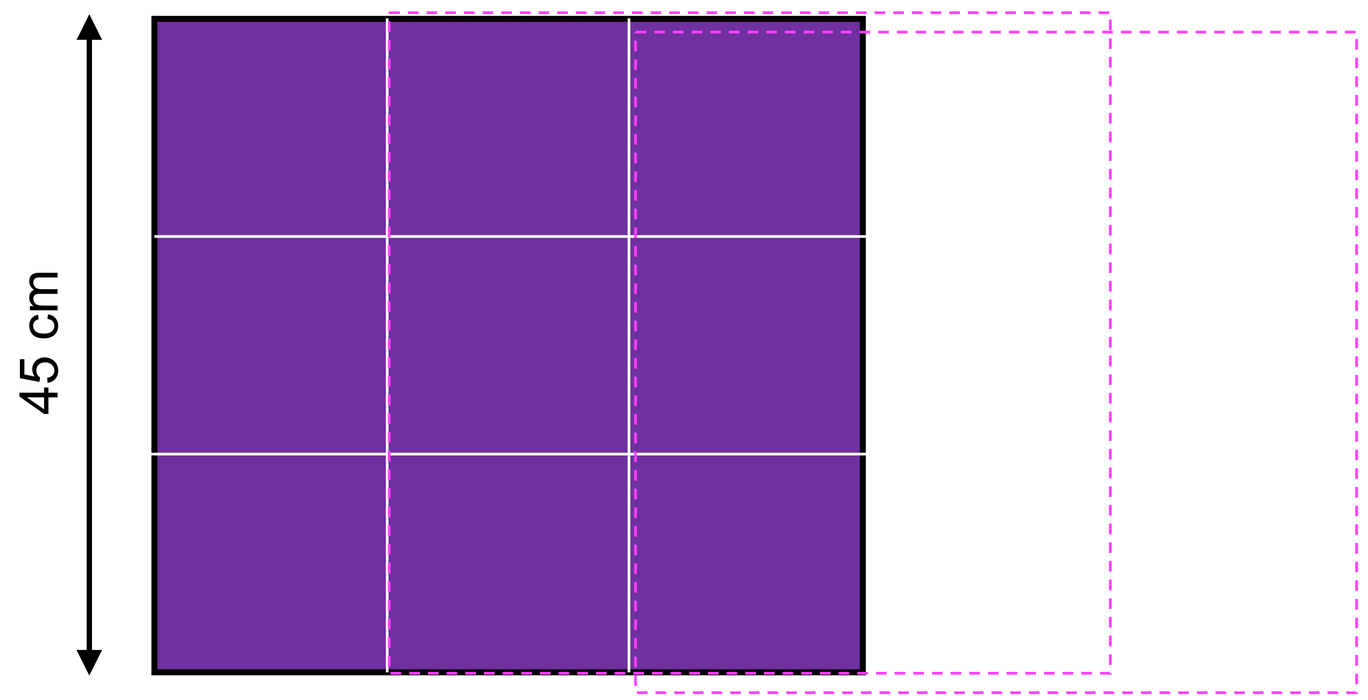

- 288 iron/scintillators
- 15.5x15.5x100 cm^3
- 3x3 grouping for subsystem
- 96 overlapping subsystems

Rates and Precision

Beam and target: 60 uA on 10 cm LH_2 => luminosity is 1.6×10^{38} cm^{-2}/s

Trigger (online)

- Elastic 37 kHz signal in full detector
- Inelastic (pion production) coincidence trigger rate ~10 kHz
- Accidental coincidence rate < 0.2 kHz
  - ~60 kHz total singles rate in ECAL > 5 GeV energy threshold
  - ~1.2MHz total singles rate in HCAL > 50 MeV energy threshold
- Temporal coincidence cut 40ns
- ~50 kHz total coincidence trigger rate

Offline analysis

- clustering, scintillator array to improve geometric cuts, tighter acceptance and ECAL cut, 4ns timing
- Accepted elastic signal reduced to 14 kHz - production statistics
- Inelastic (pion production) <0.5%, accidentals $<1\times10^{-5}$ due to higher E cut, angular precision

Beam polarization 85%

30 days runtime ⟶ Raw asymmetry statistical precision $\delta(A_{raw}) \sim 5$ ppm

⟶ $A_{PV} = -150 \pm 6.2$ ppm

Fast Counting DAQ

Readout for fast counting is now very common challenge and enabled by new, and now common, technologies. In particular, SOLID will face this challenge in measurement of PV-DIS, and this experiment will be an important testing ground for precise asymmetry measurements.

Concept very similar to the HPS DAQ, used in 2019 or NPS DAQ:

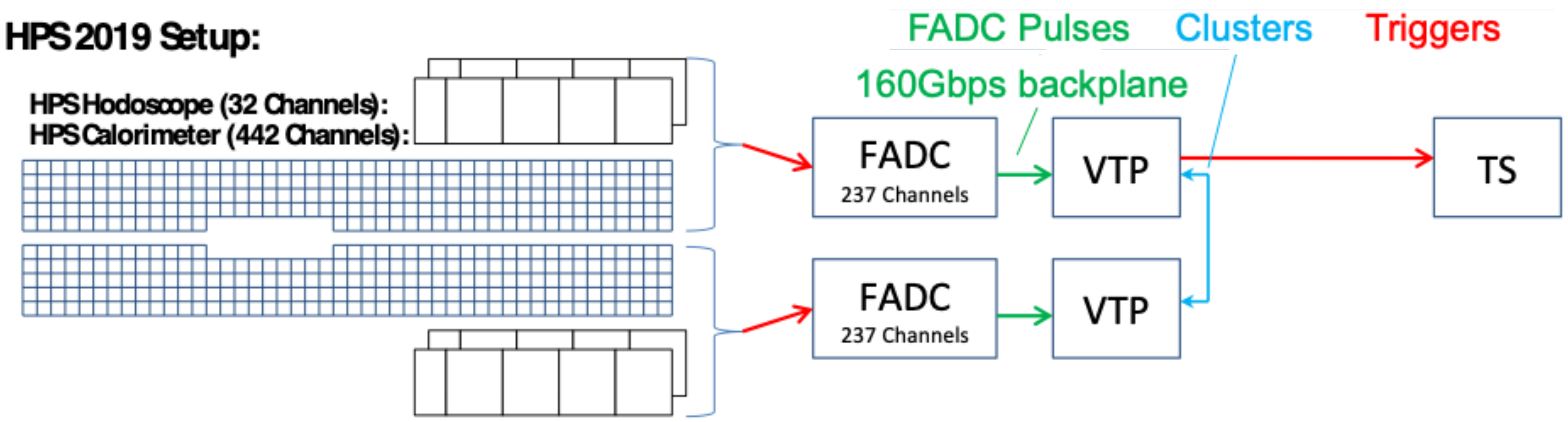

JLab **FADC250** for HCAL and ECAL readout
Provides the pulse information for a fast, "deadtime-less" trigger

VTP (VXS Trigger Processor)
Clusters in time, sums over subsystems, finds ECAL+HCAL coincidence

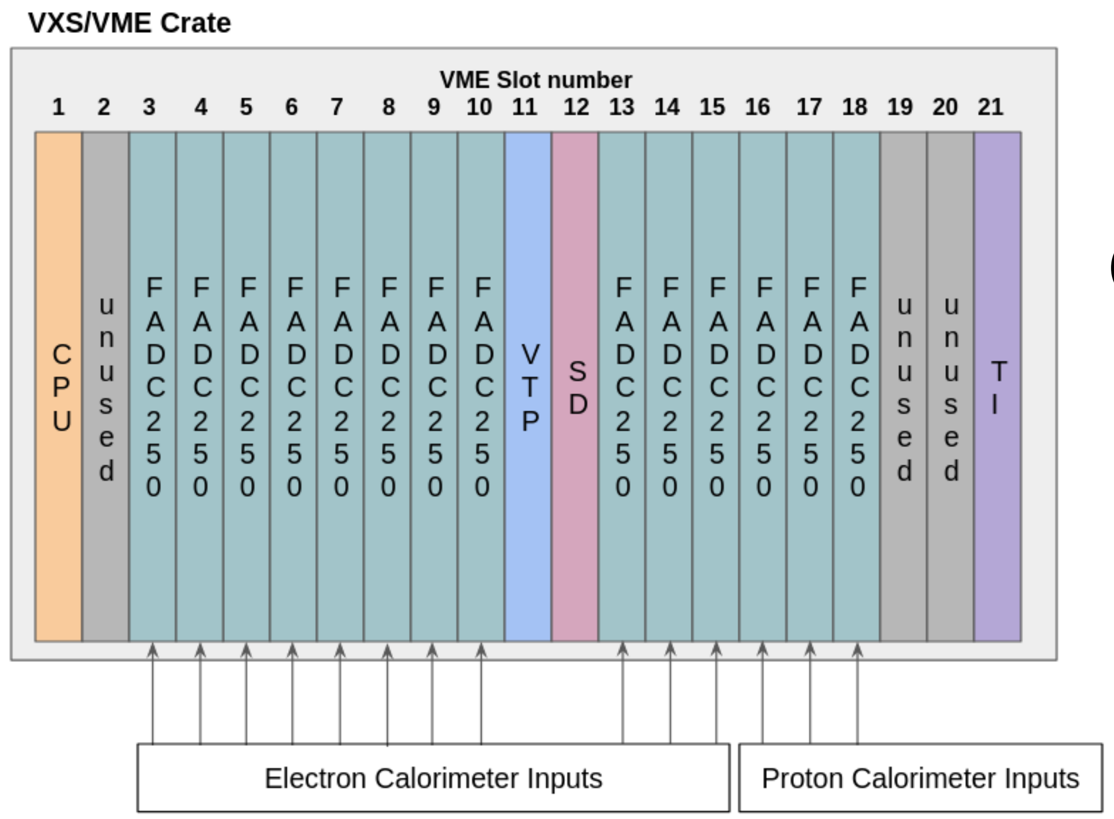

One VXS crate will handle one sixth of ECAL + HCAL, also provide external trigger for ScintArray pipelineTDC readout

Expect ~50kHz total, ~250 Mb/s data rate, distributed over 6 separate crates

Error budget

quantity	value	contributed uncertainty
Beam polarization	$85\% \pm 1.5\%$	1.8%
Beam energy	$6.6 +/- 0.003$ GeV	0.1%
Scattering angle	$15.5° \pm 0.03°$	0.4%
Beam asymmetries	<100 nm,<10 ppm	0.2%
Backgrounds	$< 0.5\%$	0.5%
G_E^n/G_{Dipole}	0.41 ± 0.04	0.6%
G_E^p/G_{Dipole}	0.75 ± 0.02	0.5%
G_{Mn}/G_{Dipole}	1.01 ± 0.02	1.7%
G_M^p/G_{Dipole}	1.08 ± 0.01	0.9%
$G_A^{Zp}/G_{\text{Dipole}}$	-0.15 ± 0.02	0.9%
Total systematic uncertainty:		3.0%

(Polarimetry precision better than 1% has been achieved for multiple experiments)

or 4.5 ppm

Statistical precision for A_{PV}: 6.2 ppm (4.1%)

There is also an uncertainty from radiative correction, is small except for a dominant “anapole” piece.

If the anapole uncertainty is not improved, this would contribute at additional 4.1 ppm (2.7%) uncertainty

Projected result

δ A_{PV} = ± 6.2 (stat) ± 4.5 (syst)

$\delta\left(G_E^s + 3.1 G_M^s\right)$ = ± 0.013 (stat) ± 0.010 (syst) = 0.016 (total)

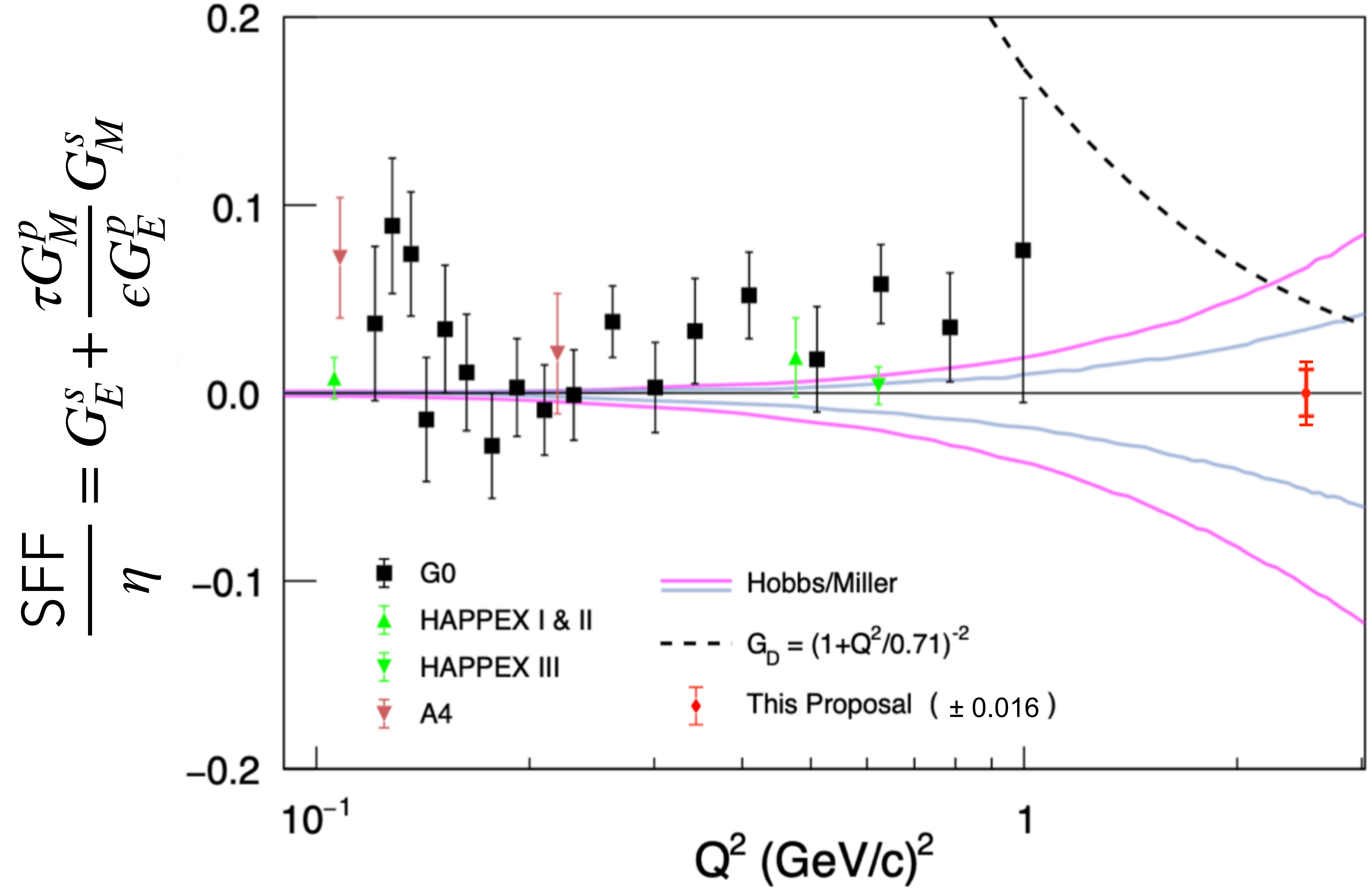

If $G_M^s = 0$, $\delta G_E^s \sim 0.016$, (about 34% of G_D)

If $G_E^s = 0$, $\delta G_M^s \sim 0.0052$, (about 11% of G_D)

The proposed measurement is especially sensitive to G_M^s

The proposed error bar reaches the range of lattice predictions, and the empirically unknown range is much larger.

An update of Fig 4 from the proposal

Summary

Kin. #	Procedure	beam, μA	time days
C1	Beam parameters	1-70	1
C2	Detector calibration	10	2/3
C3	Dummy target data	20	1/3
C4	Beam polarimetery	1-5	2
C5	Pion yield study	20	1
E1	A_{PV} data taking	60	30
	Total requested time		35

- 10+ years after the last sFF searches were performed, a new experiment is proposed for much higher Q^2, motivated by interest in flavor decomposition of electromagnetic form factors
- Projected accuracy at 11% of the dipole value allows high sensitivity search for non-zero strange form factor.
- The proposed error bar is in the range possibly suggested by lattice predictions, and significantly inside the range from the simple extrapolation from previous data
- These results will be crucial to support the interpretation of the nucleon form-factors as constraints on GPDs
- We request PAC approval of 35 days of beam time (60 uA on 10 cm long LH2 target).

Backup slides

Strawman Budget

scattering chamber	Vacuum chamber – large pipe+window	*tbd*
	Scattering chamber shift	*tbd*
ECAL/HCAL support	ECAL support	200k
	ECAL cooling	*tbd*
	HCAL support	200k
	FADCs (exist for HCAL/ECAL)	*exists*
	VTP, DAQ crates + CPUs + data links	*mostly exists*
Scintillator array construction ~7200 elements	Scint array maPMTs (125x64 channels)	250k
	Scint array extruded scint	50k
	Scint array support	100k
Scintillator array readout	Lead shield for scint array	*tbd*
	Scint Array TDC + front end	250k
	Total, a bit over	$1050k

The most expensive components (calorimeter detectors) largely exist

Pion electro-production contribution

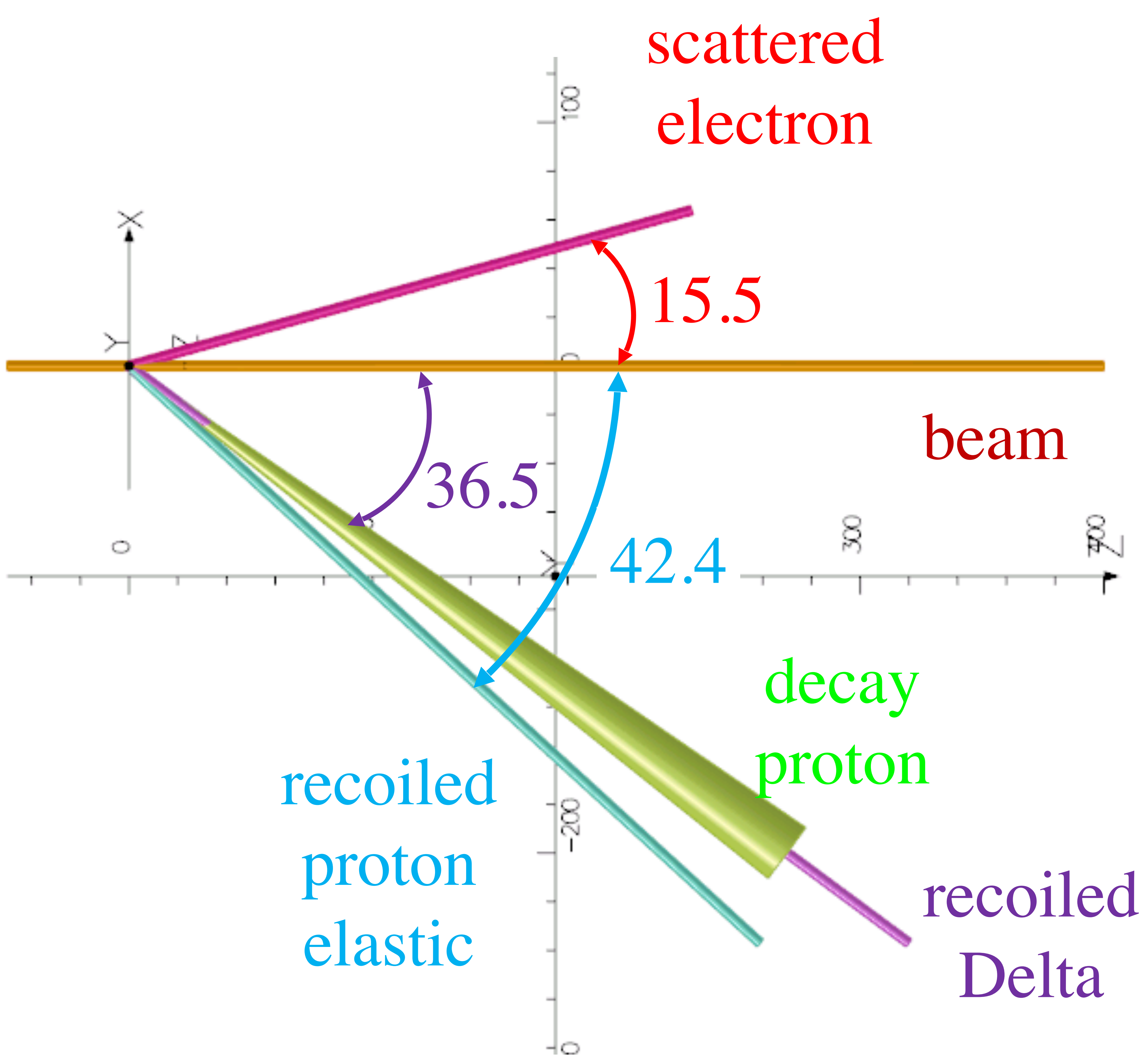

Pion production rate
above offline ECAL threshold ~ 3 kHz

Angular separation:
$6°$ (at Δ peak)
$2.8°$ (at π threshold)

Angular resolution ~$0.6°$ (polar)

Proton cone around Δ recoil, projected to polar angle:
RMS = $2°$ (so, 2.5σ separation for Δ)

Fraction to elastic rate < 0.3%

Pion-production background rate calculation

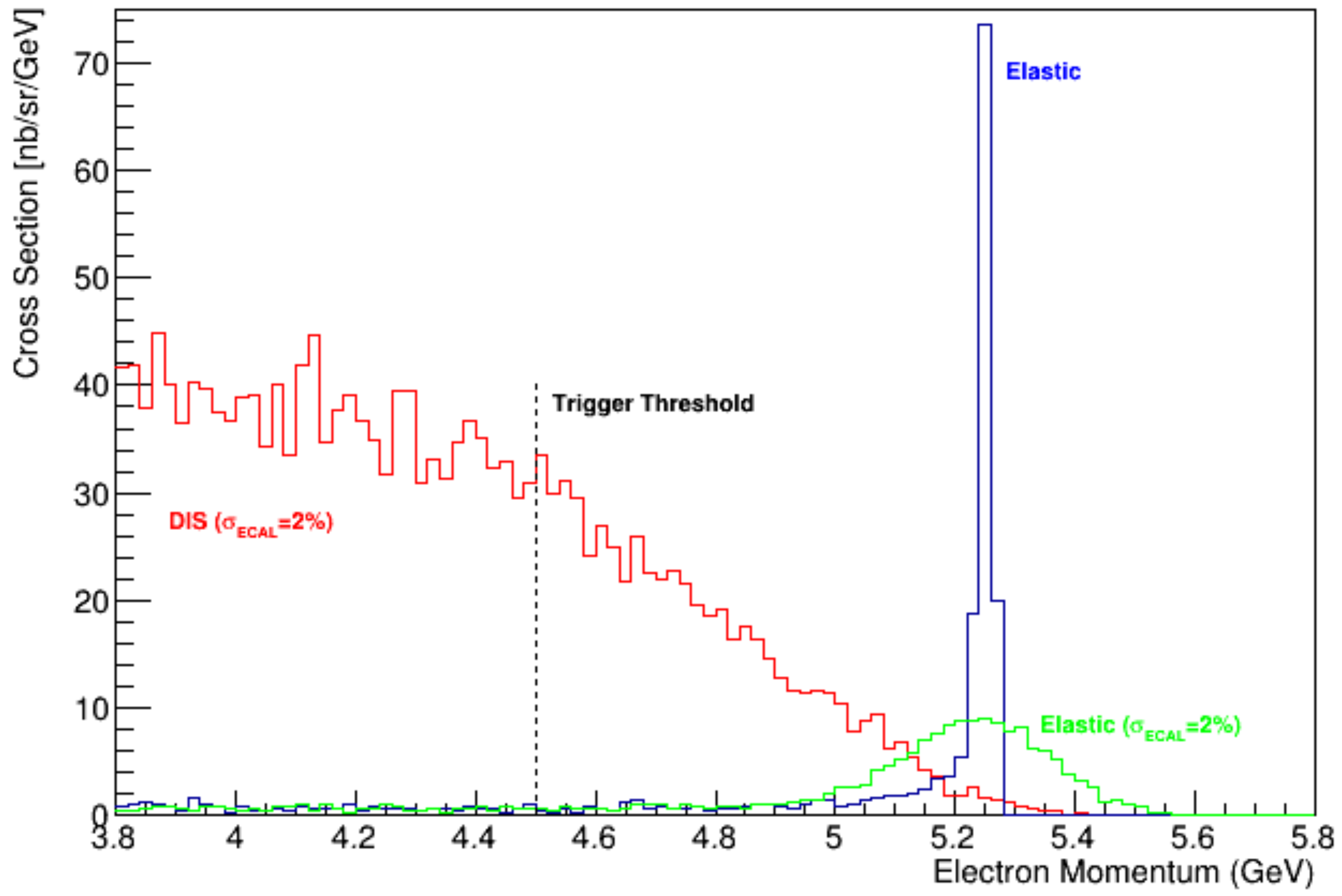

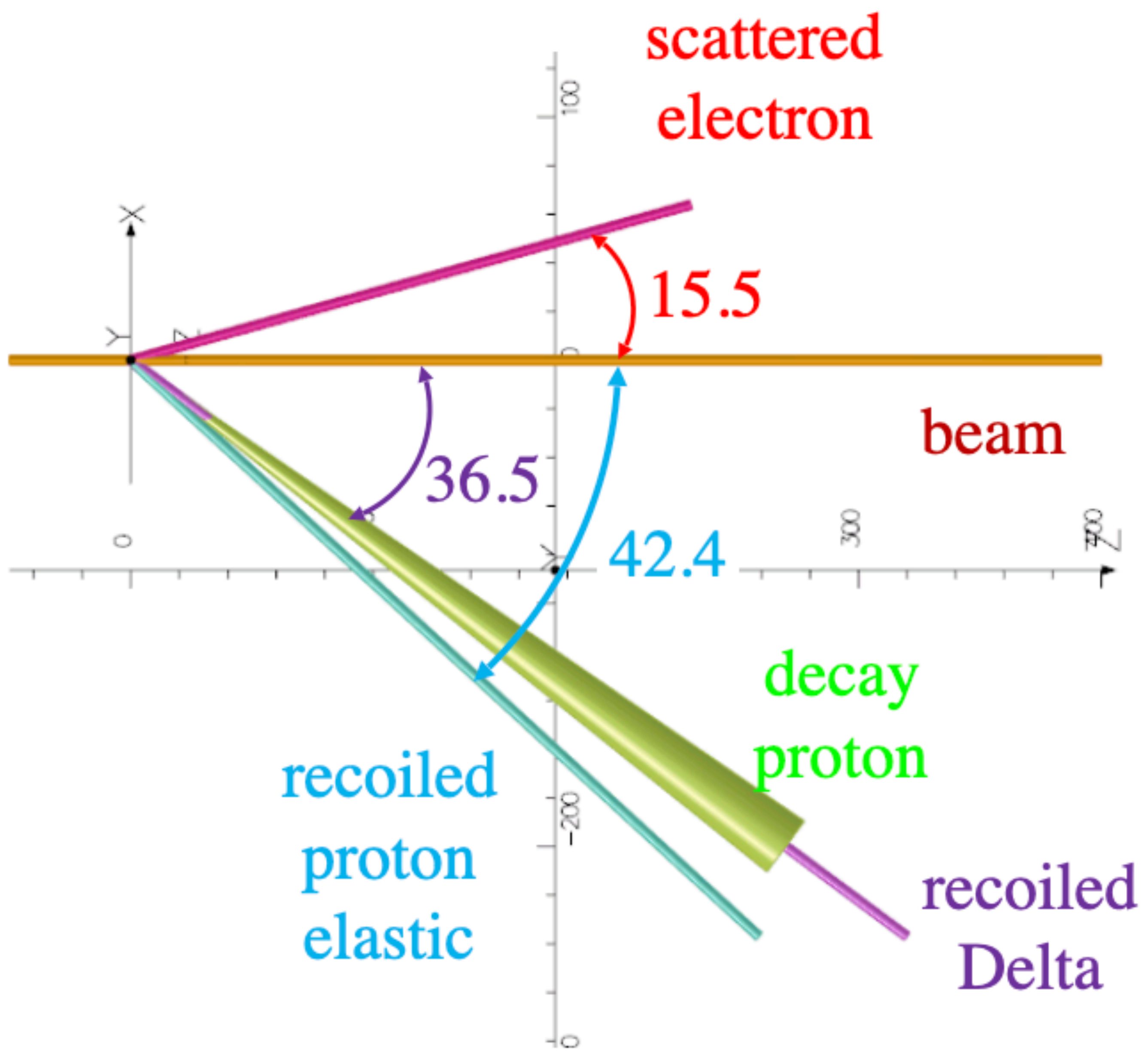

Online:
Electron arm single rate for $E_{e'}$ > 5 GeV is ~18 kHz
about 50% enters HCAL acceptance as coincidence, so ~10kHz

Offline:
electron arm single rate for E> 5.2 GeV is ~3 kHz
high angular resolution excludes >99%

Accidental background coincidence calculation

Online:
Electron arm single rate for $E_{e'} > 5$ GeV is ~18 kHz : 18 Hz/detector, 450 Hz/subsystem
Proton arm single rate 1.2 MHz : 36 kHz/subsystem
Time window in the trigger 40 ns -> total accidental coincidence rate ~ 0.2 kHz

Offline:
Time window in analysis 4 ns
Accidental rate is 0.02 Hz in high resolution part of solid angle
of sub-system where elastic rate is 70 Hz.

Next reduction due to higher threshold in offline analysis:
electron arm single rate for E> 5.2 GeV is 3 kHz-> extra factor of 5

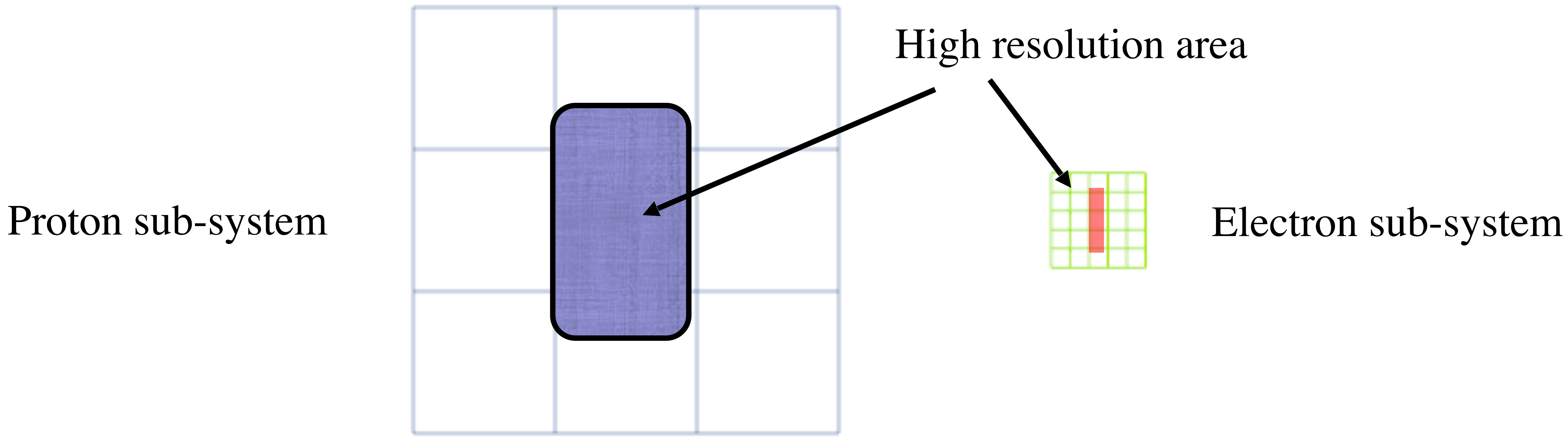

Single pion photo-production contribution

pion (ECAL) - proton (HCAL) coincidence

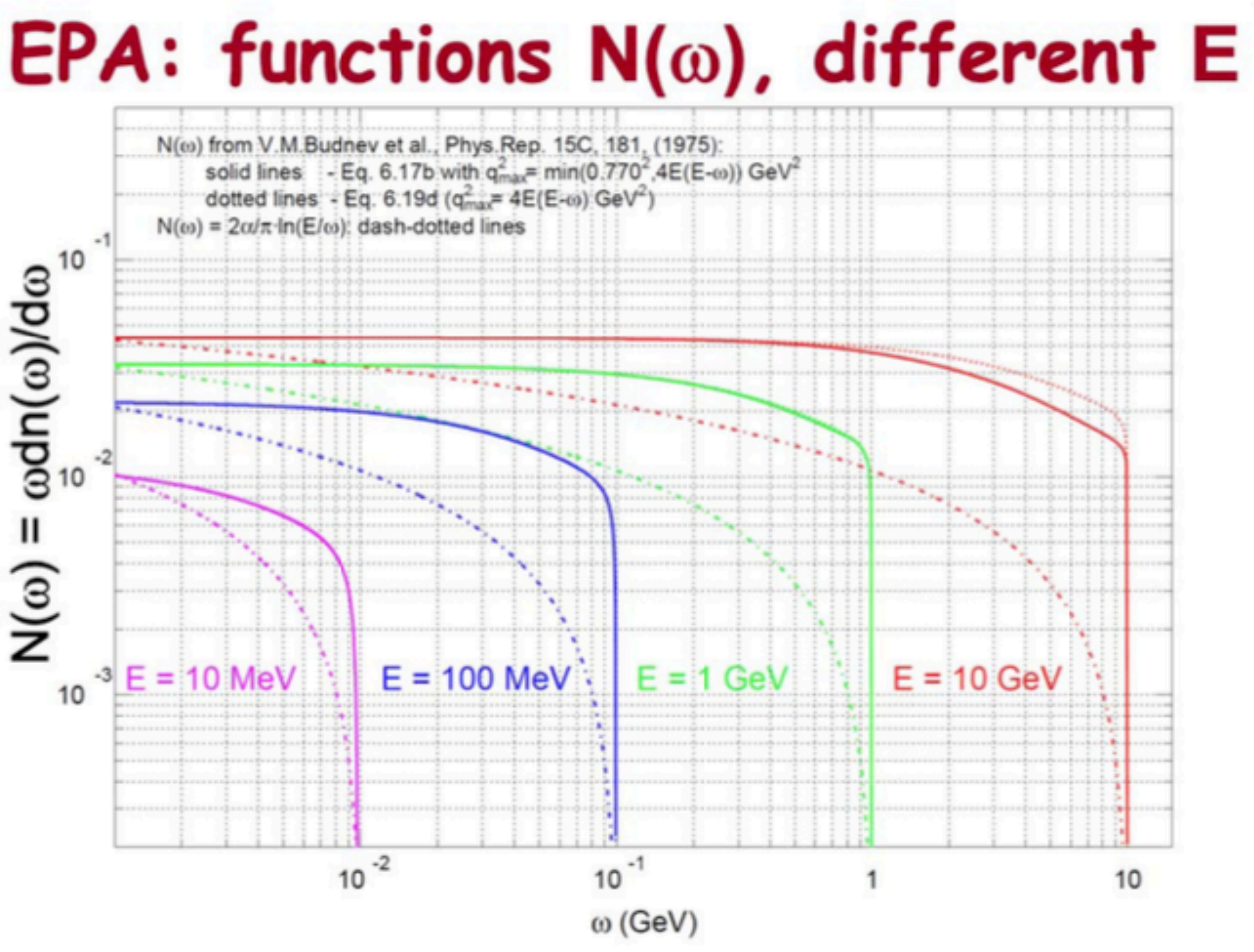

$$\frac{d\sigma}{dt}_{\gamma n\to\pi^- p} = 1.7\times 0.83\times\left(\frac{10}{s\,[\mathrm{GeV}^2]}\right)^7 (1-z)^{-5}(1+z)^{-4}\ \left(\mathrm{nb/GeV}^2\right),$$

$$N_{\pi^- p} = \frac{d\sigma}{dt}_{\pi^- p}\frac{p^2_{\pi^-}}{\pi}\Delta\Omega_{\pi^-} f_{\pi^- p}\left[\frac{\Delta E_\gamma}{E_\gamma}\frac{t_{rad}}{X_o}\mathcal{L}_{en}\right]$$

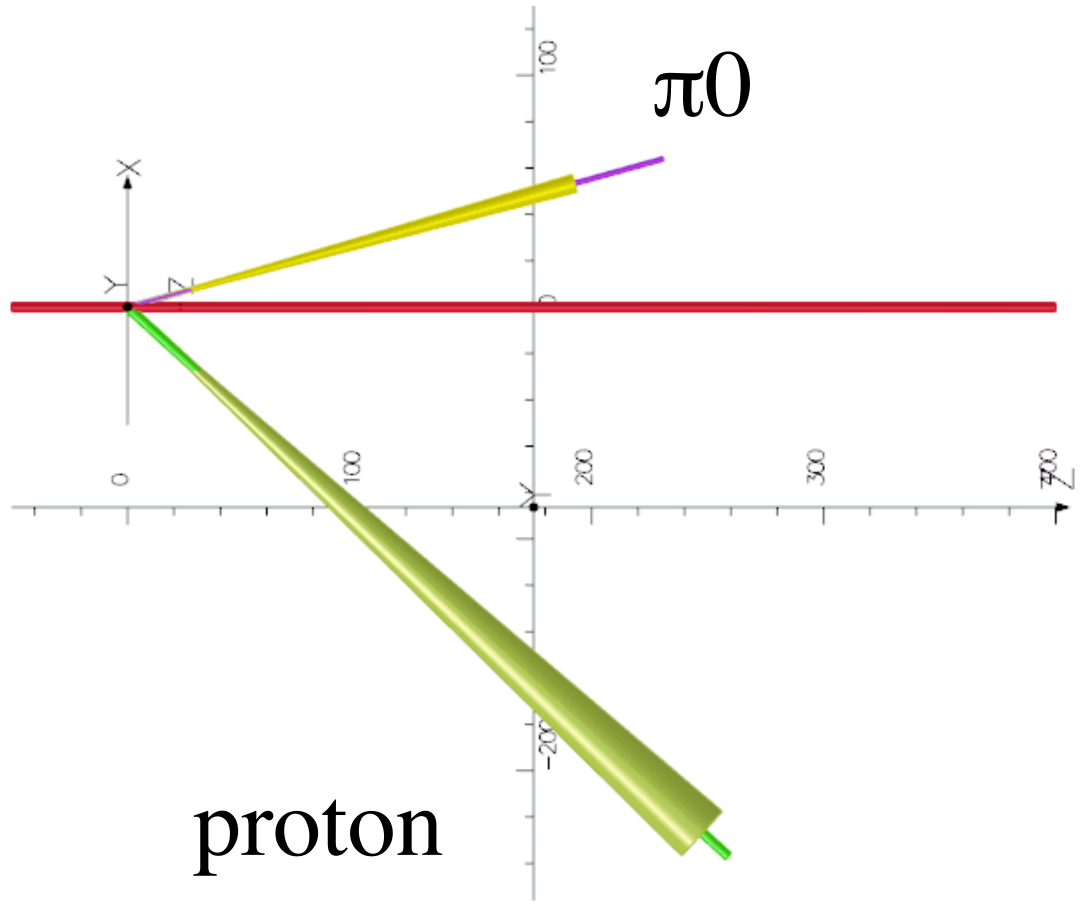

Near the end point the photon yield is going down ⟶ reduction in factor t_{rad}/X_0

$f_{\pi-p}$ takes care of the cuts on angular correlation/resolution

Remaining single pion events < 0.2% of elastic rate

Use of radiator for single pion production estimate

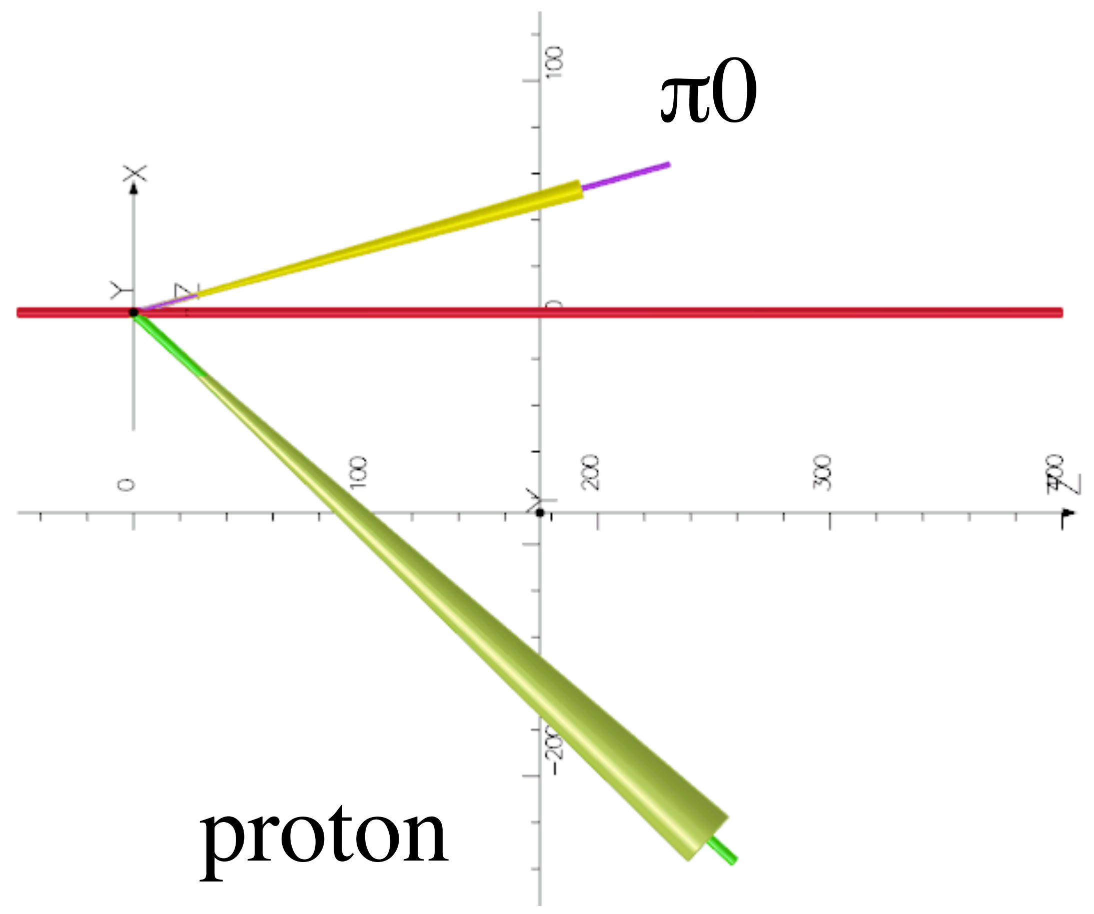

Pion Photoproduction near photon endpoint dominates pion-proton coincidence
Photoproduction will be increased by large factor (~4) using radiator
This can be well estimated, provides a check of accepted factor of this background

6% radiator was used for several WACS experiments in Halls A and C

Background events from Al

- assumed 5 mils target cell windows, ~5% nucleon
- Fermi energy smears quasi-elastic scattering distribution, about 80x suppression
- B/S < 0.1%
- a dummy target will be used to check accepted rate

Coincidence Cuts

Electron subsystems

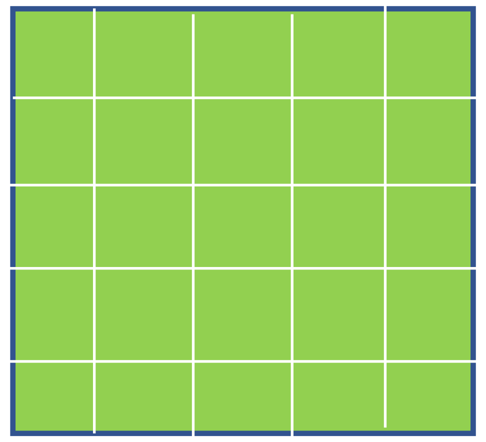

5x5

Proton subsystems

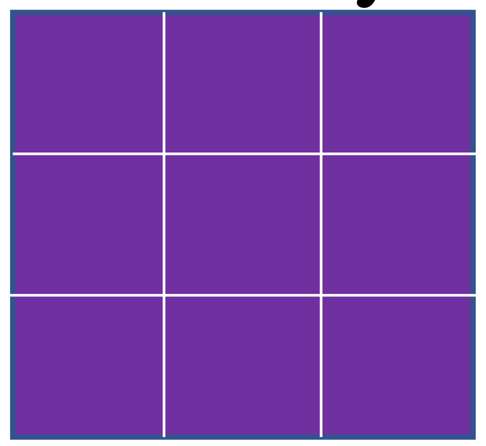

3x3

Online

- Elastic 37 kHz signal in full detector
  - 18 kHz total rate DIS in e-arm
  - 1.2 MHz (proton arm)
- 5x5(electron) & 3x3(proton) subsystem counters
- Temporal coincidence cut 40ns
- Energy cut 5GeV
- Accidental < 0.2 kHz

Electron subsystems

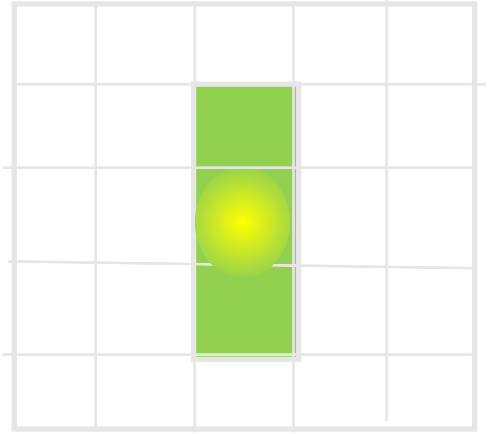

3x1

Proton subsystems

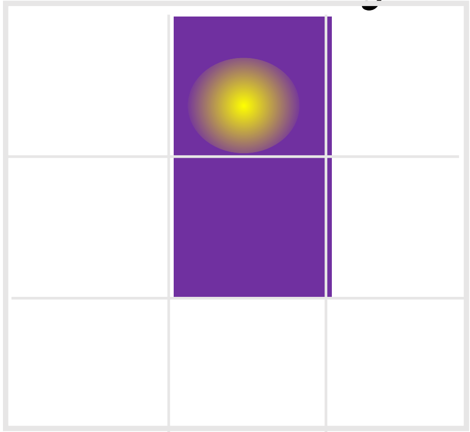

2x1

Offline

- Elastic 14.4 kHz signal
- use center of cluster to better define azimuth of each hit
  - e-arm select 3x1 subsystems hi-res area
  - p-arm 2x1 subsystems hi-res area
- reduce temporal coincident cut to 4ns
- sharpen geometric/angular cuts
- Energy cut 5.2GeV
- Ratio real/accidentals 1.6×10^5

NPS Calorimeter DAQ

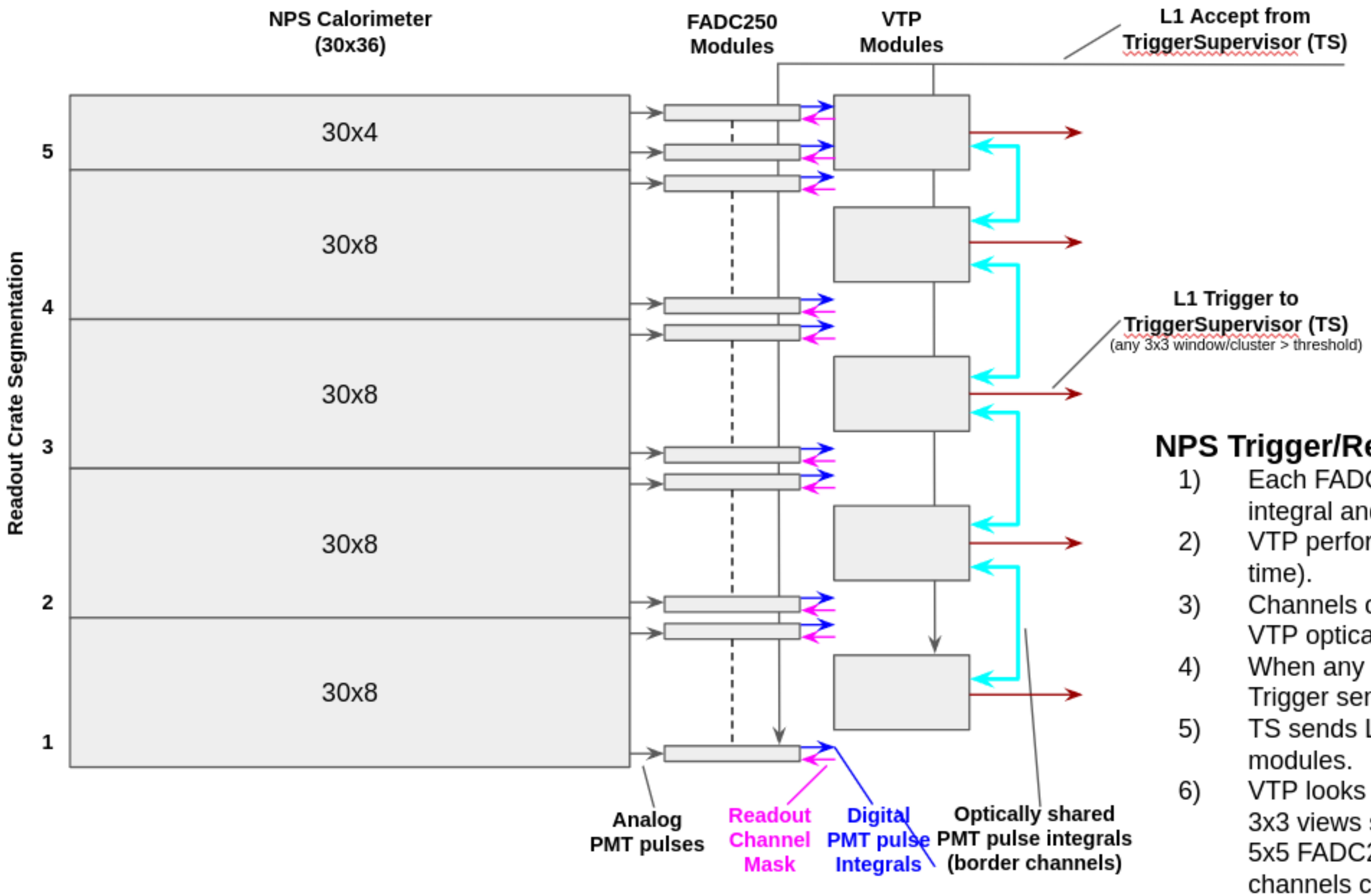

NPS Trigger/Readout Operation:

1) Each FADC digitized each crystal and reports integral and time to VTP for trigger processing.
2) VTP performs 3x3 clustering (in both space and time).
3) Channels on border of crates are shared using VTP optical connections
4) When any 3x3 view of calorimeter > threshold L1 Trigger sent to TS
5) TS sends L1 accept back to all FADC250 and VTP modules.
6) VTP looks back fixed amount of time to see which 3x3 views satisfied trigger and send corresponding 5x5 FADC250 channel mask to FADCs to readout channels centered on 3x3 trigger cluster
7) FADC250 wait for channel mask after L1 accept and readout raw waveforms with no zero suppression for the specified channels

JLab Fast Electronics FADC250 / VTP

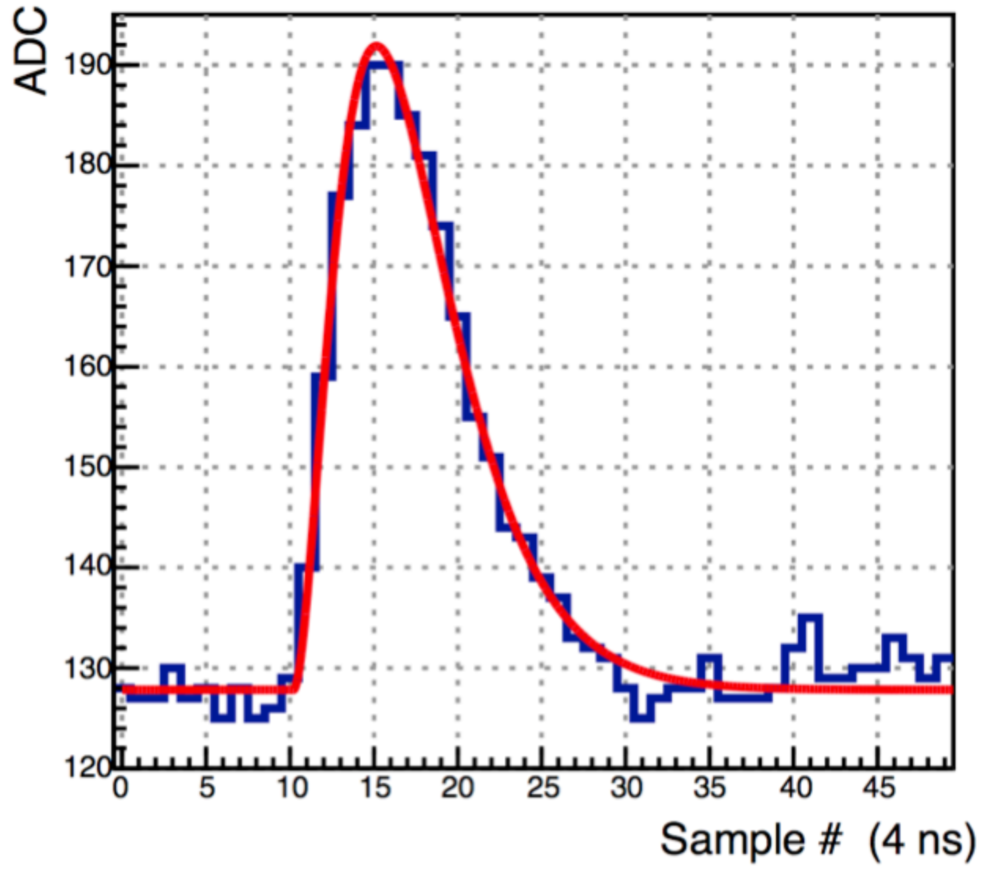

JLab FADC250 for HCAL and ECAL readout
Provides the input for a fast, "deadtime-less" trigger

FADC Trigger path: Pulse detector/integrator

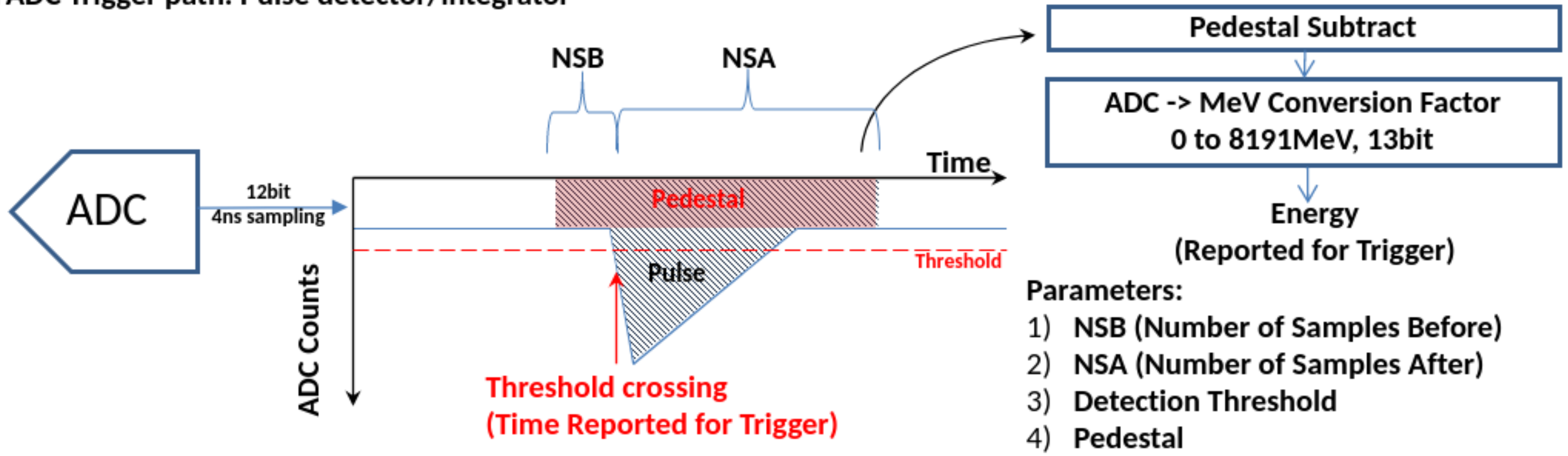

Parameters:
1) **NSB (Number of Samples Before)**
2) **NSA (Number of Samples After)**
3) **Detection Threshold**
4) **Pedestal**
5) **Gain**

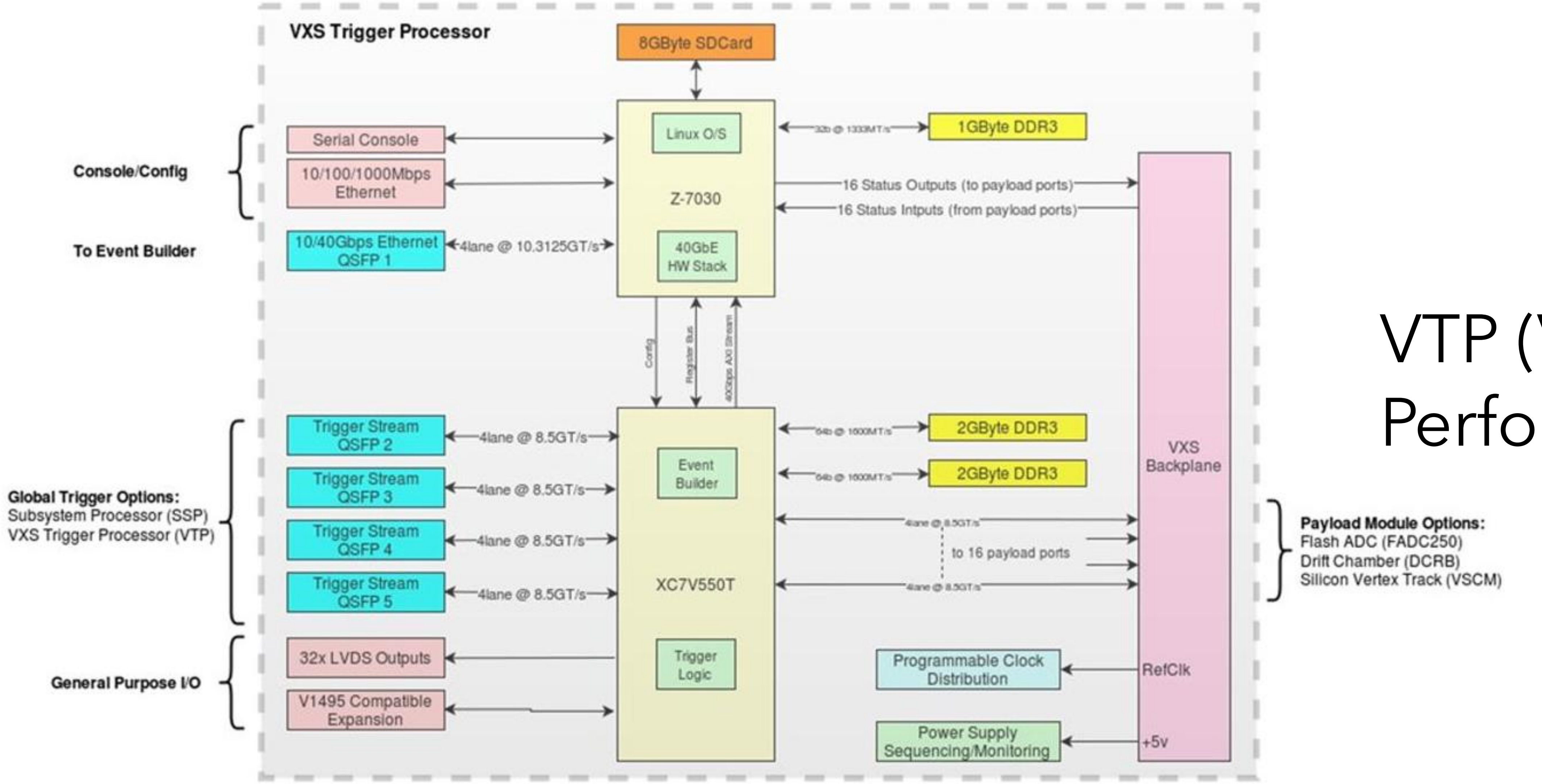

VTP (VXS Trigger Processor)
Performs the trigger logic computation

DAQ Diagram

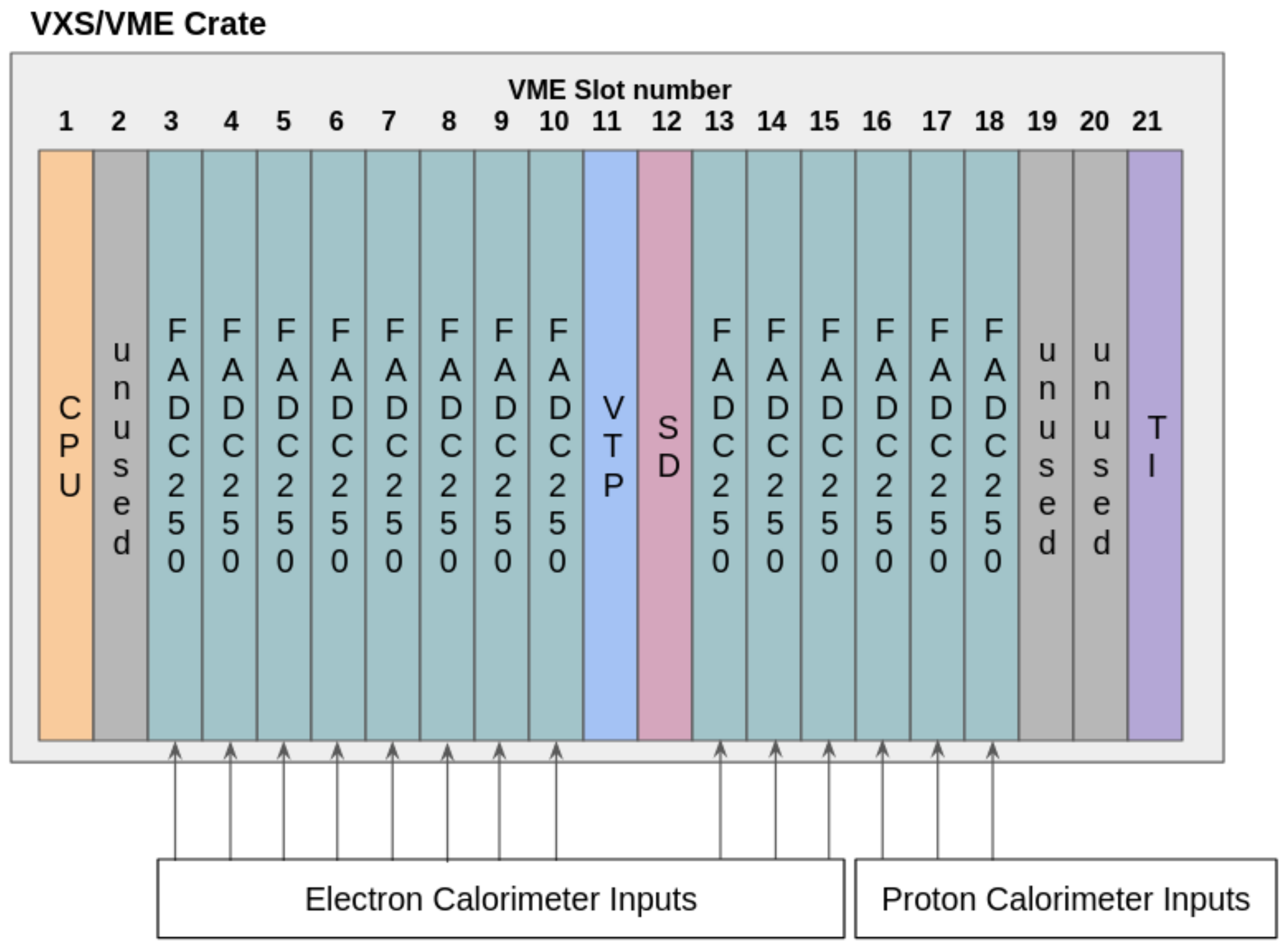

One VXS crate will handle one sector of ECAL + HCAL, also provide external trigger for ScintArray TDC readout

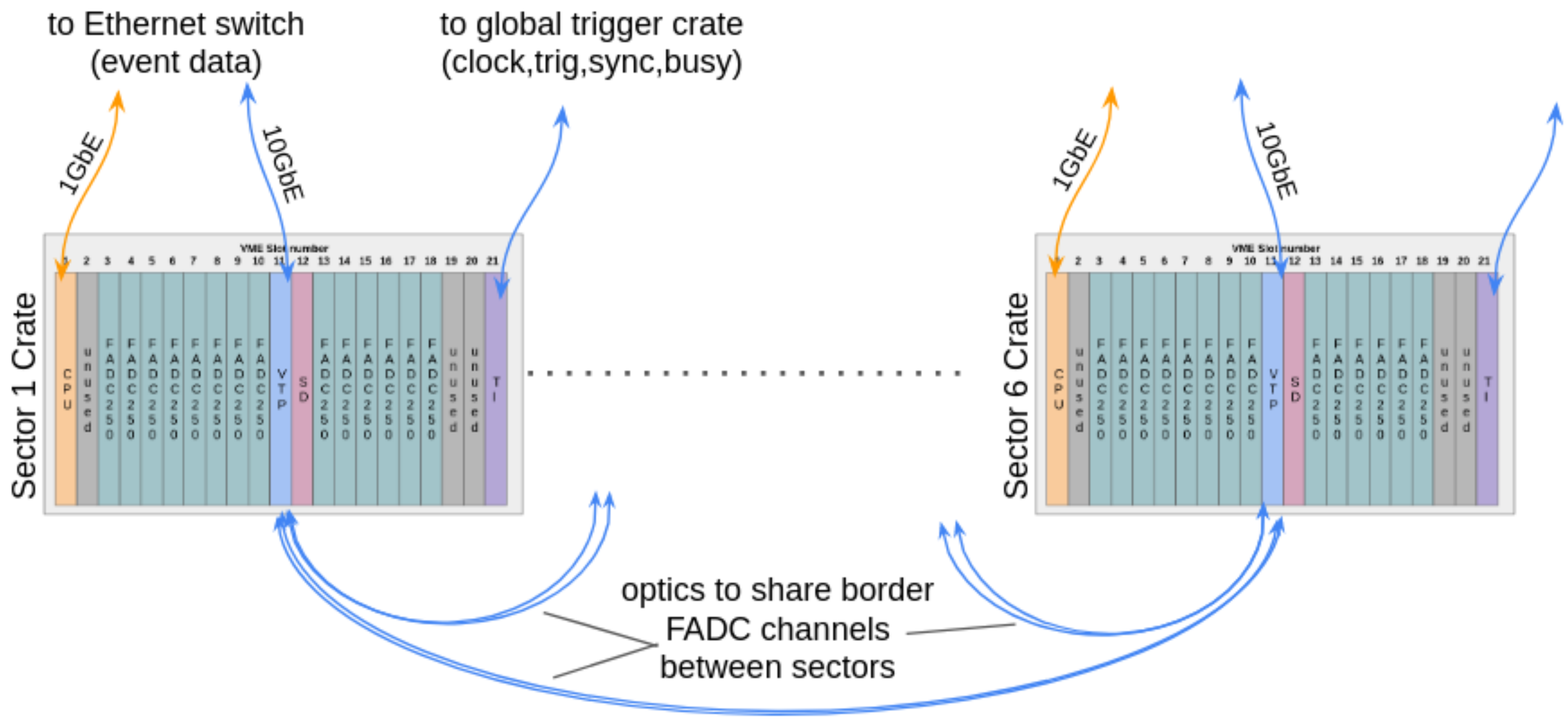

This six synchronized but independent systems will form the full DAQ

Cooling for ECAL

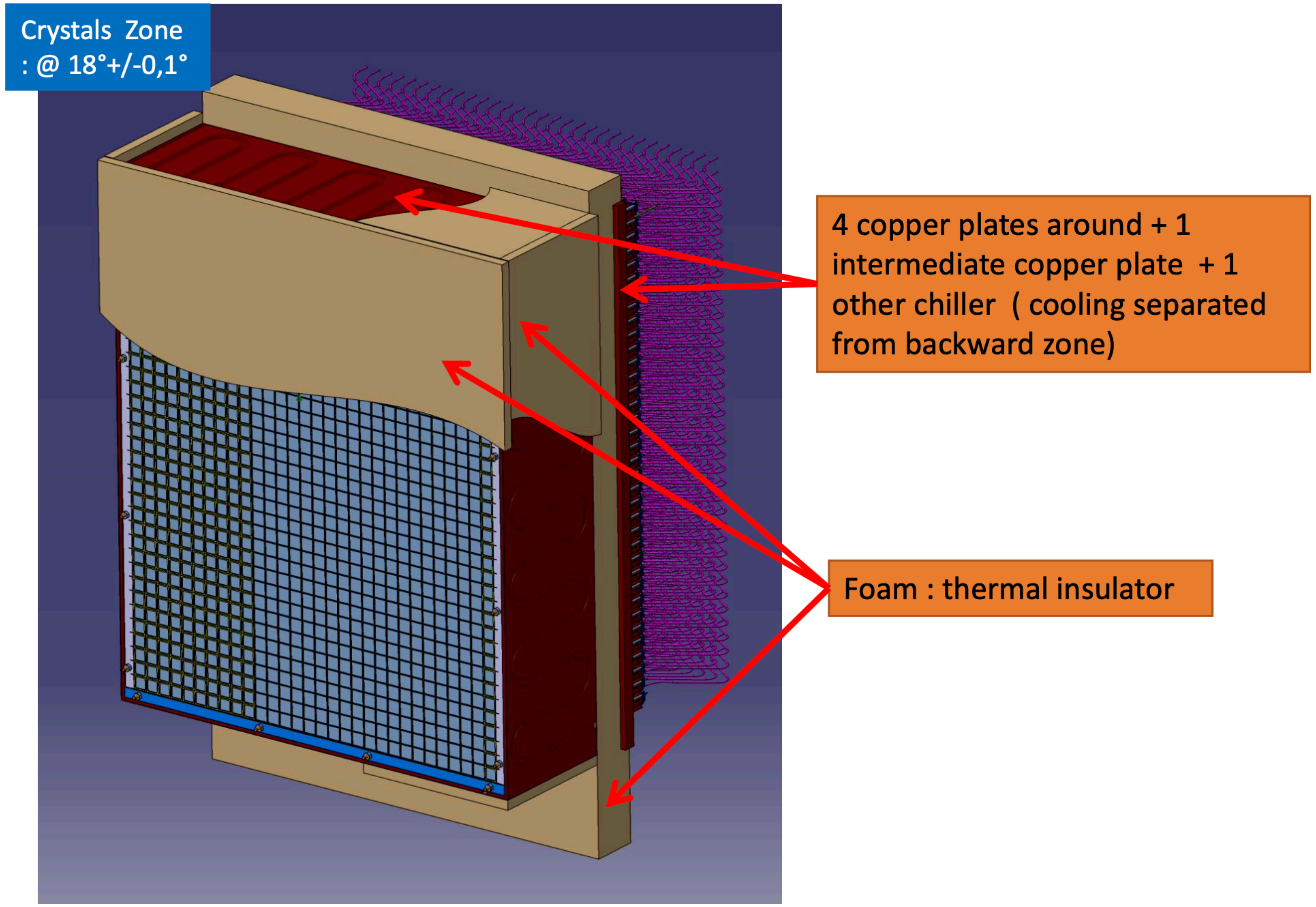

Water-cooled copper plates, foam thermal insulator

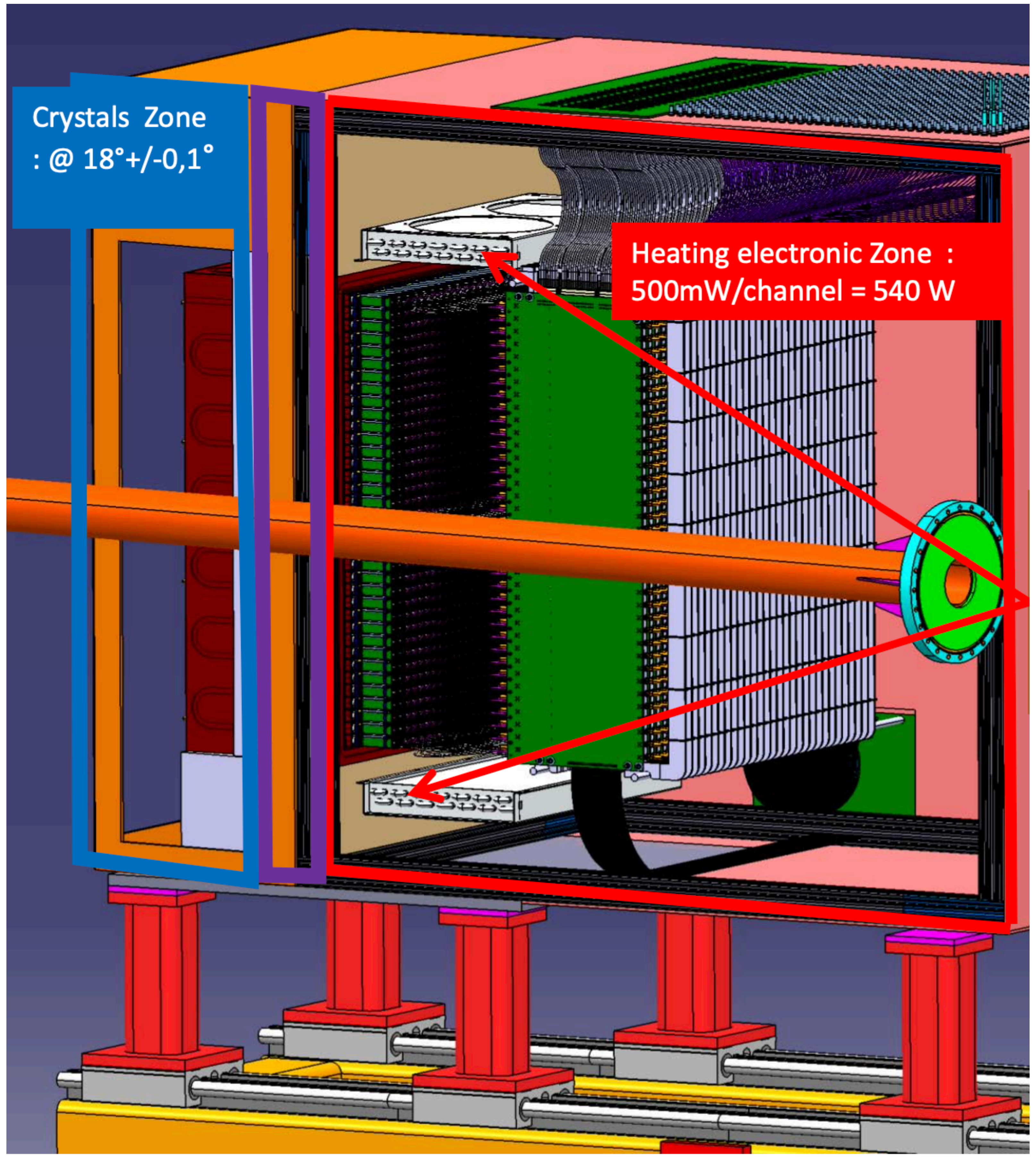

voltage dividers cooled with cooled air

Helicity-correlated Beam Asymmetries

Position differences (like angle, but angle ~10x smaller):
APV roughly proportional to Q^3 , so sensitivity $\delta A / \delta\theta \sim 3\, \delta\theta / \theta$

Assume very large (by today's standards) position difference of 200 nm, to be compared to 64cm radius of ECAL

200nm / 64 cm ~ 0.3 ppm, or 0.2%

Similarly, energy, assuming 200 nm in dispersive bpm (~1m dispersion)⟶ 0.2 ppm, or 0.15%

Azimuthal symmetry leads to excellent cancellation, so the net effects will be very small. Can be checked with regression

Charge asymmetry
Using feedback, <10ppm easily achievable. 1% calibration ⟶ 0.1ppm systematic, 0.06%

Scale of "acceptable" contributions

	Quantity	Absolute	Relative
1	Beam energy	132 MeV	2.0%
2	Scattering angle	0.34 deg	2.2%
3	GEN/G_{Dipole}		65%
4	GEP/G_{Dipole}		21%
5	GMN/G_{Dipole}		5%
6	G_A^{Zp}/G_{Dipole}		72%

The uncertainties of the parameters needed for each contribution of systematic uncertainty to match the statistical $\delta(A_{PV})/A_{PV} \sim 4.1\%$ result

EMFF accuracy at Q^2 ~2.5 GeV^2

Most sensitive to G_M^p and G_M^n
but these have been well measured

M. Diehl and P. Kroll, 2013

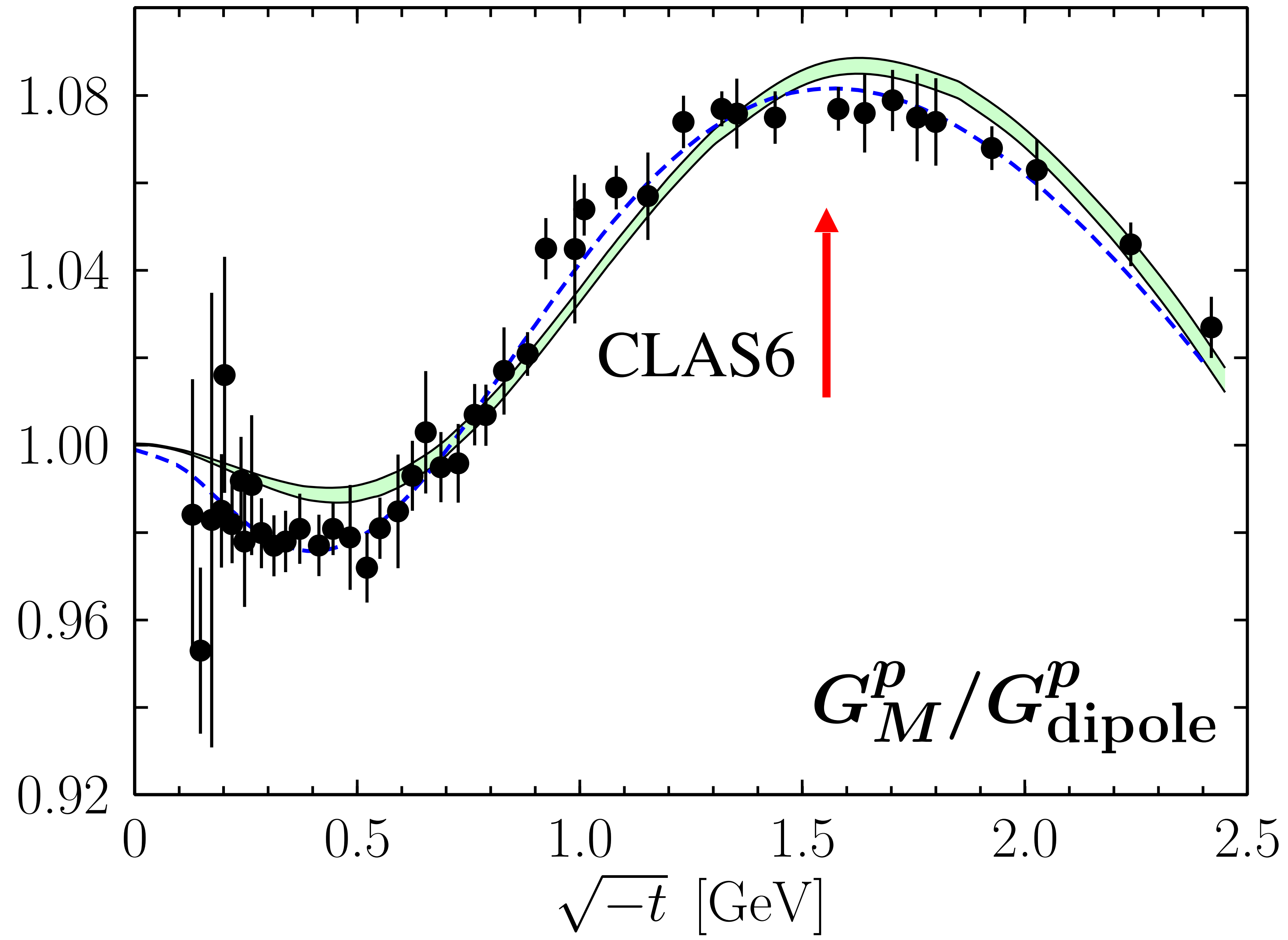

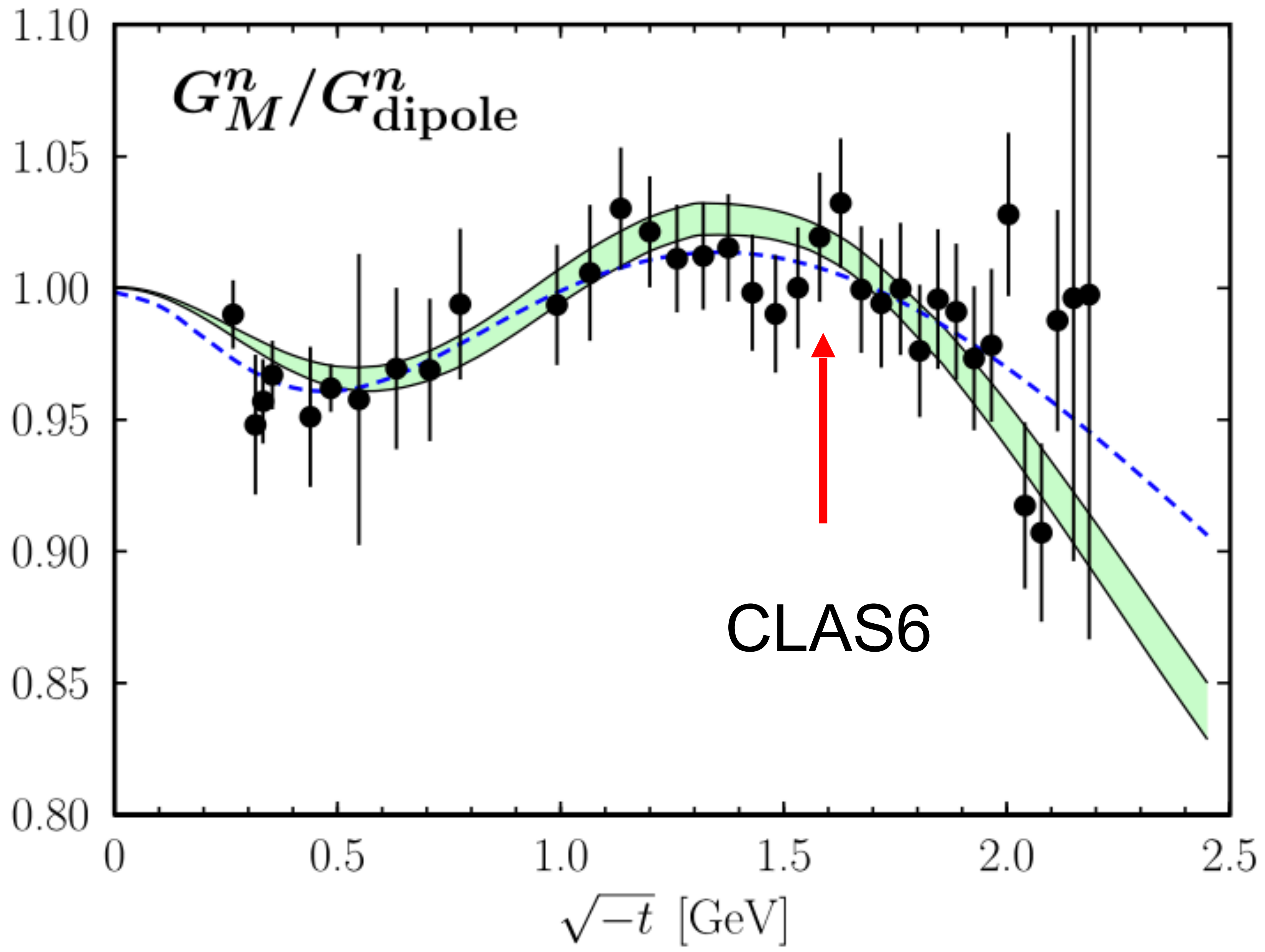

EMFF accuracy at 2.5 GeV²

M. Diehl and P. Kroll, 2013

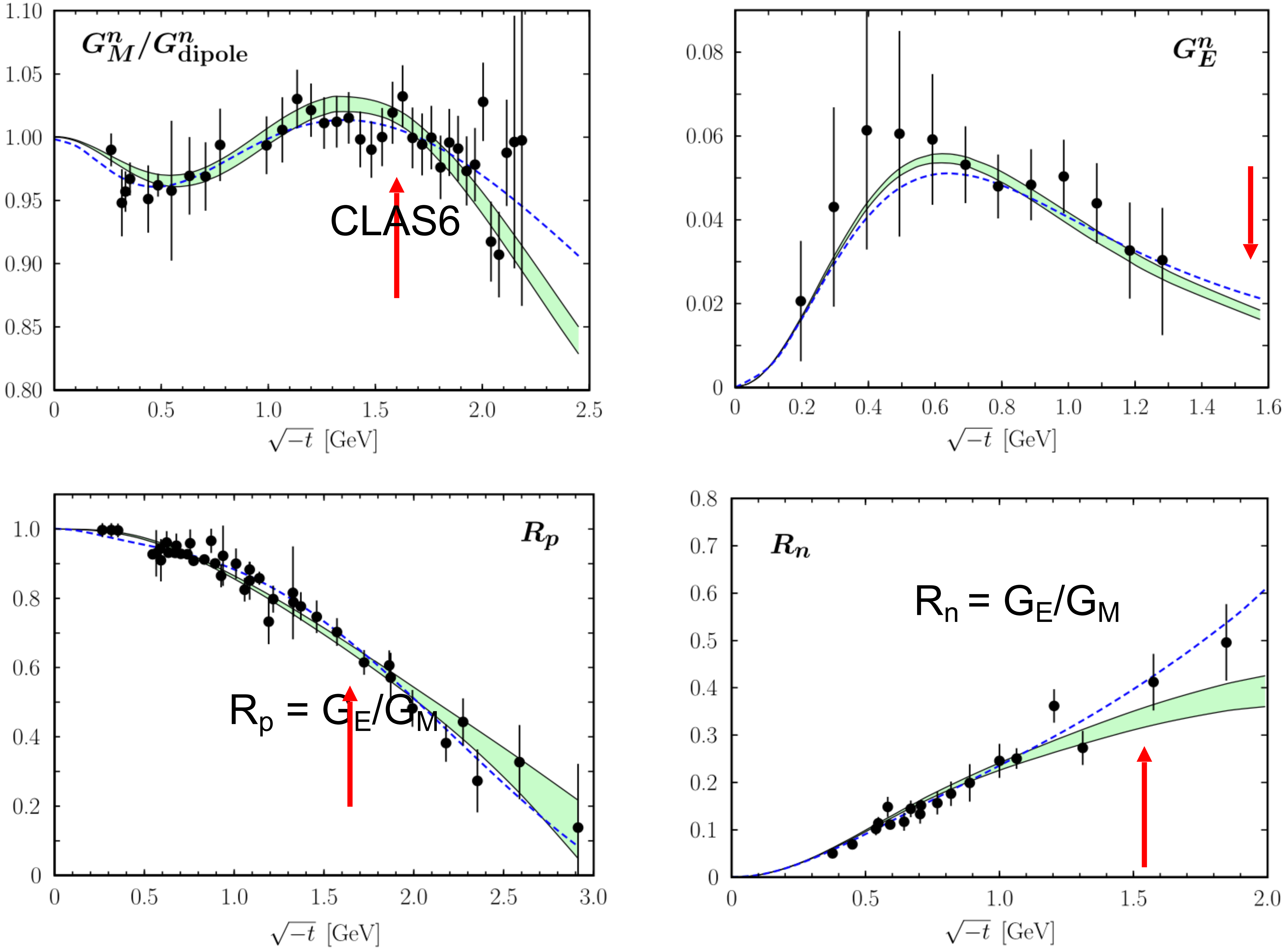

Electromagnetic Form-factors used for this calculation

Form Factor	Value at $Q^2 = 2.5$ GeV^2
$\mu_p G_E^p / G_M^p$	0.69
$G_M^p / (\mu_p G_D)$	1.08
$\mu_n G_E^n / G_M^n$	0.41
$G_M^n / (\mu_n G_D)$	1.01

V. Punjabi, C.F. Perdrisat, M.K. Jones, E.J. Brash, and C.E. Carlson: The Structure of the Nucleon

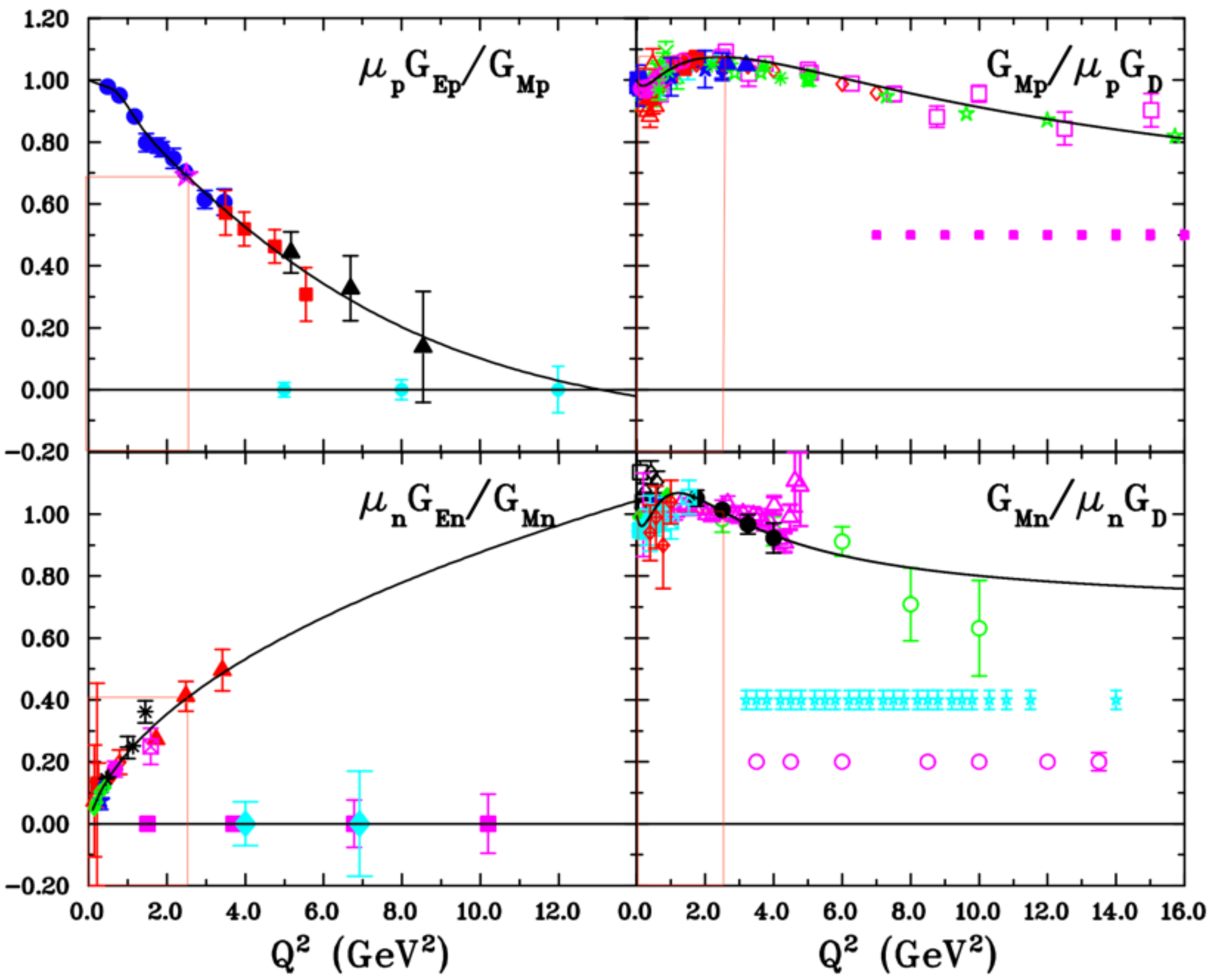

The nucleon electromagnetic form factors

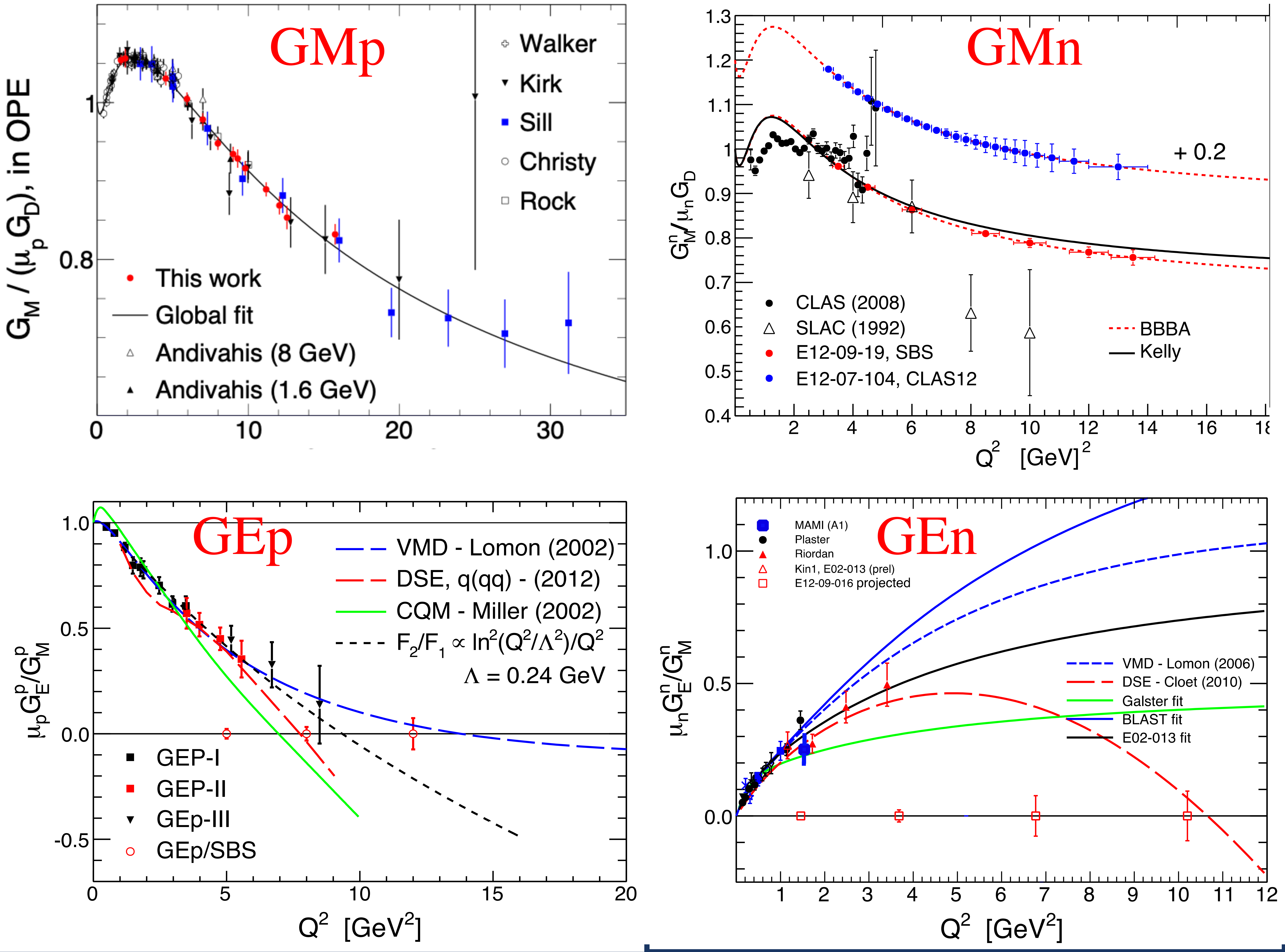

Axial Form Factor

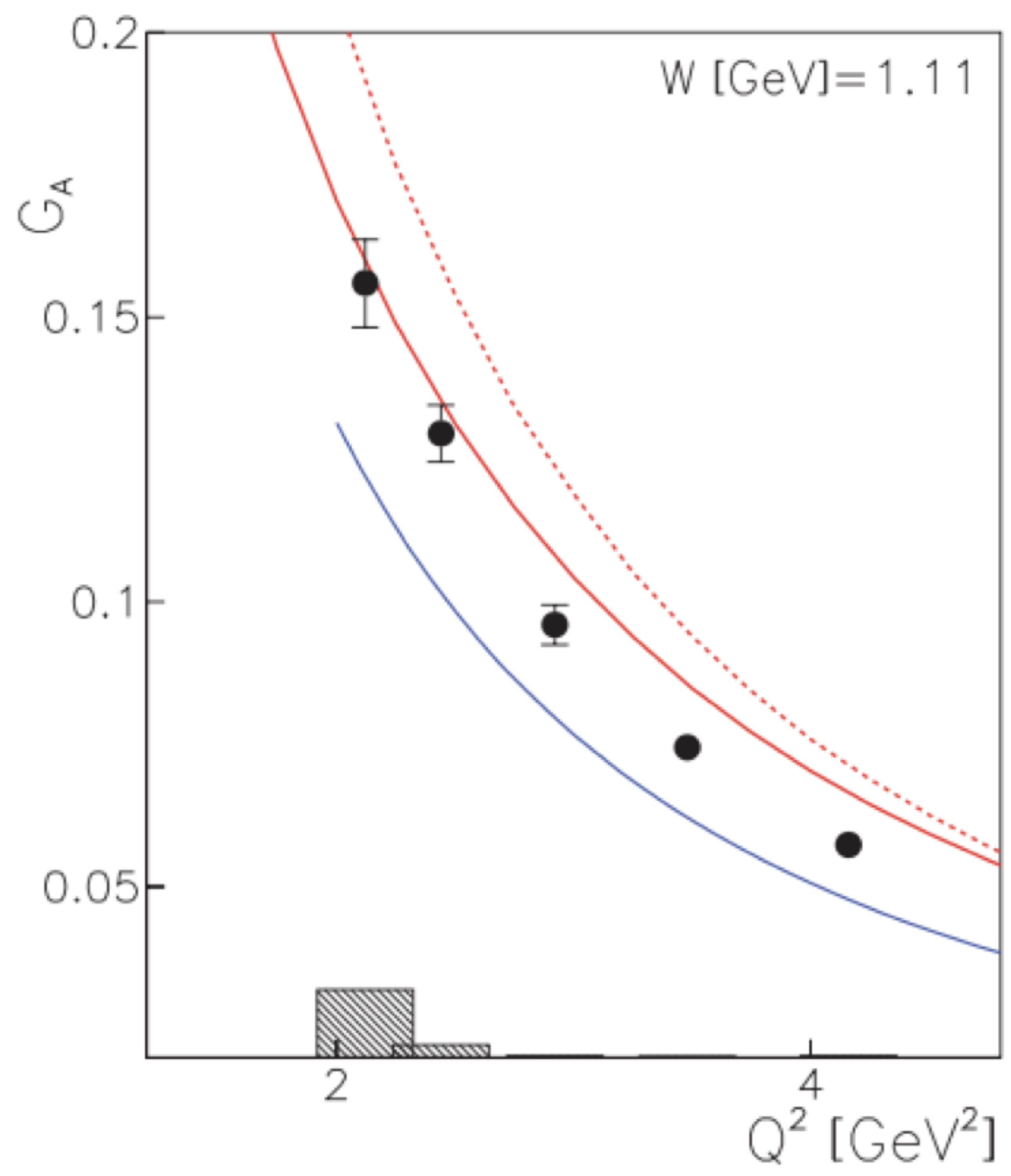

K. Park *et al.* [CLAS Collaboration],
Phys. Rev. C **85**, 035208 (2012).

- Axial form factor parameterization $G_A{}^p = 0.15$ at $Q^2 = 2.5$ GeV^2
  - *C. Chen, C. S. Fischer, C. D. Roberts, and J. Segovia, Form factors of the nucleon axial current, Physics Letters B 815, 136150 (2021)*
- Confirmed with pion photoproduction measurements
  - K. Park *et al.* [CLAS Collaboration], Phys. Rev. C **85**, 035208 (2012).
  - (~15% interpretation uncertainty)
  - I.V. Anikin, V.M. Braun, and N. Offen, Phys.Rev.D 94 (2016) 3, 034011.
- How uncertain is this measurement because of it?
  - Axial term ~6% of APV
  - ~15% uncertainty, so estimate 1% relative uncertainty on the 4% statistical measurement

Why search at high Q2?

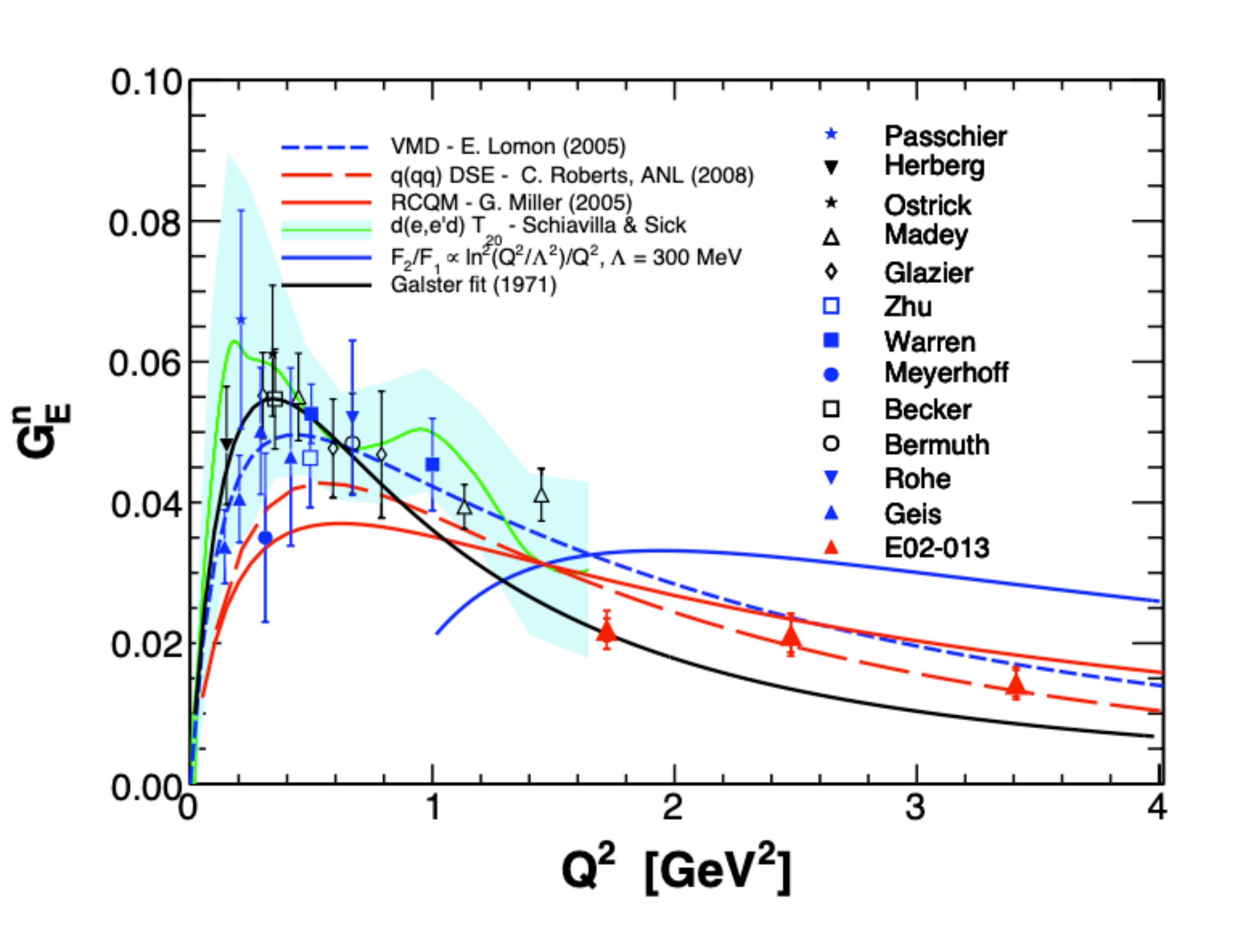

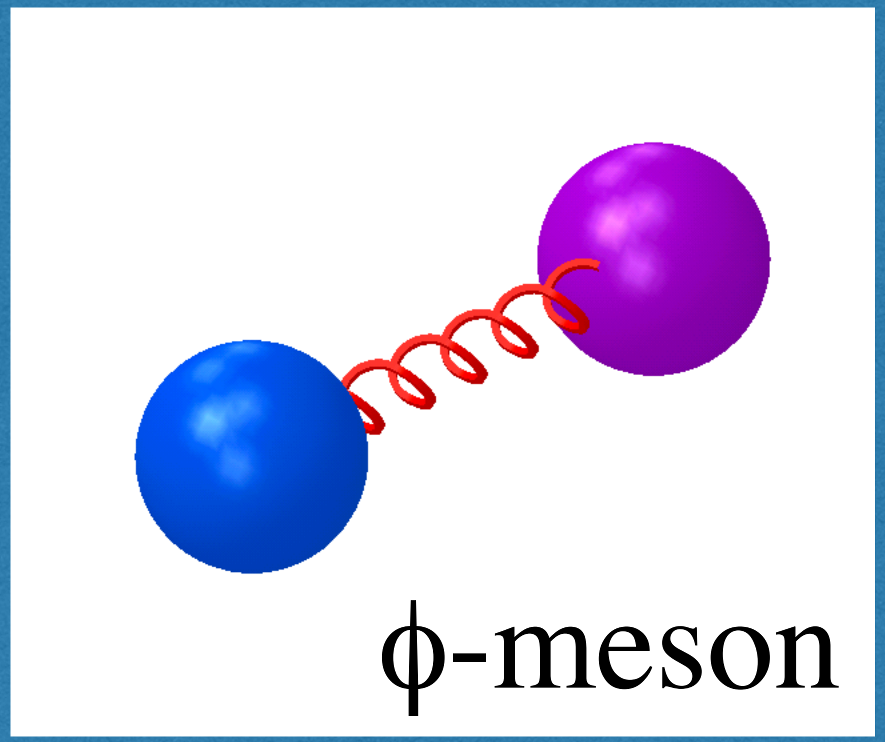

PARAMETER β IN $\phi \to \pi^0 e^+ e^-$ DECAY

VALUE (GeV^{-2})	*EVTS*	*DOCUMENT ID*		*TECN*	*COMMENT*
2.02±0.11	9.5k	[1] ANASTASI	16B	KLOE	1.02 $e^+e^- \to \pi^0 e^+ e^-$

This combined phi-pi radius ~ 0.69 fm
with a pi-0 radius of ~ 0.64 fm and
a ϕ-meson radius of ~ 0.26 fm

Electromagnetic form factors

$$F_i^p = e_u F_i^u + e_d F_i^d + e_s F_i^s \,,$$
$$F_i^n = e_u F_i^d + e_d F_i^u + e_s F_i^s \,,$$

$$\int_0^1 \mathrm{d}x \left[s(x) - \bar{s}(x) \right] = 0$$

$$F_1^s(0) = 0 \qquad F_2^s(0) = \mu_s$$

$$A_{PV} = -\frac{G_F Q^2}{4\pi\alpha\sqrt{2}} \cdot [(1-4\sin^2\theta_W) - \frac{\epsilon G_E^p G_E^n + \tau G_M^p G_M^n}{\epsilon (G_E^p)^2 + \tau (G_M^p)^2} - \frac{\epsilon G_E^p G_E^s + \tau G_M^p G_M^s}{\epsilon (G_E^p)^2 + \tau (G_M^p)^2}$$
$$+ \epsilon' (1-4\sin^2\theta_W) \frac{G_M^p G_A^{Zp}}{\epsilon (G_E^p)^2 + \tau (G_M^p)^2}]$$

A_{PV} = 150 ppm at 2.5 GeV^2 (for sFF = 0)

A_{PV} = (-226 ppm) *[0.075 + 0.542 – 6.43*($G_M^s + 0.32\, G_E^s$) + 0.038]

Q_w EMFF axial

strange form-factors

Anapole Moment

In the context of a very large discrepancy from SAMPLE, the anapole radiative correction was investigated as a possible cause

$$\tilde{G}^e_A(Q^2) = \left[\tau_3 g_A(1 + R_A^{(T=1)}) + \frac{3F - D}{2} R_A^{(T=0)} + (1 + R_A^{(0)})\Delta s\right] G_A^D(Q^2)$$

The 1-quark and many-quark corrections to the axial charges in the $\overline{MS}$ renormalization scheme.

	$R_A^{(T=1)}$	$R_A^{(T=0)}$	$R_A^{(0)}$
1-quark	−0.172	−0.253	−0.551
Many-quark	$\boxed{-0.086(0.34)}$	0.014(0.19)	–
Total	−0.258(0.34)	−0.239(0.20)	−0.551

values from Shi-Lin Zhu, S.J. Puglia, Barry R. Holstein, M.J. Ramsey-Musolf, Phys. Rev. D 62 (2000) 033008.

Suggests a coefficient on the axial term at $Q^2 = 0$:

$(1 + R_A^{(T=1)}) = 0.74 \pm 0.34$

Without improvement, this would correspond to 4.1ppb, or 2.7% of A_{PV}

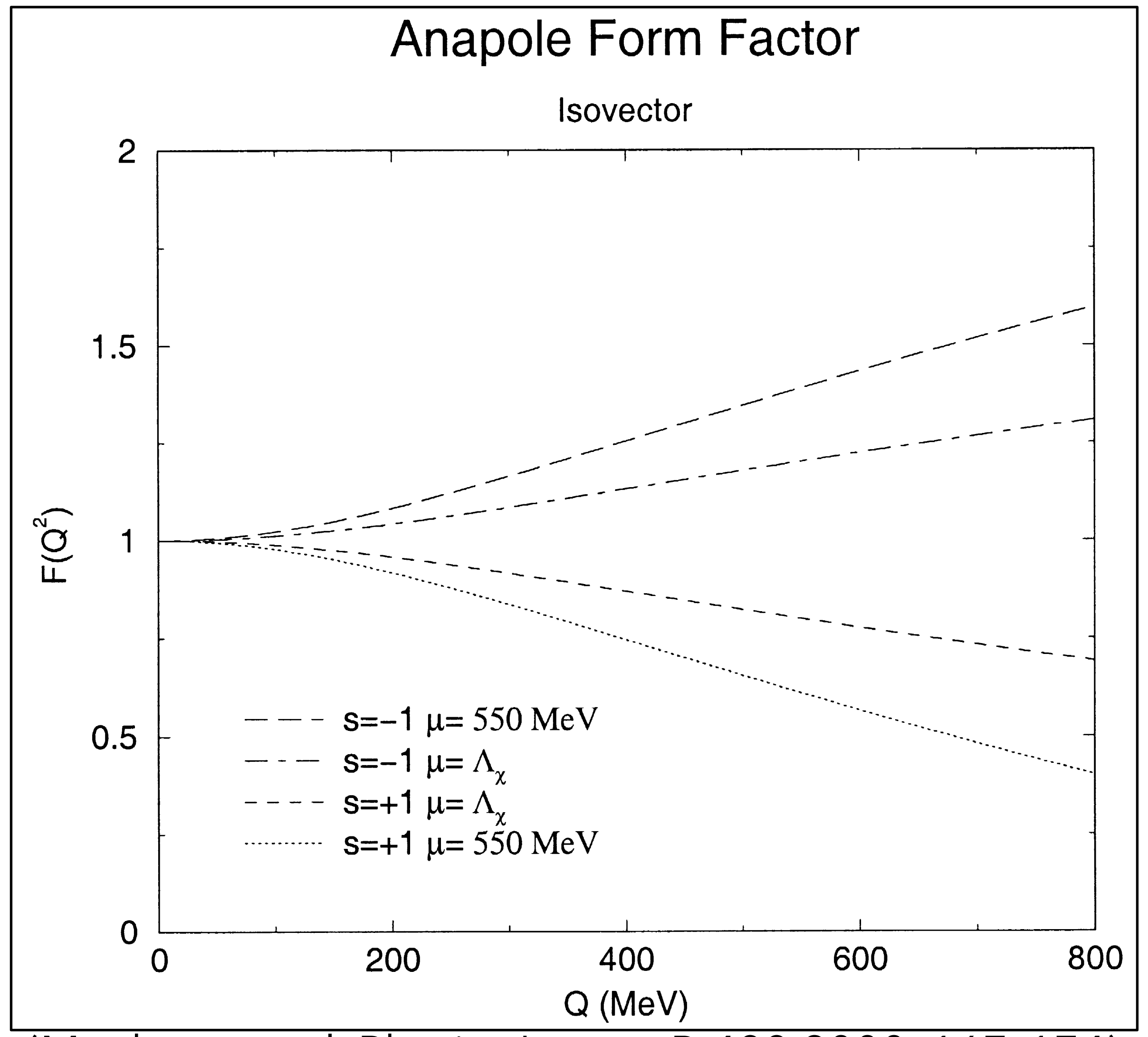

(Maekawa et al, Physics Letters B 488 2000. 167–174)

Q^2 dependence was explored at that time - suggested that it may be significant, but hasn't been evaluated since, or to high Q^2.

(Here, I believe this $F(Q^2)$ multiplies only the many-quark $R_A^{(T=1)}$= -0.086 contribution.)

Gamma-Z Box

Additional radiative correction to Q_W

$$Q_W^p = (1 + \Delta\rho + \Delta_e)\left(1 - 4\sin^2\theta_W(0) + \Delta_e'\right) + \Box_{WW} + \Box_{ZZ} + \Box_{\gamma Z}(0)$$

For Qweak, added ~0.5% uncertainty

Here, $\Box^{\mathrm{v}}_{\gamma Z}(0)$ = 0.0095 ± 0.0005 and $\Box^{\mathrm{a}}_{\gamma Z}(0)$ = -0.0036 ± 0.0004 which together is about 1.33±0.14 ppm (0.9±0.1%)

Caveat: this calculation is for forward direction. Off-forward expected to be greatly reduced (but this is also model dependent).

Axial piece smaller, didn't receive as much recent attention/update, seems stable with energy